

**ASSESSING THE PERFORMANCE OF TECHNIQUES FOR
DISAGGREGATING DAILY RAINFALL FOR DESIGN FLOOD
ESTIMATION IN SOUTH AFRICA**

Ryshan Ramlall

Submitted in partial fulfilment of the requirements for the degree of

Master of Science

Centre for Water Resources Research

School of Agricultural Earth and Environmental Sciences

University of KwaZulu-Natal

Pietermaritzburg


December 2020

PREFACE

I **Ryshan Ramlall** declare that:

- (a) The research reported in this document, except where otherwise indicated, is my original work.
- (b) This document has not been submitted for any degree or examination at any other university.
- (c) This document does not contain text, data, figures, pictures, graphs or tables from another document, unless it is specifically acknowledged as being sourced the original document. Where other sources have been quoted, then:
 - (i) their words have been paraphrased/re-written, and the general information attributed to them has been referenced, and
 - (ii) where their exact words have been used, their writing has been placed inside quotation marks, and referenced.
- (d) Where I have reproduced a publication, of which I am an author, co-author or editor, I have indicated, in detail, which part of the publication was actually written by myself alone and I have fully referenced such publications.
- (e) This document does not contain text, graphics or tables copied and pasted from the Internet, unless they are specifically acknowledged, and the source is detailed, both in the document and in the References section.

Signed:



Date: 2020/12/28

Supervisor:



Date: 25/01/2021

ABSTRACT

Design Flood Estimation (DFE) and other hydrological modelling methods are used to limit the risk of failure and ensure the safe design of infrastructure and for the planning and management of water resources. The temporal distribution of rainfall has a significant impact on the magnitude and timing of flood peak discharges. Rainfall temporal distributions are therefore an important component of DFE approaches. In order to improve DFE methods which are based on event or continuous simulation rainfall-runoff models, it is generally necessary to use sub-daily time step rainfall hyetographs as input. However, the number of recording raingauges which provide sub-daily timesteps in South Africa is relatively scarce compared to those which provide daily data. Rainfall Temporal Disaggregation (RTD) techniques can be used to produce finer resolution data from coarser resolution data. Several RTD approaches have been applied in South Africa. However, application of RTD approaches locally is relatively limited, both in terms of diversity of approaches and cases of application, compared to those developed and applied internationally. Therefore, a need exists to further assess the performance of locally applied approaches as well update the list of available approaches through inclusion of internationally developed and applied RTD techniques. A pilot study was performed in which selected locally applied and internationally applied approaches were applied to disaggregated daily rainfall data. Some approaches were applied in their original form while others were modified. Temporal distributions of rainfall were represented by dimensionless Huff curves, which served as the basis for comparison of observed and disaggregated rainfall. It was found that for daily rainfall, the SCS3, SCS4 and Knoesen model approaches performed considerably better than the other approaches in the pilot study. The RTD approaches were further assessed using data from 14 additional rainfall stations. For the additional stations, the Knoesen model disaggregated depths provided the most realistic temporal distributions overall, followed by the SCS-SA approach. In addition, an adapted form of the Triangular distribution was found to show potential for disaggregation when a generalised value for the timing of the peak was utilised.

ACKNOWLEDGEMENTS

I would like to extend my gratitude to the South African National Committee on Large Dams (SANCOLD) for the provision of funding in the form of a scholarship and for allowing me to attend the conference in 2019. This financial and experiential assistance was greatly appreciated.

This MSc was completed through the Centre for Water Resources Research (CWRR) at the University of KwaZulu-Natal. The Centre and University are greatly acknowledged for provision of funding, office space, data, administrative functions and other assistance during the course of this research.

I would like to thank my supervisor, Professor J.C Smithers for allowing me to work in his research group and for his mentorship, encouragement and support. The experiences which I gained working on this project and as part of the research group have allowed me to grow immensely as a person and as a scientist.

This project could not have been completed without the support of my close friends and family. A very special thank you is given to my father Mukesh, mother Kriya and brother Yuvesh. I also would not have gotten this far without Heidi, Snoekie, Spot and my dearest Scampy, who kept me company and kept my spirits up whenever I worked alone.

TABLE OF CONTENTS

PREFACE.....	i
ABSTRACT	ii
ACKNOWLEDGEMENTS	iii
LIST OF FIGURES	vii
LIST OF TABLES	x
LIST OF ABBREVIATIONS	xii
1. INTRODUCTION.....	1
1.1 Importance of Rainfall Data Temporal Resolutions	2
1.2 Aim and Objectives.....	3
2. APPROACHES FOR TEMPORAL DISAGGREGATION OF RAINFALL	5
2.1 Rainfall Distribution Curves	5
2.1.1 Hyetographs derived from storm event analysis	6
2.1.2 Hyetographs derived from intensity-duration-frequency (IDF) relationships	13
2.2 Disaggregation Models	15
2.2.1 Stochastic Rainfall Temporal Disaggregation models	15
2.2.2 Deterministic rainfall temporal disaggregation models	19
2.3 Summary of Methods.....	23
2.4 Chapter Discussion and Conclusions.....	27
3. GENERAL METHODOLOGY	30
3.1 Approach.....	30

3.2	General Methodology	30
3.3	Data Utilised	31
3.3.1	Characteristics of rainfall data	34
3.3.2	Assessment of the performance of the RTD methods.....	35
4.	APPLICATION OF RTD APPROACHES: PILOT STUDY	38
4.1	Data used in pilot study.....	38
4.2	Huff Curves.....	42
4.3	SCS-SA Rainfall Distributions	46
4.4	HRU 1/72 Distributions	48
4.5	Triangular Distribution	52
4.5.1	Triangular ObsTP	52
4.5.2	Triangular Median TP	55
4.6	Average Variability Method (AVM)	57
4.7	AVM-B	60
4.8	Knoesen Semi-stochastic Disaggregation Model	61
4.9	Comparison of The Performance of RTD Approaches.....	64
4.9.1	Comparison of observed and disaggregated peak intensities.....	64
4.9.2	Comparison of temporal distribution accuracy	65
4.10	Chapter Discussion and Conclusions.....	69
5.	APPLICATION OF RTD APPROACHES: ALL SITES	71
5.1	Performance of Disaggregation Approaches	71

5.1.1	Station 0555866	73
5.1.2	Station Jnk19a	76
5.1.3	Results for all selected rainfall stations	79
5.2	Chapter Discussion and Conclusions	85
6.	DISCUSSION, CONCLUSIONS AND RECOMMENDATIONS	87
6.1	Overview	87
6.2	RTD Approaches Applied in South Africa	88
6.3	Application and Performance of Selected Approaches	88
6.4	Recommendations	91
7.	REFERENCES	92

LIST OF FIGURES

Figure 2.1	Categorisation of rainfall temporal disaggregation approaches (after Knoesen, 2005)	5
Figure 2.2	Example of Huff curve for time distribution of rainfall in first quartile storms (Huff, 1990)	7
Figure 2.3	SCS 24-hour rainfall hyetographs (Chow <i>et al.</i> , 1988)	8
Figure 2.4	Synthetic design rainfall distributions for use in South Africa (Schmidt and Schulze, 1987; cited by Knoesen, 2005)	9
Figure 2.5	Temporal distribution curves for intermediate durations (HRU, 1972) ..	10
Figure 2.6	General model of the Triangular distribution hyetograph (Chow <i>et al.</i> , 1988)	11
Figure 2.7	Ranking of storms and periods for the AVM (Pilgrim <i>et al.</i> , 1969; cited by Bhuiyan <i>et al.</i> , 2010)	12
Figure 2.8	Example of design hyetographs derived from the ABM with a 1-hour timestep (Nguyen <i>et al.</i> , 2008)	13
Figure 2.9	Fitting a curve to a hyetograph with the Instantaneous Intensity Method (Chow <i>et al.</i> , 1988)	14
Figure 2.10	Schematic of the BLRP model process (Koutsoyiannis and Onof, 2001)	16
Figure 2.11	Schematic of the NSRP model process (Olsson and Burlando, 2002)	17
Figure 2.12	Discrete disaggregation model (Ormsbee, 1989)	20
Figure 3.1	Locations of rainfall stations utilised in this study	31
Figure 3.2	Percentage of rainfall days with daily total depths in each range per station	34

Figure 3.3 Percentage of rainfall days with peak intensities in each quartile per rainfall station	35
Figure 4.1 Relationship between peak intensity and daily total depth for Station C161 rainfall days	39
Figure 4.2 Relationship between time to peak and daily total depth for Station C161 rainfall days	39
Figure 4.3 Characteristics of daily rainfall parameters for Station C161	40
Figure 4.4 Huff curves for rainfall days greater than 10 mm from Station C161	43
Figure 4.5 Quartile Huff curves for daily rainfall periods from Station C161	44
Figure 4.6 Percentage of rainfall days which display peak intensities in each quartile of the total duration.....	45
Figure 4.7 Comparison of SCS distribution curves and observed daily rainfall Huff curves.....	47
Figure 4.8 Fit of the polynomial equation curves for HRU 1/72 different duration curves.....	50
Figure 4.9 Comparison of observed daily rainfall Huff curves and HRU 1/72 24-hour distribution curve	51
Figure 4.10 Derivation of straight line equations for rainfall intensity and depth values preceding and succeeding peak intensity.....	53
Figure 4.11 Comparison of observed daily rainfall Huff curves and Triangular distribution curves	54
Figure 4.12 Comparison of observed daily Huff curves and Median time-to-peak Triangular distribution curve	56
Figure 4.13 AVM 24-hourly distribution pattern at Station C161	57
Figure 4.14 Comparison of observed daily rainfall Huff curves to AVM curve	59

Figure 4.15 Comparison of observed daily rainfall Huff curves to AVM-B curve	61
Figure 4.16 Stochastic generation of distribution of rainfall depths over 24-hours....	62
Figure 4.17 Comparison of observed daily Huff curves to Knoesen model daily Huff curves	63
Figure 4.18 Regression analysis between peak intensities of rainfall days disaggregated using the Triangular ObsTP approach and observed rainfall day peak intensities for Station C161	64
Figure 4.19 MARE between observed and disaggregated 50th percentile Huff curves 66	
Figure 4.20 Total MARE across percentiles for each RTD approach	67
Figure 5.1 50 th percentile Huff curves derived from observed daily rainfall at each station.....	72
Figure 5.2 \sum MARE values for Station 0555866.....	74
Figure 5.3 \sum MARE values for Station Jnk19a	77
Figure 5.4 \sum MARE values per RTD approach for each rainfall station.....	81
Figure 5.5 \sum MARE values for RTD approaches summed across all stations	82

LIST OF TABLES

Table 2.1	Selected case studies for rainfall temporal disaggregation approaches...	23
Table 3.1	Characteristics of rainfall stations used in this assessment	32
Table 4.1	Summary of methodology for application of RTD approaches.....	41
Table 4.2	MARE values for SCS-SA distributions applied to disaggregate daily rainfall.....	47
Table 4.3	Multipliers for the 10th order polynomial equations for each duration HRU 1/72 curve used	49
Table 4.4	MARE values for the HRU 1/72 24-hour distribution applied to disaggregate daily rainfall.....	51
Table 4.5	MARE values for Triangular ObsTP approach applied to daily rainfall.	54
Table 4.6	MARE values for Triangular Median TP approach applied to disaggregate daily rainfall.....	56
Table 4.7	Derivation of 24-hourly AVM distribution	58
Table 4.8	MARE values for AVM applied to disaggregate daily rainfall.....	60
Table 4.9	MARE values for AVM-B applied to disaggregate daily rainfall.....	61
Table 4.10	MARE values for Knoesen model applied to disaggregate daily rainfall	63
Table 4.11	Comparison between observed and disaggregated peak intensities for each approach applied to daily rainfall for Station C161.....	65
Table 4.12	NSE values for comparison of observed and disaggregated Huff curves	68
Table 5.1	Comparison between observed and disaggregated peak intensities for Station 0555866 rainfall days	73
Table 5.2	NSE values for comparison of observed and disaggregated Huff curves for 0555866 rainfall days	75

Table 5.3	Comparison between observed and disaggregated peak intensities for Jnk19a rainfall days	76
Table 5.4	NSE values for comparison of observed and disaggregated Huff curves for Jnk19a rainfall days	78
Table 5.5	Total MARE values for each RTD approach per station.....	79
Table 5.6	Mean NSE values for each approach for each rainfall station.....	83

LIST OF ABBREVIATIONS

ABM	Alternating Block Method
ACRU	Agricultural Catchments Research Unit model
AVM	Average Variability Method
BLRP	Bartlett-Lewis Rectangular Pulse
BLRPG	Bartlett-Lewis Rectangular Pulse Gamma
CSM	Continuous Simulation Modelling
CUM	Continuous Universal Multifractal
DFE	Design Flood Estimation
IDF	Intensity-Duration-Frequency
IIM	Instantaneous Intensity Method
MBLRPG	Modified Bartlett-Lewis Rectangular Pulse Gamma
MOF	Method of Fragments
NSRP	Neyman-Scott Rectangular Pulse
RBLM	Randomised Bartlett-Lewis Model
RMC	Random Multiplicative Cascade
RTD	Rainfall Temporal Disaggregation
SA	South Africa
SAWS	South African Weather Service
SCS	Soil Conservation Service
USA	United States of America
NSE	Nash-Sutcliffe Efficiency

1. INTRODUCTION

Although a natural part of Earth system processes, flood occurrence has numerous negative impacts on society. These include economic losses due to infrastructure damage, loss of productivity time, injuries and loss of human life (Ward *et al.*, 2016). Therefore, the management of and prediction of floods is imperative to maintaining the overall well-being of society (Parkes and Demeritt, 2016). Design Flood Estimation (DFE) comprises of the assessment of flood risk through determining the return periods of extreme events which have the potential to impose design hazard (Rowe and Smithers, 2018). The technique is vital to ensuring that the design of hydrological and related infrastructure, planning and management of water resources is carried out with safety in consideration (Rowe and Smithers, 2018).

Rainfall is a driver of hydrological models and therefore its data is a key component in DFE techniques (Smithers and Schulze, 2002). Rainfall data is utilised to determine hyetographs and subsequently hydrographs from which the peak discharge is obtained, against which hydrological structures and management plans are designed (Arnaud *et al.*, 2007; Hassini and Guo, 2017; Rowe and Smithers, 2018). Rainfall is highly variable both temporally and spatially on any given day or for a given event (Koutsoyiannis, 2003). In order to accurately calculate flood peaks in design flood estimation, rainfall data at fine temporal scales are needed (Knoesen and Smithers, 2008).

Modelling and simulation relating to DFE is generally performed utilising daily rainfall data, due to the relative abundance and longer record lengths as opposed to sub-daily data (Smithers and Schulze, 2000; Smithers *et al.*, 2002; Pui *et al.*, 2012). However, such data may not adequately represent the important characteristics of rainfall processes occurring at sub-daily and sub-hourly scales (Smithers and Schulze, 2000; Pui *et al.*, 2012). The inadequate representation of such processes by coarser resolution data may be attributed to the non-linear nature of the formulative processes of rainfall events, which may suggest that a number of individual storms could occur within a short time period (Socolofsky *et al.*, 2001). Coarser data resolutions may also inaccurately represent the distribution of rainfall occurring at different times within the overall event period (Huff, 1967; Huff, 1990). Rainfall data at sub-daily levels is necessary for numerous hydrological applications, including *inter-alia* erosion and sediment transport monitoring, water quality modelling, flood risk assessments and the design of hydraulic structures, owing to its advantages over coarser data

in representing rainfall characteristics and modelling rainfall-runoff interactions (Engida and Esteves, 2011). However, a major disadvantage in utilising such data is that both internationally and in South Africa (SA), the number of gauges which provide data at sub-daily time steps is far less than those which provide daily-level data (Koutsoyiannis and Onof, 2001; Smithers and Schulze, 2002; Segond *et al.*, 2006; Pui *et al.*, 2012). Data at such timesteps is required for accurately modelling sub-daily processes (Smithers and Schulze, 2002). Therefore, in order to obtain adequate data at finer temporal resolutions, Rainfall Temporal Disaggregation (RTD) techniques are often employed (Pui *et al.*, 2012).

RTD methods disaggregate coarser resolution data, such as daily data, to produce data of a finer resolution, such as hourly (Koutsoyiannis, 2003). The finer resolution data is able to more accurately represent rainfall hyetographs required for design flood estimation (Koutsoyiannis *et al.*, 2003). RTD techniques have been successfully applied under South African conditions to obtain finer resolution rainfall data for DFE applications (Adamson, 1981; Lambourne and Stephenson, 1987; Weddepohl, 1988; Knoesen, 2005; Knoesen and Smithers, 2008). However, such methods may be seen as limited in variety, since a plethora of newer approaches have been developed and successfully applied internationally (Smithers and Schulze, 2002).

1.1 Importance of Rainfall Data Temporal Resolutions

The temporal distribution of rainfall intensity within storms influences the magnitude and timing of peak discharges within a catchment, and as a result, the flood-generation potential of the event (Knoesen and Smithers, 2008). In recent years, increased attention has been drawn to the implications of climate change and altered atmospheric-hydrological patterns on higher flood risks (Burn and Hag Elnur, 2002; Parkes and Demeritt, 2016; Hu *et al.*, 2018). The need for improved understanding of the non-stationarity of rainfall processes advocates for utilization of shorter-duration, finer resolution data and use of more accurate disaggregation techniques for their production.

Brunner and Sikorska-Senoner (2019) found that the temporal distribution of rainfall and the resolution utilised have a marked effect on simulated flood volumes and peak discharges, and therefore will impact on the estimated design floods. Hence, an accurate temporal distribution is particularly important for the reproduction of observed peak discharges and flood volumes. This can be attributed to the influence which the rainfall temporal distribution

has on the shape of the hyetograph and subsequently the hydrograph (Ball, 1994; ARR, 2015). Hence, rainfall data used for modelling studies must be selected with an appropriate temporal resolution and representative distribution (Brunner and Sikorska-Senoner, 2019).

The work shown in Calver *et al.* (2004) and Calver *et al.* (2005) demonstrated that utilising rainfall data with finer temporal resolutions were advantageous for accurate representation of flood peaks. Furthermore, daily data which was disaggregated to hourly provided more accurate results compared to when daily data was directly utilised. The improved accuracy in the use of finer resolution data is also relevant to rainfall extremes, whereby the rainfall distribution of high rainfall days can be better represented by use of sub-daily data compared to daily data (Westra *et al.*, 2013; Westra *et al.*, 2014).

Considering the abovementioned findings, it can be stated that the use of finer resolution data such as sub-daily may improve the overall confidence of the results of DFE applications and other forms of hydrological and climatological modelling (Frezghi and Smithers, 2008; Rowe and Smithers, 2018). This concept has applicability to the continued development of DFE in South Africa, as described by Smithers *et al.* (2016) and Rowe and Smithers (2018) in relation to Continuous Simulation Modelling (CSM) approaches. Further development of a Continuous Simulation Modelling system for DFE in South Africa has been recommended as one of the pathways for updating DFE techniques. RTD approaches are useful for generating rainfall records in the desired resolution to use in CSM, since observed rainfall records may be used as direct input to CSM approaches in order to generate simulated flow time-series (Knoesen, 2005; Rowe and Smithers, 2018). Examples of this are the SCS-SA and ACRU models which require a means to disaggregate daily rainfall to generate sub-daily hyetographs in order to estimate peak discharge. These models have been utilised for CSM development in South Africa (Rowe and Smithers, 2018; Rowe, 2019). The relevance of RTD approaches to improving DFE and other types of modelling and water resources management, as well as the comparatively limited application of newer RTD approaches in South Africa, advocates for the need to assess the feasibility of new methods for application in South Africa and subsequently update the toolbox of RTD techniques.

1.2 Aim and Objectives

The overall aim of this research is to assess the performance of various RTD methods and to recommend the adoption or adaptation of one or more of these approaches for application

under South African conditions. Achieving this aim will require the following objectives to be met:

- Reviewing literature on disaggregation approaches.
- Acquiring an understanding of previously used methods as well as recently developed approaches.
- Assessing the performance of selected methods using South African daily rainfall data, either in their original form or as adapted methods.
- Recommendation of suitable options for adoption, adaptation or development of a regionalised rainfall disaggregation method(s) for design flood estimation in SA.

An extensive literature review was conducted on approaches used for disaggregating rainfall data internationally and locally which is detailed in Chapter 2. Suitable approaches were identified based on examination of case studies of their application and based on simplicity of application, data requirements and performance in regions with similar climates to South Africa. The general methodology used in this study is detailed in Chapter 3, which is followed by detailed methodologies for the applied RTD approaches and the results of the pilot study in Chapter 4. Further investigation was performed using additional rainfall stations in Chapter 5, which is followed by the conclusions and recommendations of this research in Chapter 6.

2. APPROACHES FOR TEMPORAL DISAGGREGATION OF RAINFALL

A selection of the various commonly applied techniques for the temporal disaggregation of coarser-level rainfall data into finer resolutions are discussed in this chapter. These can be broadly classified as either distribution curves or mathematical and computational models, as shown in Figure 2.1.

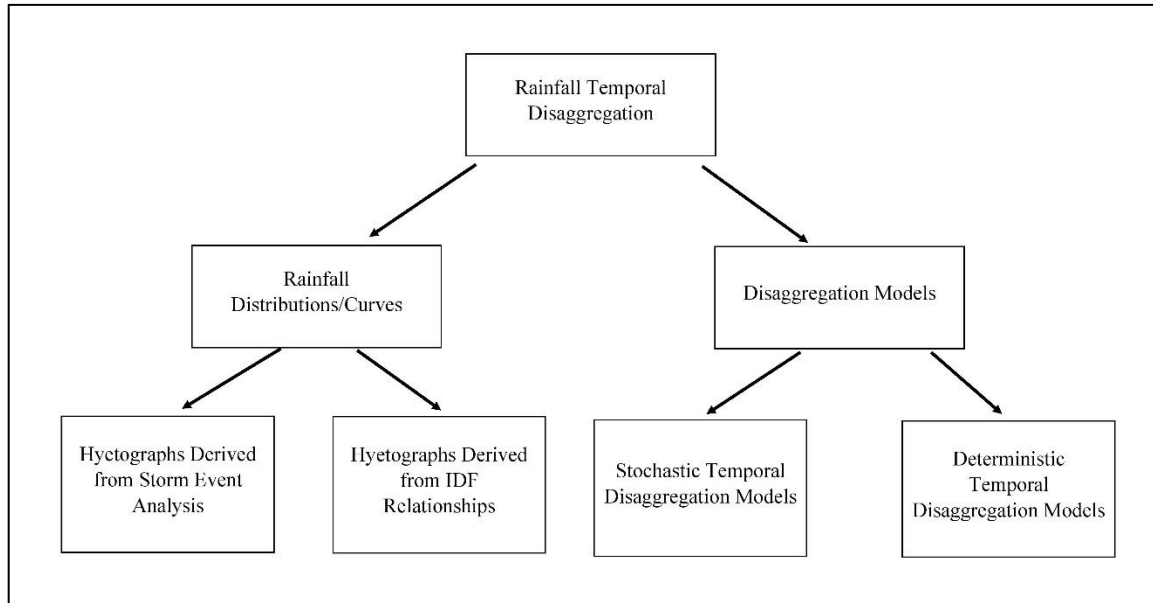


Figure 2.1 Categorisation of rainfall temporal disaggregation approaches (after Knoesen, 2005)

2.1 Rainfall Distribution Curves

A synthetic event or distribution can be developed through statistical and time sequence analysis of rainfall intensity data from nearby gauges for a particular event. Development over a large area may enable the production of a regional synthetic rainfall distribution (Chow *et al.*, 1988; Weddepohl, 1988). Temporal distribution curves have seen extensive application in South Africa for rainfall-runoff modelling and design applications (Adamson, 1981). Rainfall distributions may be divided into two broad categories; design hyetographs derived from direct analysis of storm events, and hyetographs derived using Intensity-Duration-Frequency (IDF) relationships or curves (Weddepohl, 1988).

2.1.1 Hyetographs derived from storm event analysis

2.1.1.1 Huff curves

Huff (1967) developed time distributions for heavy storms in Illinois, USA, utilizing a 12-year data record of 49 gauges from the surrounding area. Storms were defined as rainy periods with a gap of 6-hours or more between previous and successive event (Huff, 1967). The distributions were smooth curves, characterizing the average rainfall distribution with time (Figure 2.2). However, they did not show the burst characteristic of observed storms (Huff, 1967; Chow *et al.*, 1988). The time distribution models, known as the ‘Huff Curves’, employed the mass curve method and were presented as probability distributions, representing inter-storm variability and the general rainfall temporal pattern (Adamson, 1981; Chow *et al.*, 1988; Weddepohl, 1988). Huff (1967) identified a trend in rainfall that showed that a major proportion occurs in a relatively short time frame of the total event duration. This allowed for classification of events in to four major quartile groups depending on the quarter of the storm period in which contained the heaviest rainfall, as shown in Figure 2.2 (Adamson, 1981). The probability distributions allow for determination of the most suitable temporal pattern for a specific application. However, guidelines for construction of the curves in selected area are generally limited (Bonta, 2004).

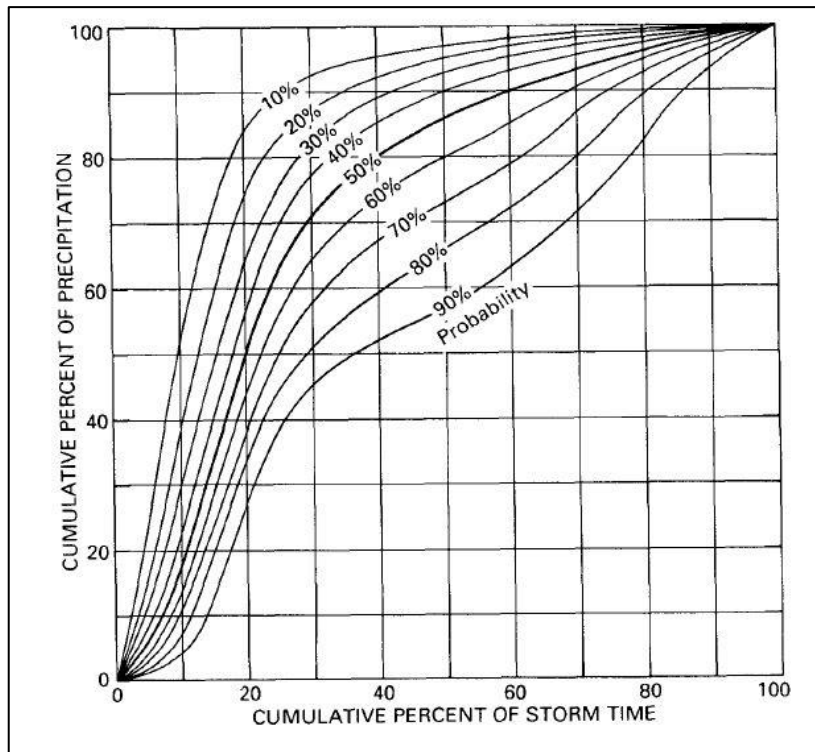


Figure 2.2 Example of Huff curve for time distribution of rainfall in first quartile storms (Huff, 1990)

2.1.1.2 SCS rainfall distributions

The United States Soil Conservation Service (SCS) developed synthetic storm hyetographs for storms of 6-24 hours in duration (Chow *et al.*, 1988). These 24-hour storm duration distribution types are related to the storm type and rainfall produced. Additional distribution types were developed after the original Type I and Type II distributions, to account for regional climatic variation, giving a total of four 24-hour duration storms, as shown in Figure 2.3 (Chow *et al.*, 1988; Knoesen, 2005). The SCS Type II distribution represents high intensity convective storms while less intensive events fall under the Type I distribution (Weddepohl, 1988). Fractional representation of the 24-hour depth values allowed for combination of different return periods into a generalised, single distribution (Weddepohl, 1988).

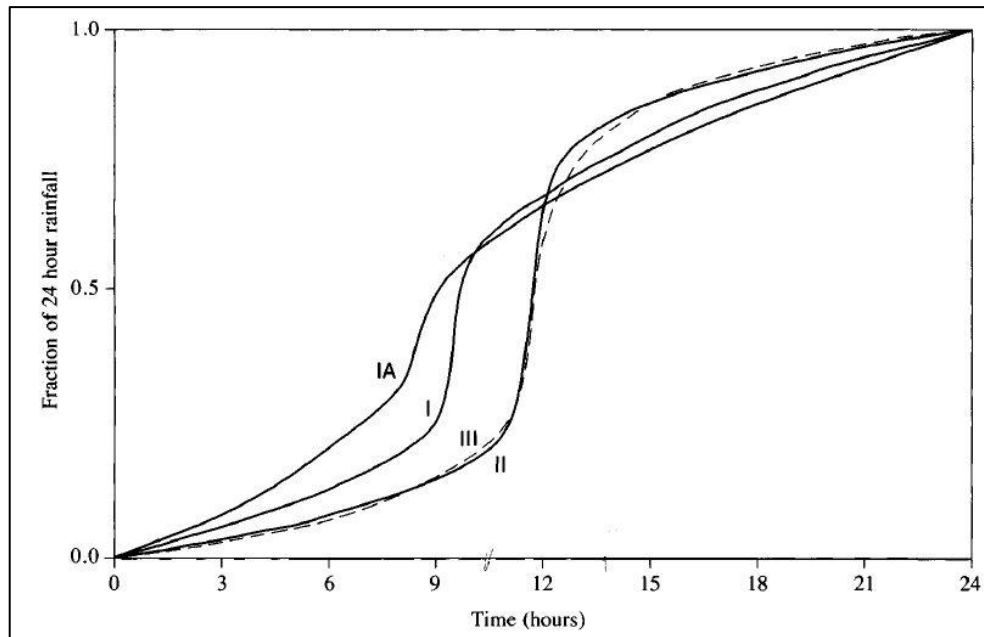


Figure 2.3 SCS 24-hour rainfall hyetographs (Chow *et al.*, 1988)

2.1.1.3 SCS-SA storm temporal distributions

The SCS distributions initially adapted for use in Southern Africa were further developed through inclusion of additional distribution types to account for higher observed intensities (Weddepohl, 1988). Four revised grouped were adopted and regionalised for use in South Africa by Schulze (1984), resulting in the SCS-SA Type 1, 2, 3 and 4 rainfall distributions (Figure 2.4). Similar to the original distributions, frontal rain producing the lowest intensity rainfall is represented by Type 1 while convective thunderstorms, likely to yield the highest design intensities, are represented by Type 4 (Schulze, 1984; Knoesen, 2005). The distributions consist of extreme rainfall depths for each sub-duration centred on the middle of 24-hours, since it is assumed to be unlikely that different duration individual rainfall intensities will correspond to the design intensities (Knoesen, 2005). The SCS-SA regionalised distributions were later further revised by Weddepohl (1988) based on an expanded digitized dataset, enabling countrywide applicability.

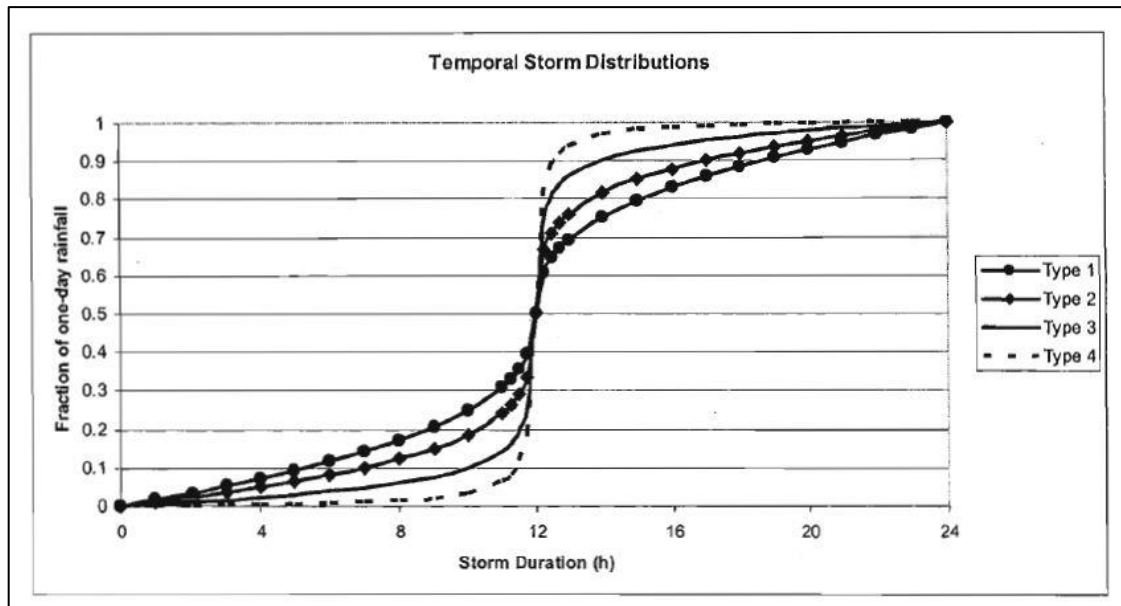


Figure 2.4 Synthetic design rainfall distributions for use in South Africa (Schmidt and Schulze, 1987; cited by Knoesen, 2005)

2.1.1.4 HRU 1/72 time distribution for intermediate durations

The time distribution for intermediate durations (HRU 1/72 method) provides a relationship between percentage of total duration and percentage of total depth. It is similar to the design of the Huff curve approach. However, rather than curves for different percentiles, curves are presented for durations between 2 hours and 24 hours, as shown in Figure 2.5.

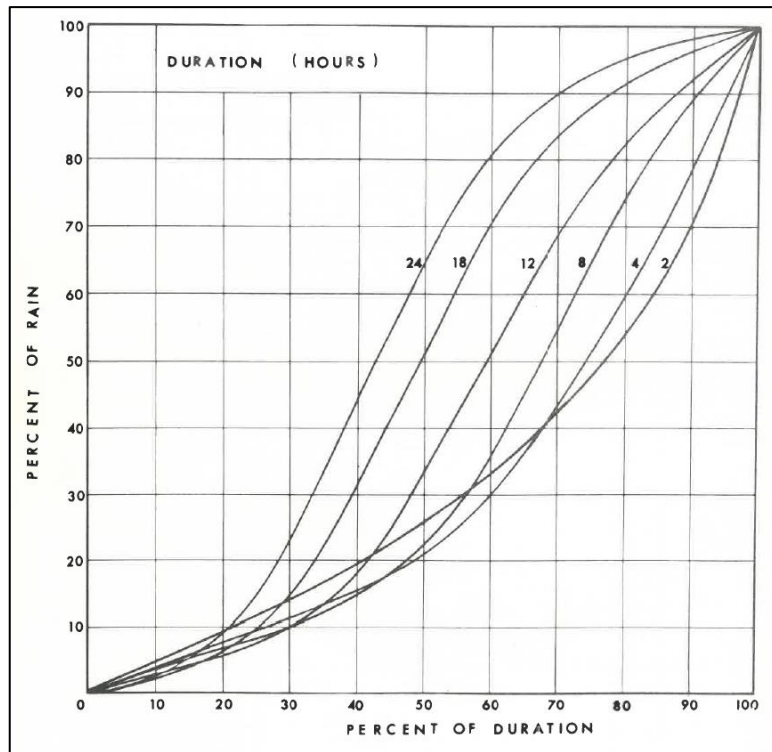


Figure 2.5 Temporal distribution curves for intermediate durations (HRU, 1972)

2.1.1.5 Triangular distribution

The Triangular distribution rests on the concept that any temporal distribution can be determined once precipitation depth P , and duration T_d are found, which allows for the height and base length of the triangle to be calculated (Chow *et al.*, 1988; Knoesen, 2005). A storm advancement coefficient r , which is the ratio of the time before peak t_a to the total storm duration, is used to determine the location of the peak intensity within the distribution, as shown in Figure 2.6 (Chow *et al.*, 1988). This value is computed as the mean of observed values for a series of storms with various durations, weighted according storm event duration. The coefficient also allows for the recession time t_b to be calculated (Knoesen, 2005). It has been shown that triangular hyetographs for heavy storms are nearly identical in shape with factors such as duration and geographic location only possessing secondary influences (Chow *et al.*, 1988). The distribution has been shown to accurately represent natural storms in applications, such as those by Lambourne and Stephenson (1987) in South Africa.

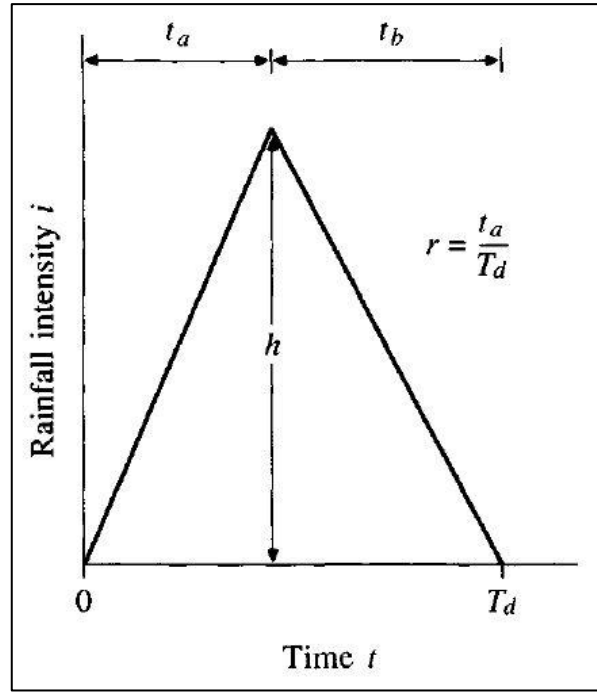


Figure 2.6 General model of the Triangular distribution hyetograph (Chow *et al.*, 1988)

2.1.1.6 Average variability method

The Average Variability Method (AVM) was developed for the determination of design rainfall temporal distributions through analysing various duration intense bursts as opposed to complete storms (Knoesen, 2005). A burst rainfall event is identified for a selected duration and zone and each period within the burst is ranked based on the depth. Following this, the rainfall depth is represented as a percentage of the total depth of the rainfall burst (Green *et al.*, 2005; ARR, 2015). This method is repeated for multiple bursts and the average rainfall percentage is determined for each rainfall period, with a weighting towards larger events, as shown in Figure 2.7 (Pilgrim *et al.*, 1969; Bhuiyan *et al.*, 2010). This averaged pattern is taken as the design rainfall burst temporal pattern for the given duration and zone (ARR, 2015). The approach is conceptually simple and has been previously extensively applied in Australia as a recommended temporal distribution (Green *et al.*, 2005; Knoesen, 2005; Bhuiyan *et al.*, 2010). However, the AVM has been shown to produce unrealistic event temporal patterns, with higher temporal correlations than observed rainfall bursts. This has resulted in its usage being reduced as a recommended distribution in Australia (ARR, 2019).

1	2	3	4	5	6	7	8	9	10	11	12	13	14	15
Date	Rain in mm	Rank	Rain in Each Period-points Period				Rank of Each Period's Rainfall Period				% of Rain in Period of Each Rank			
			1	2	3	4	1	2	3	4	1	2	3	4
20.11.32	176	1	32	48	48	48	4	2	2	2	27	27	27	18
20.03.14	168	2	30	44	44	50	4	2.5	2.5	1	30	26	26	18
29.09.43	166	3	48	46	31	41	1	2	4	3	29	28	25	19
26.10.22	157	4	42	65	35	15	2	1	3	4	41	27	22	10
09.03.13	153	5	18	50	45	40	4	1	2	3	33	29	26	12
25.10.19	150	6	40	27	41	42	3	4	2	1	28	27	27	18
20.11.61	140	7	35	35	35	35	2.5	2.5	2.5	2.5	25	25	25	25
19.01.26	139	8	36	48	40	15	3	1	2	4	35	29	26	11
25.09.51	137	9	44	20	37	36	1	4	2	3	32	27	26	15
15.06.49	133	10	42	40	35	16	1	2	3	4	32	30	26	11
Average							2.55	2.20	2.50	2.75	31	27	26	16
Standard Deviation							1.25	1.11	0.66	1.13	4.6	1.5	1.4	4.8
Assigned Rank							3	1	2	4				
Period							1	2	3	4				
Final Pattern (% of Total Rainfall)							26	31	27	16				

Figure 2.7 Ranking of storms and periods for the AVM (Pilgrim *et al.*, 1969; cited by Bhuiyan *et al.*, 2010)

2.1.1.7 Monobe model

The Monobe model was developed by Na and Yoo (2018) for distributing design rainfall depths obtained from analysis of observed rainfall data in Seoul, Korea. The approach was based on an equation of the distribution of cumulative rainfall R_t (mm) up to a specified time t , as shown in Equation 2.1.

$$R_t = \frac{R_T}{T} \left(\frac{T}{t} \right)^n t \quad (2.1)$$

The design rainfall depth R_T (mm), and rainfall duration T (h) were the main variables in addition to a constant n of an assumed value of 2/3 (Na and Yoo, 2018). The derived rainfall intensity data for development of the temporal distribution was taken as the difference between the cumulative rainfall depths of the current and previous time periods. Once the peak value was located, the second highest rainfall intensity is positioned alternately around the peak, until all intensities are distributed for the storm duration (Na and Yoo, 2018).

2.1.2 Hyetographs derived from intensity-duration-frequency (IDF) relationships

2.1.2.1 Alternating block method

The Alternating Block Method (ABM) is a simplistic approach for utilising an Intensity-Duration-Frequency (IDF) relationship to construct a design rainfall hyetograph (Chow *et al.*, 1988). The storm duration ($T_d = n\Delta t$) is divided into n equal time increments of duration Δt and for a particular return period, rainfall intensity is derived from the IDF curve for each duration ($\Delta t, 2\Delta t, 3\Delta t \dots$) and the corresponding rainfall depth is computed as a product of intensity and duration (Chow *et al.*, 1988; Knoesen, 2005). The rainfall amount to be added for each of the equal time increments Δt is taken as the difference between successive depths, after which they are re-ordered to allow the maximum depth to occur at the centre of the total storm duration T_d (Chow *et al.*, 1988). The remaining incremental depths are then alternately placed in descending order on either side of the maximum depth to form the design hyetograph, as shown in Figure 2.8 (Nguyen *et al.*, 2014). Although simple in design, the ABM has been shown to be effective in representing peak rainfall depths from observed events (Na and Yoo, 2018).

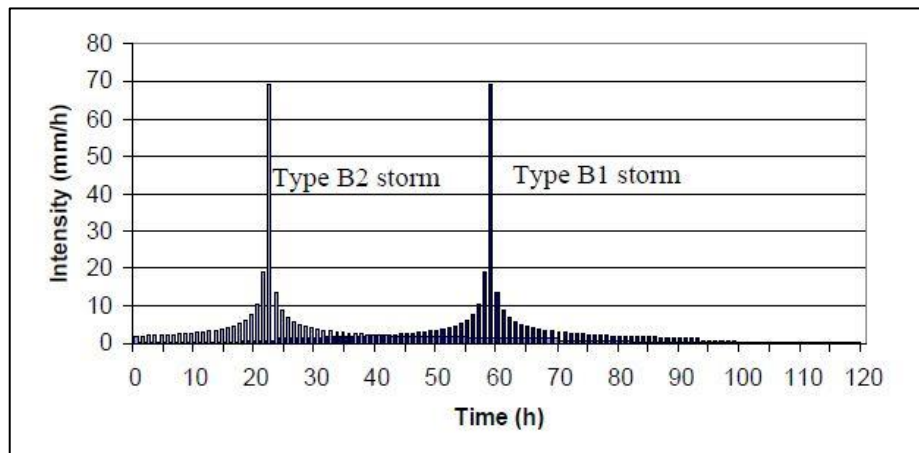


Figure 2.8 Example of design hyetographs derived from the ABM with a 1-hour timestep (Nguyen *et al.*, 2008)

2.1.2.2 Instantaneous intensity method

The Instantaneous Intensity Method (IIM), also known as the Keifer and Chu (1957) method or Chicago design storm is based on the premise that an equation defining an IDF curve or relationship can be used to develop equations for determining temporal variation of intensity in a design hyetograph (Chow *et al.*, 1988). It assumes that rainfall depth for a period of

duration (time interval) around the storm peak T_d is equal to the depth given by the IDF curves, which similar to the ABM approach (Chow *et al.*, 1988; Knoesen, 2005). However, intensity is considered to vary for the entire storm duration, allowing for the location of the peak to change but not the magnitude (Chow *et al.*, 1988). The distribution of alternating rainfall intensities i preceding and succeeding, the peak, t_a and t_b , respectively, are assumed to form a hyetograph, as shown in Figure 2.9. The relationship of these points to T_d is given by Equation 2.2. The approaches employs a storm advancement coefficient r , shown in Equation 2.3, in the same manner as the Triangular distribution (Prodanovic and Simonovic, 2004; Na and Yoo, 2018). The total amount of rainfall R within time T_d is given by the area under the curves in Equation 2.4 (Chow *et al.*, 1988).

$$T_d = t_a + t_b \quad (2.2)$$

$$r = \frac{t_a}{T_d} \quad (2.3)$$

$$R = \int_0^{rT_d} f(t_a) dt_a + \int_0^{(1-r)T_d} f(t_b) dt_b \quad (2.4)$$

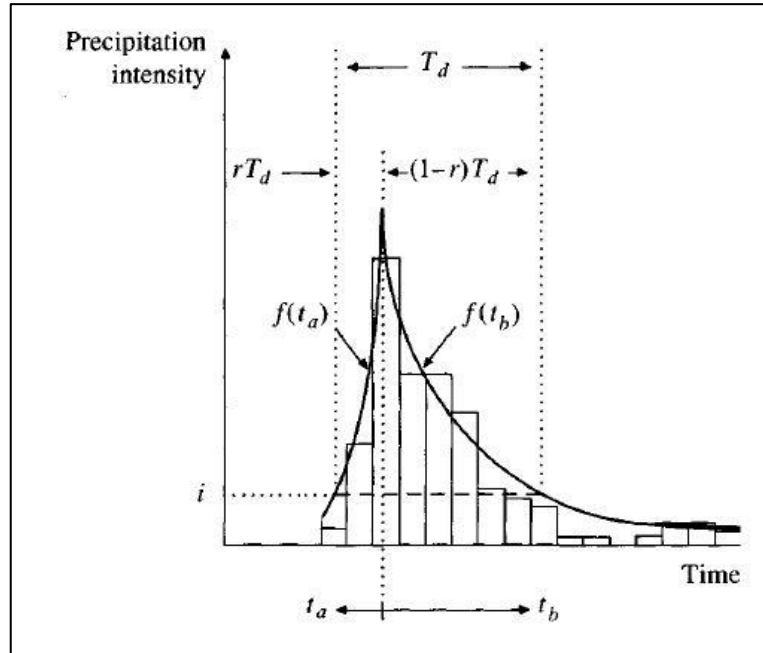


Figure 2.9 Fitting a curve to a hyetograph with the Instantaneous Intensity Method (Chow *et al.*, 1988)

2.2 Disaggregation Models

The second main category of RTD approaches contains mathematical and computational disaggregation models, which can be either stochastic or deterministic in nature. There are a considerable number of stochastic, deterministic and semi-deterministic models which have been applied for RTD. However, only a few of the more commonly applied examples are discussed in this section.

2.2.1 Stochastic Rainfall Temporal Disaggregation models

2.2.1.1 Bartlett-Lewis models

Bartlett-Lewis models are Poisson cluster models which generally represent major observable characteristics of rainfall, including rain-cell clustering within storms in continuous time periods, utilizing simple stochastic assumptions and limited physically-related parameters (Segond *et al.*, 2006). They can be calibrated to different climates, are widely applicable and capable of reproducing important rainfall characteristics at various spatial resolutions (Koutsoyiannis and Onof, 2001). Variants of the original approach described by Rodriguez-Iturbe *et al.* (1987), include the Bartlett-Lewis Rectangular Pulse Model (BLRP), Modified BLRP (MBLRP), Randomized Bartlett-Lewis Model (RBLM) and Bartlett-Lewis Rectangular Pulse Gamma (BLRPG) (Rodriguez-Iturbe *et al.*, 1987; Entekhabi *et al.*, 1989; Glasbey *et al.*, 1995; Koutsoyiannis and Onof, 2001; Smithers and Schulze, 2002; Pui *et al.*, 2012). The general concept of the commonly applied BLRP approach assumes that the occurrence of storm cell origins t_i follows a Poisson process with rate λ . Cell origins t_{ij} of each storm i follow a Poisson process with rate β . Cell arrivals of each storm i are exponentially distributed, with parameter γ , and terminate after a given time v_i . Cells durations w_{ij} are exponentially distributed with parameter η and a uniform intensity X_{ij} for the specific distribution, as shown in Figure 2.10 (Rodriguez-Iturbe *et al.*, 1987; Smithers, 1998; Koutsoyiannis and Onof, 2001). The BLRP model may be considered one of the most widely utilized available stochastic approaches for RTD internationally. It has been shown to adequately represent important statistical rainfall characteristics at different time scales (Smithers and Schulze, 2000; Koutsoyiannis and Onof, 2001). The cluster design permits flexible representation of complex rainfall processes at various time-scales in a fairly simplified manner (Kossieris *et al.*, 2018).

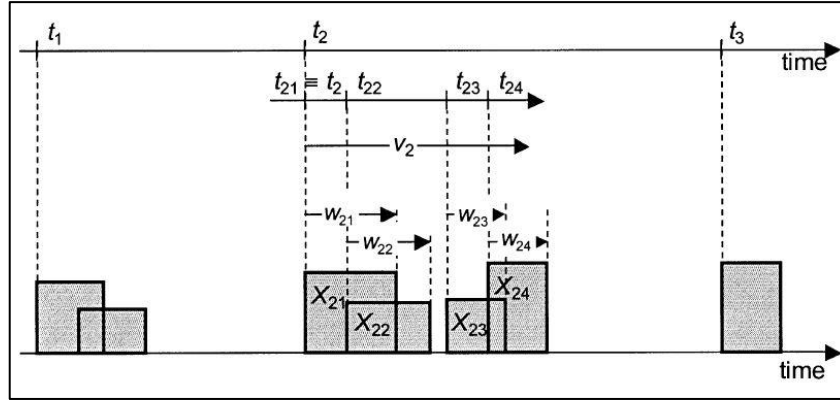
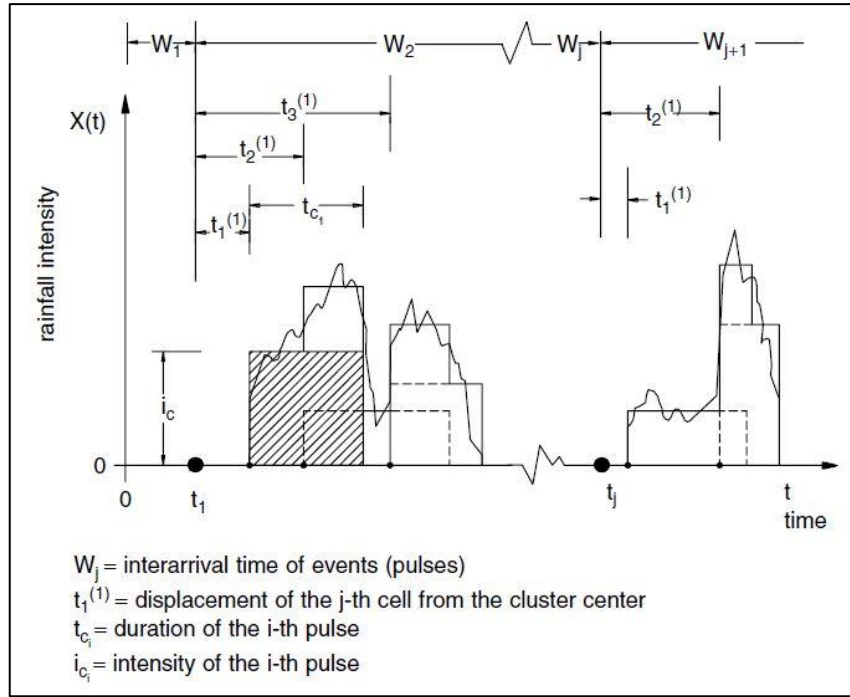


Figure 2.10 Schematic of the BLRP model process (Koutsoyiannis and Onof, 2001)

2.2.1.2 Neyman-Scott models

Neyman-Scott models are similar to Bartlett-Lewis models in that they are Poisson cluster-based and have several variants, depending on the rainfall depth of each rain cell distributed over a specific time period (Cowpertwait, 1991). The cell positions are governed by a set of identically-distributed and independent random variables characterizing time intervals between the storm origin and new cell formation (Entekhabi *et al.*, 1989). The commonly utilised Neyman-Scott Rectangular Pulse (NSRP) model characterises rainfall as a series of storms with individual storms consisting of a set of rectangular pulse cells defining events (Hingray *et al.*, 2002; Frost *et al.*, 2004). The superposition of pulses is used to describe the profile of the storm, as shown in Figure 2.11 (Olsson and Burlando, 2002). NSRP displays natural generalisation of spatial point processes, for design applications requiring spatial representation of processes (Cowpertwait, 1991). Model parameters adequately represent seasonal and climatological characteristics of rainfall-generating mechanisms (Olsson and Burlando, 2002). However, it displays inadequate preservation of dry and wet periods of events, which may potentially be associated with a lack of inherent scaling behaviour in the construction of rectangular pulse models (Entekhabi *et al.*, 1989; Olsson and Burlando, 2002).



The approaches are relatively simplistic and have been extensively applied for generating higher resolution rainfall time series, producing results which adequately matched observed data characteristics (Lisniak *et al.*, 2013; Müller and Haberlandt, 2018). However, the exact nature of the underlying relationship between turbulence and rainfall, is not explicitly clear (Pui *et al.*, 2012). Furthermore, issues of parameter transferability have been noted in semi-arid regions, due to higher inter-annual rainfall variability (Güntner *et al.*, 2001).

2.2.1.4 Method of fragments

The Method of Fragments (MOF) or Analog method is a non-parametric technique which resamples based on a vector of fragments, or analog days, which represent the ratio between sub-daily and daily rainfall at a particular time step. Disaggregated sequences are obtained through multiplication of the available coarser-level values by the designated proportion vector (Li *et al.*, 2018). It does not consider a relationship between continuous and aggregate rainfall (Pui *et al.*, 2012; Carreau *et al.*, 2019). The MOF produces rainfall sequences which display persistence attributes similar to the observed data. This is achieved through maintaining temporal dependence at the daily timescale and employing non-parametric disaggregation logic for creating sub-daily timesteps which also display dependence (Pui *et al.*, 2012). The approach is conceptually simple and has been shown to perform well against other disaggregation approaches such as Poisson cluster models (Carreau *et al.*, 2019). Furthermore, it considers the influence of yearly changes in sub-daily temporal patterns and the magnitude of rainfall (Pui *et al.*, 2012). However, some variations may be considered data-intensive (Li *et al.*, 2018).

2.2.1.5 Regionalized daily rainfall disaggregation model

Knoesen (2005) adapted a daily-to-hourly rainfall disaggregation model developed in Australia by Boughton (2000) for use in South Africa. The original stochastic approach was based on a dimensional hyetograph, and was initially designed for design flood estimation procedures in combination with daily rainfall generators (Boughton, 2000; Knoesen, 2005). A major component of the model involved consideration of the distribution of the fraction of the daily rainfall total occurring in the hour of maximum rainfall R , which indicates the degree of uniformity (Knoesen and Smithers, 2008). These fractions were used to form rainfall clusters, which were organized as random patterns to reproduce possible variations in the daily rainfall distribution (Knoesen and Smithers, 2008). Modification allowed for

reproduction of synthetic hourly rainfalls displaying characteristics of the daily observed rainfall data distributions (Knoesen, 2005; Knoesen and Smithers, 2008). The modified and regionalised model were found to adequately reproduced rainfall statistics at the test stations. However, it was less suited to simulating event characteristics of the phasing properties of rainfall, and at locations with lower fractions of daily rainfall totals occurring in the maximum hour (Knoesen and Smithers, 2008).

2.2.2 Deterministic rainfall temporal disaggregation models

2.2.2.1 The constant model

This highly simple disaggregation approach assumes a constant rainfall intensity for the rain hour (Hingray and Ben Haha, 2005). The disaggregated time steps produced within rain hours are all wet and the model has no parameter. Assessment in producing important rainfall event statistical characteristics found that the Constant model underestimates rainfall variability and extremes (Hingray and Ben Haha, 2005). For 10-minute rainfall, the model gave lower limits of standard deviation, skewness and the peak value for return periods. The model was also found to overestimate 10-minute rainfall autocorrelations and occurrence probability (Hingray and Ben Haha, 2005). Hence it is a simple but relatively poor-performing model for rainfall temporal disaggregation.

2.2.2.2 Ormsbee discrete disaggregation model

Ormsbee (1989) reasoned that historical rainfall data at one-hour time steps were too coarse to adequately represent hydrological response on small catchments. Uniform distributions employed for disaggregation were identified to potentially underestimate peak discharges (Ormsbee, 1989). Hence a discrete disaggregation model, with both a deterministic and stochastic pathway, was developed for improving upon this limitation. The model assumed proportionality between the rainfall distribution within the central hour t of a 3-hour moving sequence and the hourly distribution over the 3-hour sequence, as shown in Figure 2.12. This allowed for disaggregation of hourly rainfall volumes into three 20-minute volumes V_t^1 , V_t^2 , V_t^3 (Ormsbee, 1989). The 20-minute rainfall volumes are expressed as fractions of the total volume V_T , as given by Equation 2.6. The central hour volume can be disaggregated into 20-minute rainfall volumes as shown in Equations 2.7, 2.8 and 2.9, and the rainfall intensities are then determined by division of the rainfall volume by the disaggregation time interval (Ormsbee, 1989).

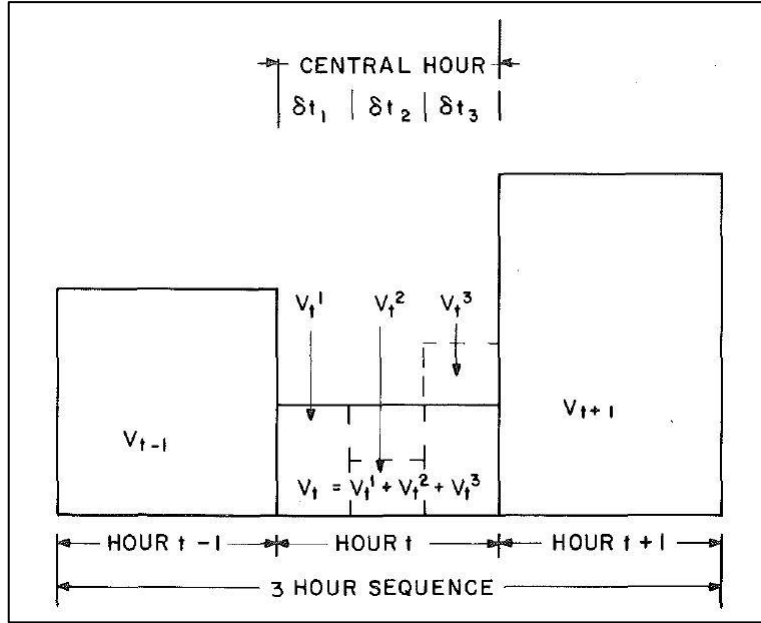


Figure 2.12 Discrete disaggregation model (Ormsbee, 1989)

$$V_T = V_{t-1} + V_t + V_{t+1} \quad (2.6)$$

$$V_t^1 = V_t * \left(\frac{V_{t-1}}{V_T} \right) \quad (2.7)$$

$$V_t^2 = V_t * \left(\frac{V_t}{V_T} \right) \quad (2.8)$$

$$V_t^3 = V_t * \left(\frac{V_{t+1}}{V_T} \right) \quad (2.9)$$

2.2.2.3 Ormsbee continuous disaggregation model

The Continuous Disaggregation Model developed by Ormsbee (1989) was based on a continuous distribution approach, applicable for disaggregating to time intervals of 1-30 minutes. The rainfall volume is deterministically distributed, in a similar approach to the Discrete Disaggregation model, allowing for the distribution in each hour to be explicitly defined according to rainfall sequence types. A rainfall sequence index table is used to define the rainfall sequence type in the first hour of the continuous sequence (Ormsbee, 1989). Following this, the central hour is then disaggregated into T time intervals of δt minutes,

among which the total volume of rainfall for the central hour V_t is distributed, as shown in Equation 2.10. The probability associated with each time interval $P(\delta t_i)$ is determined using Equations 2.11a, 2.11b and 2.12, with t^* being the time parameter for different rainfall sequence types. The expanded set of equations can be found in Ormsbee (1989). After complete distribution of the total volume for the hour, the process is repeated for the next hour containing measurable rainfall (Ormsbee, 1989).

$$V_t^i = V_t * P(\delta t_i), \text{ for } i = 1, \dots, T \quad (2.10)$$

$$F(t) = \frac{V_{t-1}t}{V_t^*} - \frac{(V_{t-1}-V_t)t^2}{2V_t^*t^*}, \text{ for } 0 \leq t < t^* \quad (2.11a)$$

$$F(t) = \frac{(V_t+V_{t-1})t^*}{2V_t^*} + \frac{V_t(t-t^*)}{V_t^*} - \frac{(V_t-V_{t+1})(t-t^*)^2}{2V_t^*(60-t^*)}, \text{ for } t^* \leq t \leq 60 \quad (2.11b)$$

$$P(\delta t_i) = P(t_{i-1} \leq \tau \leq t_i) = F(t_i) - F(t_{i-1}) \quad (2.12)$$

2.2.2.4 Chaotic approach to rainfall temporal disaggregation

Deterministic chaos is the notion that seemingly irregular behaviour in simple deterministic systems may be a result of the influence of non-linear interdependent variables (Sivakumar *et al.*, 2001). Sivakumar *et al.* (2001) identified that stochastic approaches generally display disconnection between model structure and the underlying physics of rainfall processes. A new framework utilizing the concept of deterministic chaos was proposed to firstly study transformation between rainfall temporal scales, and improve upon the limitations of stochastic approaches (Sivakumar *et al.*, 2001). A simple chaotic disaggregation model was formulated and applied. The approach could be used to take a rainfall series X_i , with values $i = 1, 2, \dots, N$ at temporal resolution T_1 , and obtain values for series $(Z_i)_k$, where $k = 1, 2, \dots, p$ at a higher resolution T_2 , with $p = (T_1/T_2)$. It is assumed that the values of series X_i are distributed into series $(Z_i)_k$ according to Equations 2.13 and 2.14, with $(W_i)_k$ as the distributions of weights of X_i to $(Z_i)_k$. An additional assumption is that information regarding the historical distribution of weights and time series is available, in order to determine the future distributions of the weights and series values, with $i = n + 1, \dots, N$, and N always being equal to the total number of points. The initial step for determining the distribution of weights $(W_{n+1})_k$ involves the reconstruction of the time series for X_i , $i = 1, 2, \dots, n + 1$ for resolution

T_1 using Equation 2.15. The second step involves assuming a functional relationship between the vectors Y_j as shown in Equation 2.16, with F_T derived using the local approximation method. Disaggregation of X_{n+1} is performed based on Y_j and its neighbours, which are given by the minimum values of $\|Y_j - Y_j\|$. The expanded set of equations and variates can be found in Sivakumar *et al.* (2001).

$$(Z_i)_k = (W_i)_k X_i \quad (2.13)$$

$$\sum_{k=1}^p (W_i)_k = 1 \quad (2.14)$$

$$Y_j = (X_j, X_{j+\tau}, X_{j+2\tau}, \dots, X_{j+(m-1)\tau}), \text{ for } j = 1, 2, \dots, (n+1) - (m-1)\tau/\Delta t \quad (2.15)$$

$$Y_{j+T} = F_T(Y_j) \quad (2.16)$$

The model performed reasonably well and seemed more suited to the application than a stochastic framework. However, there was need for further study on the occurrence of chaos in rainfall data (Sivakumar *et al.*, 2001). Other studies which have discussed chaotic approaches have labelled them as controversial, due to the assumptions utilised and limited available literature on applications (Rodriguez-Iturbe *et al.*, 1987; Koutsoyiannis, 2003; Segond *et al.*, 2006).

2.3 Summary of Methods

The applications of the above approaches and the key findings describing their characteristics are summarized in Table 2.1 for comparison of their strengths and weakness.

Table 2.1 Selected case studies for rainfall temporal disaggregation approaches

Category	Approach	Case study	Location	Key findings
Hyetographs derived from storm event analysis	Huff Curves	Huff and Angel (1992)	Nine states in the USA	<ul style="list-style-type: none"> Curves developed from a dense raingauge network were applicable over nine states because of similar climate and rainfall.
		Bonta (2004)	USA	<ul style="list-style-type: none"> Curves can be developed using point data. Potential for regionalisation; a single set can be applied over a large area.
	Triangular Distribution	Lambourne and Stephenson (1987)	Vanderbiljpark, South Africa	<ul style="list-style-type: none"> Triangular hyetograph was adequate for design applications. More accurately represents natural storms than Chicago and Uniform distributions.
	AVM	Green <i>et al.</i> (2005)	Australia	<ul style="list-style-type: none"> An unsmoothed single design pattern AVM temporal distribution for design flood applications should be based on the 10 highest events for a duration Approach is still applicable for estimating probable maximum floods despite higher intensity distributions being available.
		Bhuiyan <i>et al.</i> (2010)	Australia	<ul style="list-style-type: none"> AVM for determining design rainfall temporal patterns successfully showed climate change-related changes in regional rainfall temporal patterns since original derivation

Category	Approach	Case study	Location	Key findings
Hyetographs derived from storm event analysis	The Monobe Model	Na and Yoo (2018)	Seoul, Korea	<ul style="list-style-type: none"> Model overestimates rainfall peaks in comparison to ABM, Huff curves and the IIM May be useful in design calculations where over-design is intended for safety but requires testing under different climatic conditions.
Hyetographs derived from IDF relationships	ABM	Na and Yoo (2018)	Seoul, Korea	<ul style="list-style-type: none"> Approach was the best suited for estimation of annual maximum rainfall events that closely matched observed rainfall data.
	IIM	Marsalek and Watt (1984)	Canada	<ul style="list-style-type: none"> Unrealistic temporal distribution due to assumption that the design storm contains all maximum intensities for the various durations. Design hyetograph should consider antecedent conditions during computation. Inadequate for application for development of design storms for Canadian rainfall data.
		Na and Yoo (2018)	Seoul, Korea	<ul style="list-style-type: none"> In comparison to the Alternating Block Method, Huff curves and Monobe model, the approach was the most accurate in producing peak values close to observed data.
Stochastic Models	BLRP model	Koutsoyiannis and Onof (2001)	London, UK Arizona, USA	<ul style="list-style-type: none"> Model could generate hourly-level data capable of aggregating to observed daily totals. Approach was applicable in cases where limited hourly data was available for fitting. Performed well in maintaining statistical properties of the rainfall process, including proportions of dry and wet period, coefficients of variation and skewness of rainfall intensities.

Category	Approach	Case study	Location	Key findings
Stochastic Models	BLRPG and MBLRP models	Smithers <i>et al.</i> (2002)	South Africa	<ul style="list-style-type: none"> • Historical data statistics were well replicated by both models. • Design rainfall events estimated by BLRPG model were more accurate. • Derivation of BLRPG parameters using only available daily data allows for estimation of short-duration data values down to 1-hour time frames.
	NSRP model	Frost <i>et al.</i> (2004)	Multiple Australian cities	<ul style="list-style-type: none"> • Model adequately reproduced rainfall characteristics of observed pluviograph data records. • Less capable of reproducing wet-spells and dry-spells, possibly due to the range of statistics for which it is calibrated.
	RMC model	Güntner <i>et al.</i> (2001)	Brazil UK	<ul style="list-style-type: none"> • Highly accurate in reproducing rainfall characteristics at an hourly time step, with performance being generally better for semi-arid tropical rainfall. • Extreme values were accurately estimated in Brazil, while overestimated in the UK temperate climate.
	RMC, Microcanonical and Canonical models	Pui <i>et al.</i> (2012)	Australia	<ul style="list-style-type: none"> • For daily-to-hourly disaggregation, canonical approach underestimated extreme rainfall values while microcanonical generally overestimated. • Models performed reasonably well in simulating statistical rainfall properties such as the mean values and dry periods but not as well as MOF

Category	Approach	Case study	Location	Key findings
Stochastic Models	MOF	Pui <i>et al.</i> (2012)	Sydney, Perth, Cairns and Hobart in Australia	<ul style="list-style-type: none"> For daily-to-hourly disaggregation, MOF performed better than other models such as RMC and RBLM in preserving important rainfall event statistical characteristics as well as estimating extreme values.
		Li <i>et al.</i> (2018)	Singapore China	<ul style="list-style-type: none"> MOF approaches were capable of reproducing characteristics of site-specific historical rainfall data. Regionalised and multi-site approaches were found to better represent annual extremes and antecedent precipitation values, making them more viable for capturing the variability in the historical rainfall data.
Deterministic models	Constant model	Hingray and Ben Haha (2005)	Lausanne, Switzerland	<ul style="list-style-type: none"> Underestimates rainfall variability and extremes. Overestimates autocorrelations and occurrence probability.
	Ormsbee discrete disaggregation model	Hingray and Ben Haha (2005)	Lausanne, Switzerland	<ul style="list-style-type: none"> Underestimates rainfall variability and extremes. Overestimated autocorrelations at 10-minute timesteps. Model may be unsuitable when these need to be maintained at high resolution timesteps.
	Ormsbee continuous disaggregation model	Ormsbee (1989)	West Virginia and Kentucky, USA	<ul style="list-style-type: none"> Model adequately predicts first three rainfall moments. Performance is improved with 15-minute data. Employing synthetic distributions instead of average distributions produced more accurately predicted peak flow frequencies.
	Chaotic approach	Sivakumar <i>et al.</i> (2001)	Mississippi, USA	<ul style="list-style-type: none"> Model was found to yield reasonable disaggregation results. Chaotic framework seemed to be more suitable for modelling temporal scale transformation dynamics than a stochastic framework.

2.4 Chapter Discussion and Conclusions

Improving the accuracy of design flood estimates and other forms of hydrological and climatological modelling, may require the use of data at finer resolutions than the traditional daily timestep. However, a point of concern is the relatively limited availability of sub-daily rainfall data, in comparison to daily data, both internationally and locally. As a result, RTD approaches have been applied to generate finer resolution data from coarser resolution data and to extend data records. Relative to international research and development, such approaches available for use in South Africa may be considered limited in terms of the variety which have been applied and adapted in the past. Hence, there is potential for updating approaches used, through review of newer approaches applied internationally and assessing their viability for adoption for disaggregation of available daily rainfall to derive realistic temporal distributions of rainfall.

The RTD approaches identified through review of the literature on the subject, could be broadly classified as either rainfall distribution curves or disaggregation models. A given disaggregation approach which is applied should ideally formulate a hyetograph which can give a realistic representation of sub-daily rainfall. The applied approach should disaggregate the daily values to the sub-daily level, while maintaining the characteristics of the rainfall process and the increments being able to be summed back up to the daily total.

Rainfall distributions are used in design and modelling applications for determining the distribution of rainfall depths or intensities throughout the duration of a storm. These synthetic distributions may be used to derive hyetographs and determine the location of peak discharges within the storm duration. While the approaches may require substantial historical records in certain cases, some could be adapted for use with observed daily data with short record lengths. Furthermore, approaches such as the Huff curves and AVM have shown potential for regionalisation. Therefore, curves could be developed and possibly regionalised based on general storm patterns for use in disaggregating daily rainfall into sub-daily incremental intensity values.

Stochastic model approaches generally simulate hourly-level data using statistical parameters derived from the observed daily data. An element of randomness is included in sampling procedures. Therefore, despite their proven adequacy for producing sub-daily data capable of aggregation to daily-level, such approaches may not be suitable for production of

realistic hyetographs with sub-daily increments. However, since rainfall processes are, by nature, complex, it is unlikely that a model will be able to completely and accurately describe event characteristics. Hence, the use of stochastic models which may produce results similar to observed data, is still justifiable. Furthermore, such approaches are highly applicable to continuous simulation modelling in which the aim is to exhaustively simulate potential outcomes for rainfall event processes. Deterministic model RTD approaches are less commonly applied than stochastic models or distribution approaches, due to their parameters being more physically-related to rainfall processes, which in some cases, are difficult and time-consuming to derive. Therefore, the variety of models identified was comparatively limited. As previously mentioned, the rainfall process is highly complex, dynamic and difficult to accurately represent with limited data. Therefore, an approach which considers deterministic chaos may more accurately represent rainfall physical characteristics than a purely stochastic or deterministic method.

Several commonly applied disaggregation approaches were identified. The case studies reviewed provided general indications of the strengths and weaknesses of each approach under which contexts they may be the most applicable. Approaches which have been successfully applied in South Africa include the SCS-SA distributions, Triangular distributions, Huff Curves, BLRP models and an adapted semi-stochastic regionalised disaggregation model. These approaches fell into the categories of rainfall distributions and stochastic models. Other approaches which were reviewed that have not seen substantial application in South Africa include the AVM, Ormsbee discrete and continuous models, Chaotic approach and MOF. The AVM was previously extensively applied in Australia, which has a similar climate to South Africa, as a recommended temporal distribution. The Ormsbee discrete and continuous deterministic disaggregation models, while not extensively applied, are applicable for disaggregation of hourly data to sub-hourly data. The Chaotic approach discussed may be considered semi-deterministic and more accurate than stochastic frameworks in some cases. Internationally, the MOF approach has shown to perform well in disaggregating with adequate reproduction of rainfall trends and could be used if appropriately developed for local conditions. The above models and their applications internationally have shown promising results and could be adapted for use in South Africa.

The focus of this study is the disaggregation of daily rainfall data into sub-daily data. Furthermore, approaches which are utilised should ideally be relatively simplistic in terms

of input parameters, while producing sub-daily data that results in realistic temporal distributions. In addition, the approaches which are found to perform well should display potential to be recommended for future research into regionalisation. Based on the literature review and case studies, the approaches which appear most suited to the aims of this study are the Huff curves, HRU 1/72 Distributions, SCS-SA, Triangular Distribution, AVM and the Knoesen Semi-stochastic model.

The methodology for selection of data for application of the approaches and the general methodology for assessment of the performance of the RTD approaches is detailed in Chapter 3. The methodology for application of these approaches and the adaptations, where necessary, for disaggregation of daily rainfall data are described in Chapter 4, which includes the results of the pilot study.

3. GENERAL METHODOLOGY

3.1 Approach

A pilot study was used to develop procedures to apply the methods and to develop performance indices to assess and compare the performance of the methods. This chapter outlines the selection of rainfall station data for use in application of the RTD approaches. In the pilot study, rainfall data from Station C161 in the UKZN research catchments database was utilised for development of the methodology for application of the approaches and assessment of results. Details on the methodology and results of the pilot study are contained in Chapter 4. Thereafter, the RTD approaches were applied to daily rainfall data from the additional 14 stations using the same methodology utilised in the pilot study. Results of this application are presented in Chapter 5.

3.2 General Methodology

The digitised rainfall data was used to delineate daily rainfall for 24-hour periods from 08:00 to 08:00 the following day. The identified and delineated rainfall days were analysed for characteristics in rainfall peak intensity (mm.h^{-1}), total depths (mm), and time to peak as a fraction of the total duration. RTD approaches selected from the literature outlined in Chapter 2 were applied to the daily rainfall data. The daily rainfall total depths were disaggregated to produce hyetographs, and these were then compared to the hyetographs from the observed daily rainfall data. Huff curves were generated from the observed and disaggregated rainfall hyetographs. These provided general distributions of rainfall and served as the basis for comparison of the observed and disaggregated rainfall distributions.

It should be noted that some of the disaggregation approaches were modified for application on daily rainfall. The modifications were made according to the following assumptions:

- Data which was provided in the digitised database was accurate. It was evident that long periods of low rainfall values displayed may be an artefact of the digitisation and interpolation procedure between two digitised points used for the derivation of the rainfall depths from the original rainfall chart data.
- It is acknowledged that not all of the RTD approaches selected for application are designed for application on daily rainfall data as obtained from the rainfall stations used

in this study. Therefore, the methods were either applied directly or in a modified manner, as detailed in Chapter 4.

- Huff curves provide smoother distributions than actual rainfall temporal distributions.

3.3 Data Utilised

Rainfall data was obtained through the CWRR - University of KwaZulu-Natal research catchments database, which includes data extracted from breakpoint digitized autographic rainfall charts from historical research sites and historical data previously supplied by SAWS (Smithers and Schulze, 2001). One station was randomly selected from each of the 15 relatively homogenous extreme rainfall clusters identified by Smithers (1998) and Smithers and Schulze (2000). The data for each station were inspected to determine if the record was of sufficient length and if the record was relatively continuous, without extensive periods of missing values. When a selected station was found to be unsuitable, another station was randomly selected for the cluster. This was repeated until 15 stations were obtained. The locations of the selected stations are detailed in Figure 3.1 and the characteristics of the selected stations are summarised in Table 3.1.

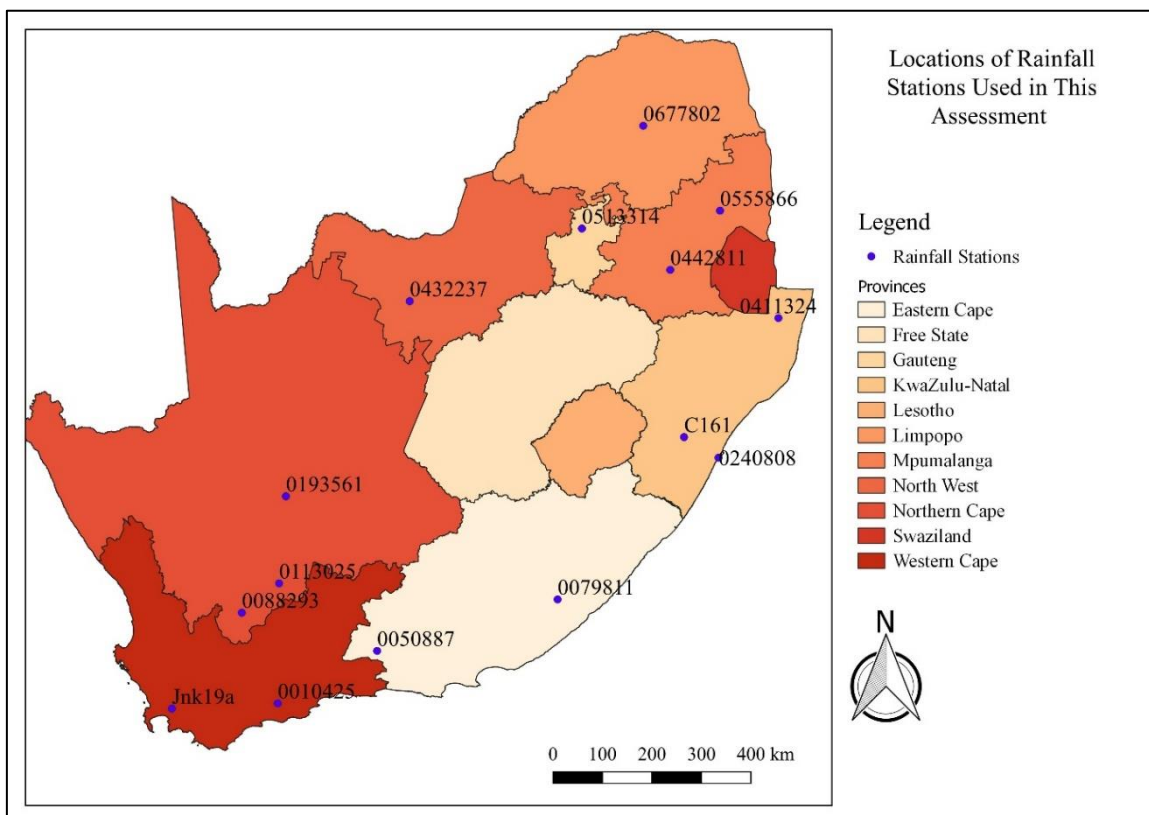


Figure 3.1 Locations of rainfall stations utilised in this study

Table 3.1 Characteristics of rainfall stations used in this assessment

Station Number	Quaternary Catchment	SCS Rainfall Zone	Homogenous cluster (Smithers, 1998)	Coordinates (longitude, latitude)	Altitude (m)	MAP (mm)	Record (start – end)	Available record (years)
0513314	A23D	3	1	28° 10' 59.88", -25° 43' 59.88"	1330	674	1964/11/01 - 1992/06/13	29
0555866	X22J	2	2	30° 58' 59.88", -25° 25' 59.88"	671	752	1973/05/02 - 1992/10/30	20
C161	U20H	3	3	30° 13' 37.92", -29° 35' 12.84"	1340	974	1976/11/23 - 1991/04/09	15
0193561	D54	3	4	21° 49' 0.12", -30° 21' 0"	962	175	1962/01/03 - 1996/06/01	35
0677802	A71A	2	5	29° 27' 0", -23° 52' 0.12"	1230	458	1954/01/03 - 1992/11/25	39
Jnk19a	G22F	2	6	18° 56' 56.04", -33° 58' 21"	282	1095	1944/10/01 - 1995/12/31	52
0411324	W45A	2	7	32° 10' 59.88", -27° 24' 0"	73	571	1966/08/06 - 1981/11/30	16
0240808	U60D	2	8	30° 57' 0", -29° 58' 0.12"	8	986	1957/01/06 - 1992/11/26	36
0010425	H90C	2	9	21° 15' 0", -34° 4' 59.88"	137	377	1985/07/01 - 1996/06/01	12
0050887	L30A	2	10	23° 30' 0", -33° 16' 59.88"	840	233	1960/02/15 - 1996/06/01	37
0442811	C11F	3	11	29° 58' 0.12", -26° 31' 0.12"	1694	722	1969/11/02 - 1996/05/17	28
0113025	D55E	3	12	21° 31' 0.12", -31° 55' 0.12"	1264	181	1957/01/01 - 1996/05/31	40

Station number	Quaternary catchment	SCS Rainfall Zone	Homogenous cluster	Coordinates (longitude, latitude)	Altitude (m)	MAP (mm)	Record (start – end)	Available record (years)
0079811	S60C	2	13	27° 28' 0.12", -32° 31' 0.12"	899	752	1964/01/01 - 1996/06/01	33
0432237	C32B	3	14	24° 37' 59.88", -26° 57' 0"	1234	437	1961/01/02 - 1996/05/28	36
0088293	D51A	3	15	20° 40' 0.12", -32° 22' 59.88"	1459	339	1959/09/01 - 1996/05/31	38

3.3.1 Characteristics of rainfall data

Rainfall days were identified from the 15-minute data available for the selected rainfall stations. Daily rainfall was computed for periods between 08:00 to 08:00 the next day, as per the standard timeframe used in South Africa. Furthermore, following the methodologies in studies such as Huff (1967) and Walker and Tsubo (2003), rainfall days with total depths less than 10 mm were excluded in the assessment. Rainfall days were sorted into depth ranges. The distribution of rainfall days in each depth range per station can be seen in Figure 3.2.

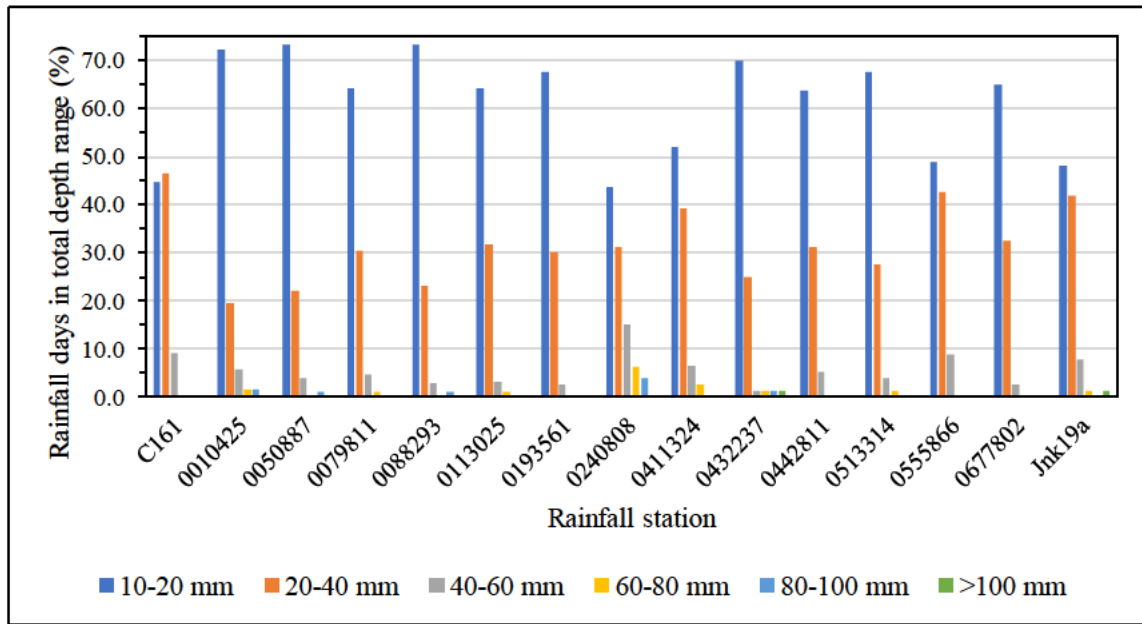


Figure 3.2 Percentage of rainfall days with daily total depths in each range per station

It can be seen that the majority of rainfall days have total depths in the 10-20 mm and 20-40 mm ranges for all stations. The temporal distributions of rainfall on these rainfall days will therefore have a greater influence on the generalised temporal distributions produced for each rainfall station.

The quartile in which the peak of the rainfall occurs is a representation of the period of the rainfall day in which the highest rainfall intensity occurs. The quartiles can be determined by dividing the total duration into four quarters, giving the first, second, third and fourth quartiles. Early peaking rainfall days would display a peak intensity in the first or second quartiles while, later peaking rainfall days would display peaks in the third or fourth

quartiles. The distribution of the percentage of rainfall days which display peaks in each quartile thus influences the shape of the set of dimensionless Huff curves produced. The percentage of rainfall days with peak intensities in each quartile for each station can be seen in Figure 3.3.

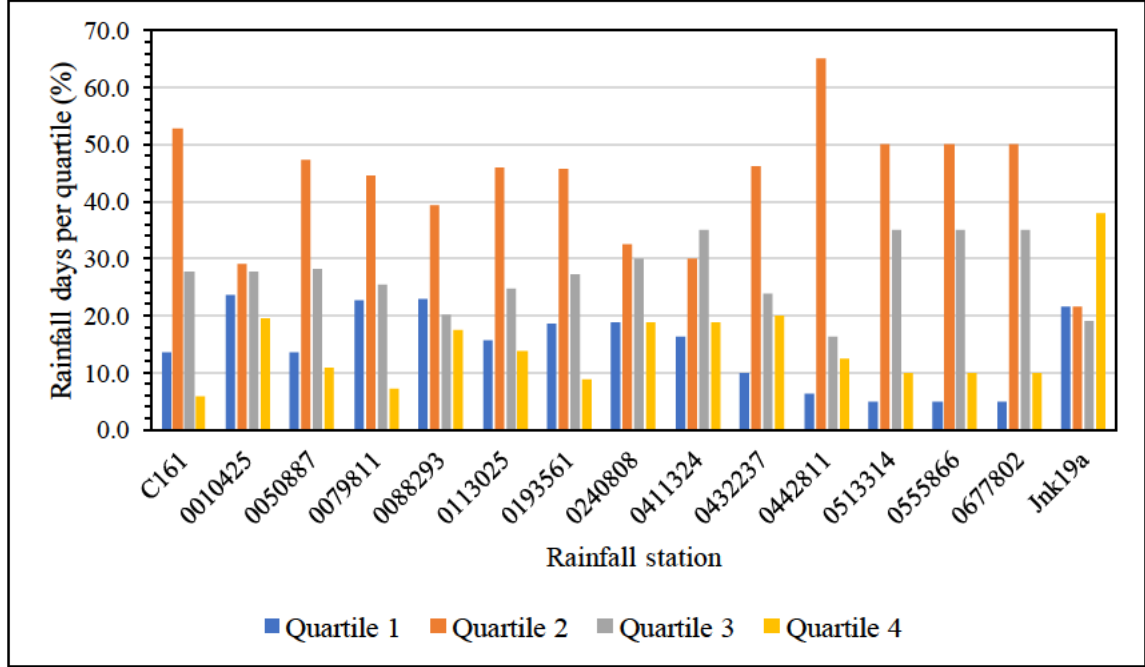


Figure 3.3 Percentage of rainfall days with peak intensities in each quartile per rainfall station

The majority of rainfall days for the selected stations display peaks in the second quartile of their respective durations. The second highest concentration is in the third quartile peaking. Hence, the generalised temporal distributions of rainfall produced are likely to display a higher proportion of rainfall in the middle to later sections of the duration.

3.3.2 Assessment of the performance of the RTD methods

3.3.2.1 Mean Absolute Relative Error (MARE)

The performance of the disaggregation approaches was determined through analysis of Huff curves produced using the observed 15-minute data and disaggregated daily data. The Mean Absolute Relative Error (MARE), a single value which quantifies the performance of disaggregation approaches and distributions was used as a measurement of the difference between a percentile Huff curve generated from the disaggregated daily data and the percentile curve derived from the observed 15-minute data, as shown in Equation 3.1. The

total MARE (Σ MARE) represents the total value for all percentiles and is given by Equation 3.2.

$$\text{MARE}_j(\%) = \frac{\sum_{n=0.1}^S |X_n - D_n|}{S} * 100 \quad (3.1)$$

$$\Sigma \text{MARE}(\%) = (\text{MARE}_{10\text{th}} + \text{MARE}_{20\text{th}} + \dots + \text{MARE}_{90\text{th}}) \quad (3.2)$$

where:

j = percentile (10th, 20th, ..., 90th),

X_n = observed dimensionless depth at dimensionless time = n ,

n = dimensionless duration fraction (0.1, 0.2, ... 1.0),

D_n = disaggregated dimensionless depth at dimensionless time step = n , and

S = number of dimensionless duration fraction values.

3.3.2.2 Nash-Sutcliffe efficiency (NSE)

The Nash-Sutcliffe efficiency (NSE) is a normalised statistic which can be used to indicate how well the plot of observed versus simulated data fits the 1:1 line (Moriasi *et al.*, 2007). The NSE is utilised in addition to the MARE to determine the performance of the disaggregation approaches, by means of comparison of observed and disaggregated Huff curve increments. The NSE ranges between $-\infty$ and 1.0, with a value of 1.0 being the optimal value. Values between 0.0 and 1.0 are considered acceptable levels of performance (Moriasi *et al.*, 2007). The NSE is determined according to Equation 3.3.

$$\text{NSE} = \left[\frac{\sum_{i=1}^n (Y_i^{\text{obs}} - Y_i^{\text{sim}})^2}{\sum_{i=1}^n (Y_i^{\text{obs}} - Y^{\text{mean}})^2} \right] \quad (3.3)$$

where:

Y_i^{obs} = the i^{th} observation for the constituent being evaluated,

Y_i^{sim} = the i^{th} simulated value for the constituent being evaluated,

Y^{mean} = the mean of observed data for the constituent being evaluated, and

n = the total number of observations.

3.3.2.3 Percent Bias (PBIAS)

The peak intensity values of the observed and disaggregated rainfall days are also compared. In addition to Pearson correlation (r) values, the Percent Bias (PBIAS) statistic was utilised. PBIAS can be used to determine the average tendency of simulated, in this case disaggregated, values to be larger or smaller than the observed data values (Moriassi *et al.*, 2007). The optimal value of PBIAS is 0.0. Positive values indicate model underestimation bias, and negative values indicate model overestimation bias. PBIAS is determined according to Equation 3.4.

$$PBIAS (\%) = \left[\frac{\sum_{i=1}^n (Y_i^{obs} - Y_i^{sim}) * 100}{\sum_{i=1}^n (Y_i^{obs})} \right] \quad (3.4)$$

where:

Y_i^{obs} = the i^{th} observation for the constituent being evaluated,

Y_i^{sim} = the i^{th} simulated value for the constituent being evaluated, and

n = the total number of observations.

Chapter 4 which follows details the relationships between rainfall day parameters which were identified, and the methodology used for application of each RTD approach. The results from the applications are described as well as a comparison between the results of each approach.

4. APPLICATION OF RTD APPROACHES: PILOT STUDY

This chapter details the methodology used in the pilot study for application of disaggregation approaches to daily rainfall data as well the results of assessment of performance. RTD approaches were selected from those identified from the literature review, contained in Chapter 2, on the basis of the following criteria:

- a) Ease of application with the available data in terms of the number of input parameters required.
- b) Reported performance in case studies, both in South Africa and internationally.
- c) Potential for regionalisation and suitability to daily rainfall data.

Based on the above criteria, the following RTD models and distributions were selected for assessment in this study:

- Huff Curves as a means of comparing observed and disaggregated distributions
- SCS-SA Rainfall Distributions,
- HRU 1/72 24-hour distribution,
- Triangular Distribution,
- Average Variability Method (AVM),
- Knoesen Semi-stochastic Disaggregation model

4.1 Data used in pilot study

Rainfall Station C161 located at Cedara, KwaZulu-Natal was selected for use in the pilot study to develop the methodology for application of the RTD approaches and assess their performance. The pilot study involved assessment of the suitability of the selected RTD approaches for application on daily rainfall.

Daily rainfall depths were computed from the Station C161 data using the 15-minute data available. Daily rainfall was computed for periods between 08:00 to 08:00 the next day. Furthermore, following the methodologies in studies such as Huff (1967) and Walker and Tsubo (2003), rainfall days with total depths less than 10 mm were excluded in the assessment, resulting in a total of 110 rainfall days for use in the assessment. Rainfall days were analysed to determine characteristics and relationships between the depth ranges, daily peak intensities, and the general temporal distribution of rainfall as can be seen in Figure 4.1, Figure 4.2 and Figure 4.3.

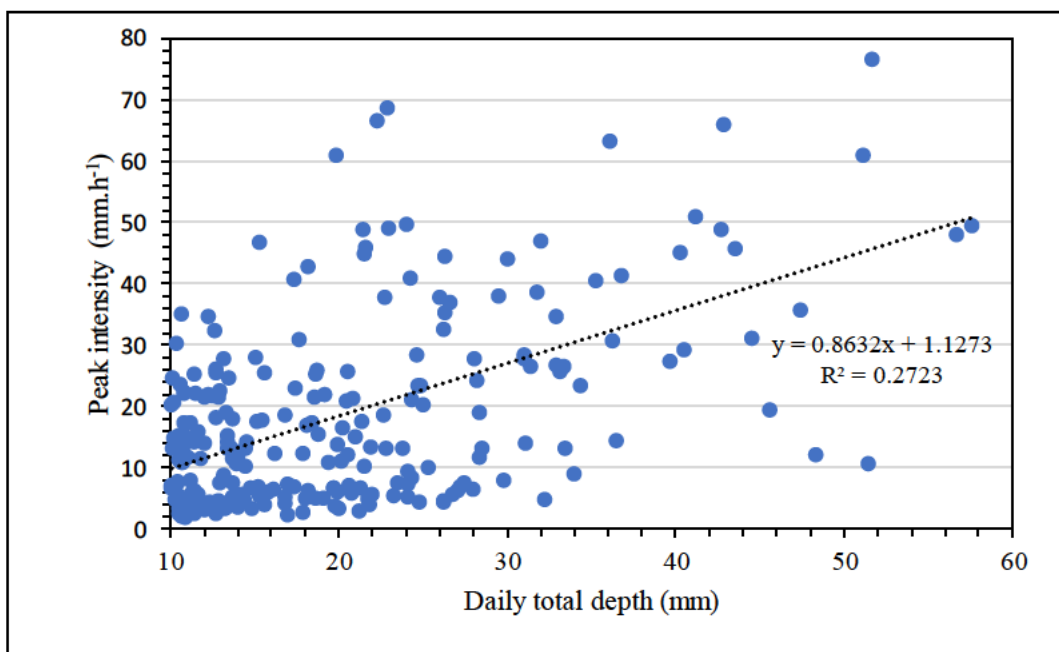


Figure 4.1 Relationship between peak intensity and daily total depth for Station C161 rainfall days

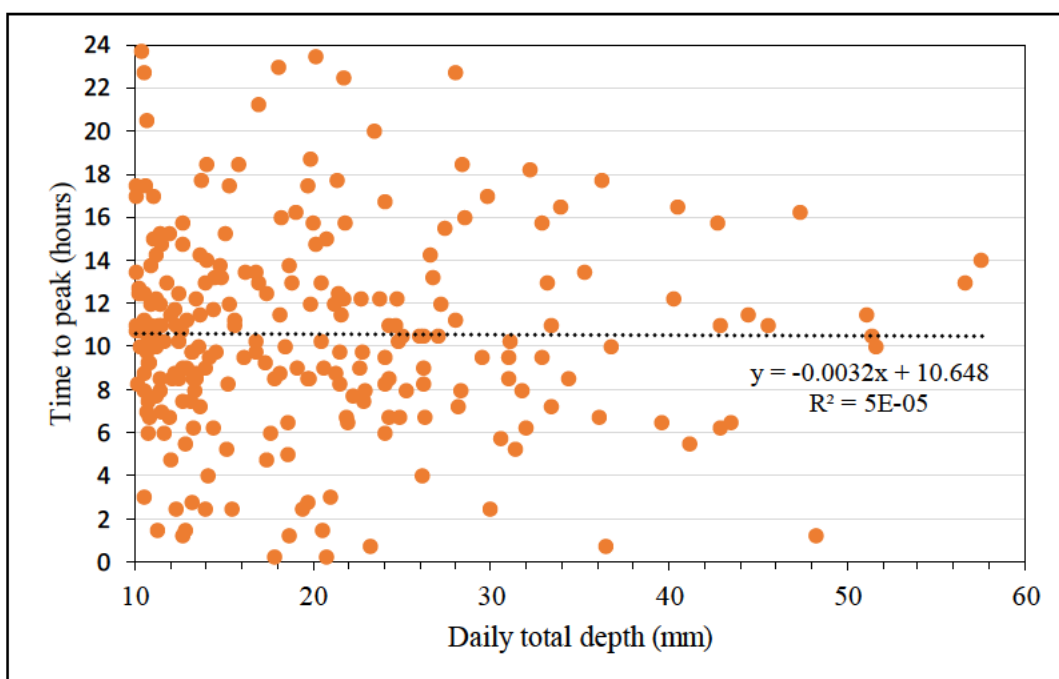


Figure 4.2 Relationship between time to peak and daily total depth for Station C161 rainfall days

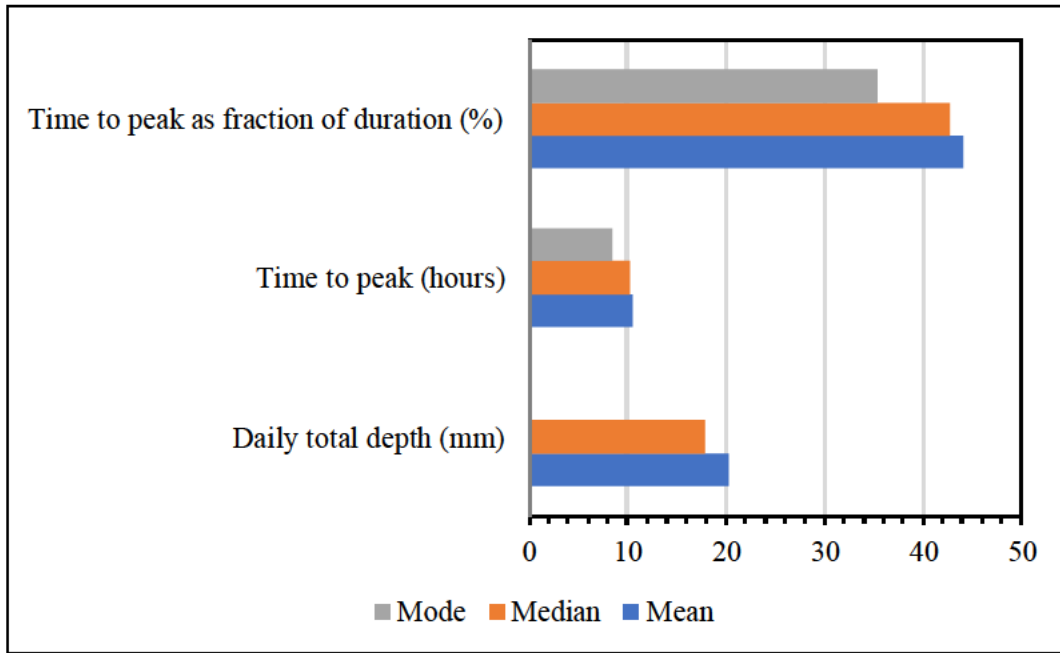


Figure 4.3 Characteristics of daily rainfall parameters for Station C161

It can be seen that the relationship between daily total depth and peak intensity is not particularly strong, as expressed by the R^2 value of 0.27 and a Pearson correlation of 0.52. A greater disparity in the relationship is seen for daily totals greater than 30 mm and peak intensities greater than 20 mm.h⁻¹. In general, the regression analysis shows that lower peak intensities may result in a relatively lower total daily depth. However, some rainfall days with higher totals display low peak intensities, and some rainfall days with high peak intensities display relatively lower total depths.

With regards to the relationship between time-to-peak and daily total depth, no direct correlation is apparent. A small exception to this is a degree of clustering between 6-12 hours for time-to-peak for the daily totals between 10-15 mm. However, in general, time-to-peak varies considerably for rainfall days greater than 10 mm in total depth in the Station C161 record. It can be seen that there are a higher proportion of rainfall days in the lower end of the range, between 10 mm and 30 mm in total depth. The median and mean total depths are found in this range and are given as 17.87 mm and 20.33 mm, respectively. Hence the temporal distribution such rainfall days will have a stronger influence on the general temporal distributions which will be shown by the Huff curves. The median, mean and mode of the time to peak as a fraction of the total daily duration values were determined to be 42.71 %, 44.09 % and 35.42 %, respectively. Hence, the peak 15-minute rainfall intensity generally occurs towards the middle of the rainfall day, in the second quartile of the duration.

A summary of the application of RTD approaches to daily rainfall is detailed in Table 4.1.

Table 4.1 Summary of methodology for application of RTD approaches

Approach	Summary of application methodology
Huff Curves	Curves developed using the depths of rainfall at each 15-minute interval of the 24-hour (08:00 to 08:00) duration for each rainfall day.
SCS-SA	Dimensionless depth fractions provided by distribution were used to produce a distribution of the total daily depth over a 24-hour duration (SCS-SA distributions).
HRU 1/72	The HRU 1/72 24-hour distribution was used to disaggregate daily total depths.
Triangular Distribution	Triangular distributions were determined by using the available daily rainfall total depth and 24-hour duration to calculate the peak intensity for rainfall day (Triangular ObsTP approach). In the second approach, the median time-to-peak derived from the observe data rainfall days was determined and used to derive distributions (Triangular Median TP approach).
AVM	A modified version of the AVM was derived according to the table detailed in the literature review of the approach in Chapter 2. The AVM was derived using the distribution of daily rainfall displayed by the 10 highest rainfall days in the record, with 4 6-hour section of rainfall percentages used to construct the 24-hour distribution. The 24-hour distribution was used to disaggregate daily depths (AVM approach). The second version of the modified AVM approached used in this assessment (AVM-B) was derived using 96 sections of 15-minutes in duration.
Knoesen Semi-stochastic Disaggregation Model	The total depth of each rainfall day was used as input to the model to stochastically generate a distribution of depths over 24-hours.

4.2 Huff Curves

Huff Curves were developed according to the methodology outlined in Bonta (2004). Percentiles are generalised probabilistic representations of dimensionless rainfall events or daily rainfall durations (24-hour periods) plotted against the corresponding dimensionless accumulated depths. For example, the 90th percentile curve shows that 90% of the accumulated daily rainfall has occurred and therefore, 90% of all other rainfall temporal distribution profiles lie below this curve (Bonta, 2004). A short python script was created to produce cumulative depths from daily rainfall. The cumulative values were then used to produce dimensionless plots, from which percentile depth values were extracted for each fraction of the dimensionless duration and used to produce the curves for different percentiles.

The Huff curves generated for 24-hour periods (08:00-08:00), developed from the observed 15-minute interval data for the selected rainfall days in the Station C161 record can be seen in Figure 4.4. These were separated into different quartiles according to the timing of the peak rainfall intensity of the rainfall day relative to the total duration. This was performed in order to represent the differences in dimensionless rainfall trends between early and late peaking rainfall days as shown in Figure 4.5. For the purposes of this study, the daily rainfall peak intensity refers to the highest 15-minute rainfall intensity of the 96 15-minute depths associated with each rainfall day. The curves derived from the 15-minute depths will be referred to as the observed daily Huff curves for purposes of comparison with curves derived from disaggregated depths. The percentage of rainfall days which display the peak 15-minute rainfall intensity in each quartile of the 24-hour duration can be seen in Figure 4.6.

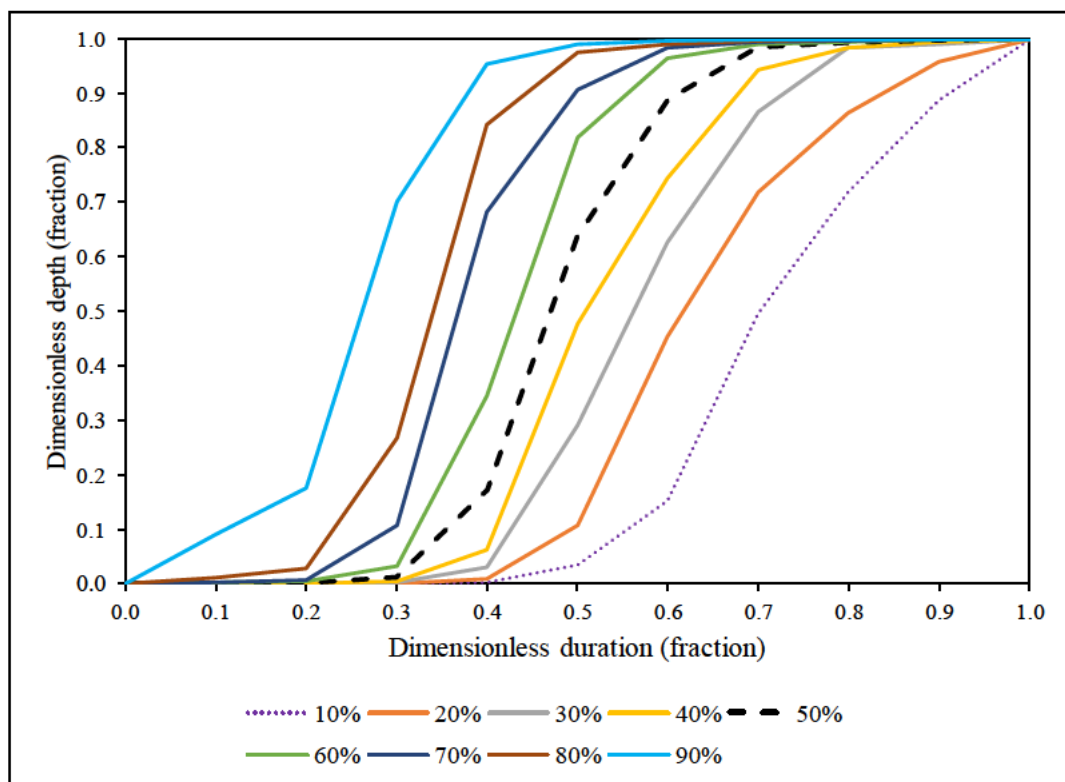


Figure 4.4 Huff curves for rainfall days greater than 10 mm from Station C161

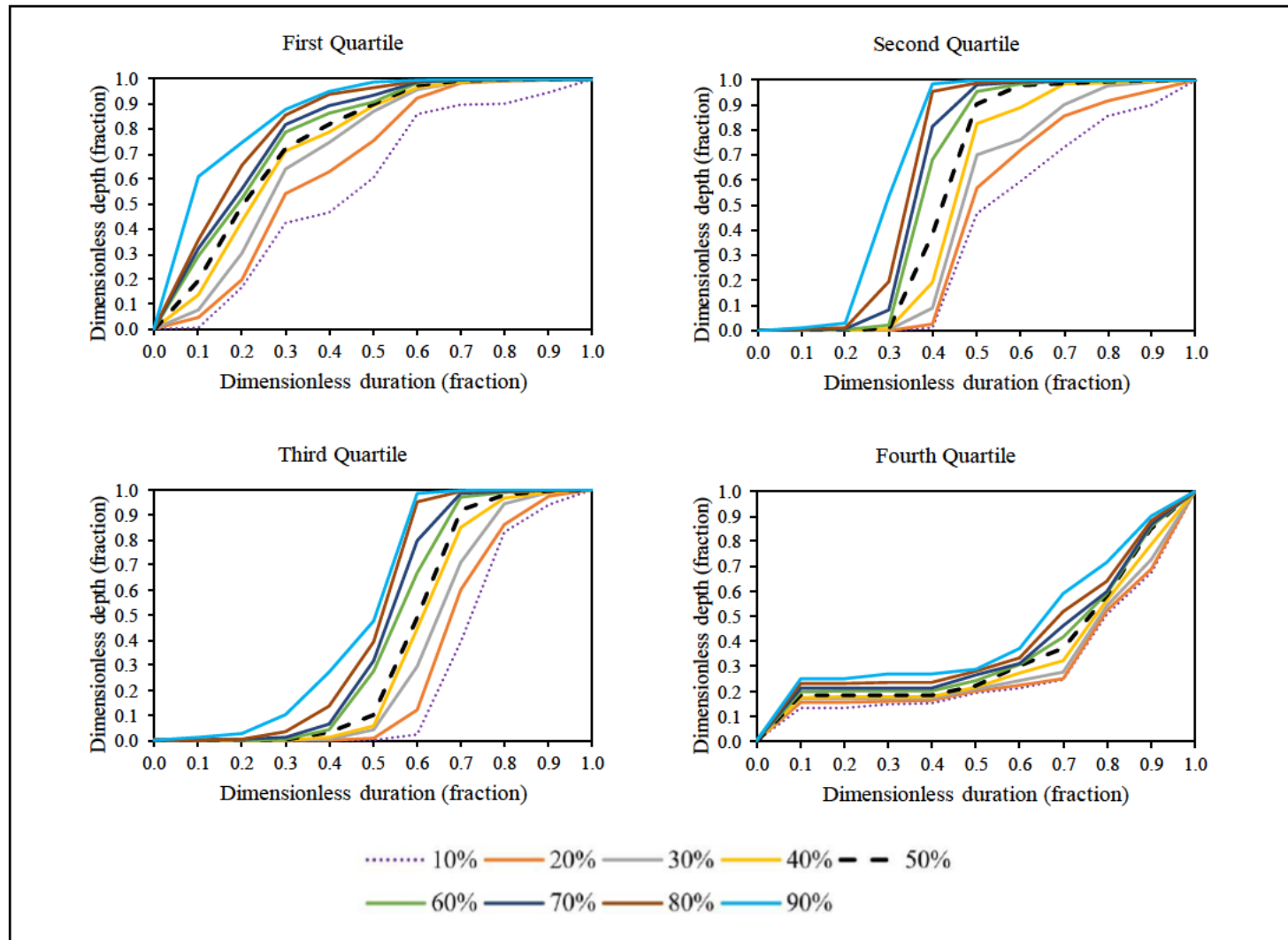


Figure 4.5 Quartile Huff curves for daily rainfall periods from Station C161

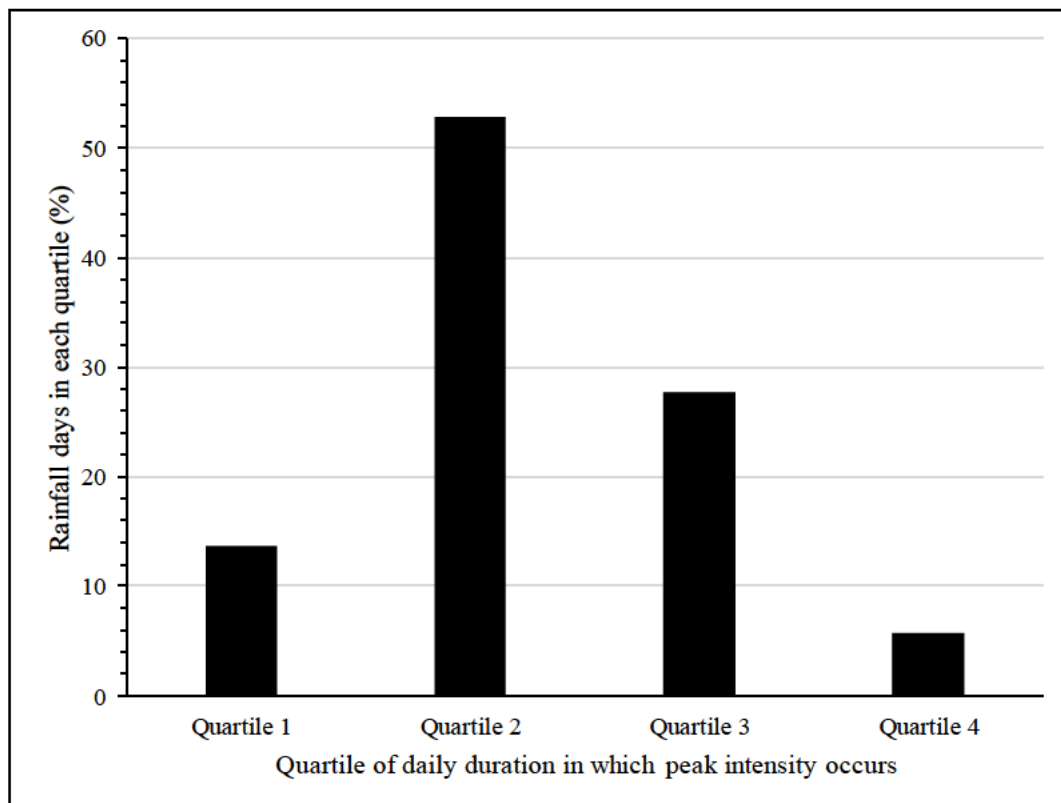


Figure 4.6 Percentage of rainfall days which display peak intensities in each quartile of the total duration

The Huff curves produced for the observed rainfall days are relatively similar in shape for each percentile. However, the higher percentile curves display a higher proportion of rainfall occurring earlier in the daily duration than the lower percentile curves. It can be seen that the 50th percentile curve shows that the majority of rainfall occurs between the second and third quartiles and begins to plateau in the fourth quartile. For the lower percentiles, the trend is lagged, with a greater proportion of rainfall occurring later in the duration. Conversely, the higher percentiles present a greater proportion of rainfall occurring earlier in the duration. However, the first quartile of the rainfall day, up to 20% of duration, displays a considerably lower proportion of rainfall throughout the percentiles.

The temporal distribution of daily rainfall periods are further expressed by the quartile Huff curves. It can be seen that the second and third quartile Huff curves most resemble those which were developed using rainfall days not separated by quartile of peak occurrence. Furthermore, the curves in these quartiles are quite similar, while those in the first and fourth quartiles are considerably different. With regards to the first quartile curves, the lower percentiles display variability in the form of peaks and troughs throughout the duration and

are therefore less regular in shape. In the fourth quartile, the curves display a relatively uniform distribution of rainfall through the first, second and third quartiles of the duration, with a late peak in the fourth quartile which results the majority of the total daily rainfall being produced. The irregularity of the curves may be potentially due to less rainfall days being used to form these quartiles, resulting in less smoothing of the curves

4.3 SCS-SA Rainfall Distributions

The SCS-SA distributions as detailed in Chapter 2 were applied to the selected rainfall days. It is acknowledged that the correct approach for applying the SCS-SA method is to select a single appropriate distribution for a rainfall station based on the SCS-SA rainfall region type. However, in this study all of the SCS-SA distributions were applied in order to determine if this would yield considerable differences in results or if distributions could be used to characterise rainfall temporal distributions outside of their recommended regions.

For purposes of application, the depth fractions at each increment of the 24-hour distribution, as given by the distribution curves, were multiplied by the daily rainfall total depths. This resulted in a cumulative distribution of the total daily depth, which was used to determine the actual rainfall depth at each of the 96 15-minute increments of the 24-hour period from 08:00 to 08:00.

The disaggregated rainfall depth distributions obtained through application of the SCS-SA distributions (SCS1, SCS2, SCS3 and SCS4) were used to generate Huff curves. The SCS-SA distributions are fixed distributions and therefore, single Huff curves are produced for each distribution, which resemble the original 24-hour distributions. Comparison of the SCS-SA disaggregated dimensionless Huff curves to the observed daily rainfall Huff curves can be seen in Figure 4.7. The MARE values for comparison with the percentile curves is shown in Table 4.2.

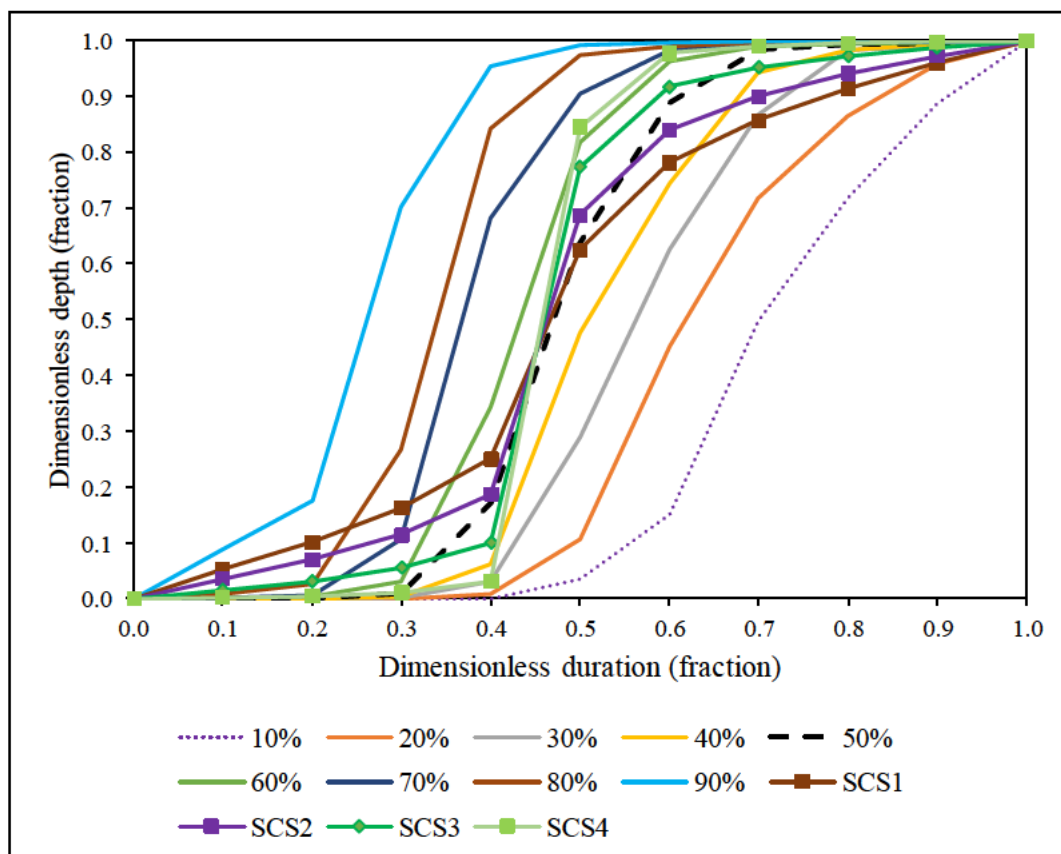


Figure 4.7 Comparison of SCS distribution curves and observed daily rainfall Huff curves

Table 4.2 MARE values for SCS-SA distributions applied to disaggregate daily rainfall

Variable	Percentile									Σ
	10 th	20 th	30 th	40 th	50 th	60 th	70 th	80 th	90 th	
SCS1 MARE (%)	26.1	17.8	12.3	9.4	7.9	10.7	14.8	17.7	24.0	140.6
SCS2 MARE (%)	26.4	18.1	11.8	8.2	5.1	8.2	12.3	16.3	23.6	130.2
SCS3 MARE (%)	26.9	18.6	11.6	7.0	4.2	5.1	10.4	14.5	23.2	121.5
SCS4 MARE (%)	27.3	19.0	11.8	7.9	5.0	4.2	9.1	13.9	22.7	120.9

The SCS3 distribution dimensionless curve appears to provide a considerably closer approximation of the observed 50th percentile Huff curve than the SCS1 or SCS2 distributions. However, some evidence of underestimation and overestimation is displayed at different points in the duration. For the later sections of the duration, it appears very similar to the observed 40th percentile curve, while in the middle sections, it is closer to the 60th percentile observed Huff curve. The SCS4 distribution dimensionless curve appears similar to 30th, 40th and 50th percentile observed Huff curves in the early sections of the duration, which account for a considerably small percentage of the total rainfall. However, for the middle and later sections of the duration, the SCS4 curve is most similar to the observed 60th percentile curve, and displays a relatively uniform distribution of rainfall beyond 60% of the duration. Overall, the SCS4 approximates the observed curve better.

4.4 HRU 1/72 Distributions

The HRU 1/72 distributions were selected from the range of 2-hour to 24-hour distributions provided in the HRU 1/72 report for characterising design storms (HRU, 1972). The distributions associated with the approach each provide a dimensionless distribution of percentage of total depth per corresponding percentage of total duration. Therefore, the approach is also similar to the Huff curve method. In order to obtain the 15-minute rainfall depths, a 10th order polynomial equation was fitted to the cumulative curves produced through multiplication of the depth fractions by the total depths. This followed the methodology used by Bonta (2004) in the application of Huff curves. The polynomial equations enabled the fraction of the total depth (y) to be determined at each 15-minute time-step (x) of the 24-hour duration. Equation 4.1 shows the general formula of the 10th order polynomial equation for each curve. The multipliers for the equations of each duration curve are given in Table 4.3.

$$y = (C10 * x^{10}) + (C9 * x^9) + (C8 * x^8) + (C7 * x^7) + (C6 * x^6) + (C5 * x^5) + (C4 * x^4) + (C3 * x^3) + (C2 * x^2) + (C1 * x^1) \quad (4.1)$$

Table 4.3 Multipliers for the 10th order polynomial equations for each duration
HRU 1/72 curve used

Multiplier	2-hour curve	4-hour curve	8-hour curve	12-hour curve	24-hour curve
<i>C10</i>	503.11	429.79	-1017.49	1301.52	-257.22
<i>C9</i>	-1969.23	-1631.76	4067.55	-4953.55	1028.95
<i>C8</i>	2947.94	2352.67	-6161.30	7107.52	-1557.87
<i>C7</i>	-1858.31	-1417.40	3893.59	-4217.10	972.01
<i>C6</i>	0.00	0.00	0.00	0.00	0.00
<i>C5</i>	700.74	470.84	-1451.40	1306.82	-292.61
<i>C4</i>	-422.84	-256.64	875.99	-684.59	107.69
<i>C3</i>	112.30	58.49	-234.11	155.49	2.81
<i>C2</i>	-13.82	-5.49	29.13	-15.97	-3.33
<i>C1</i>	1.12	0.50	-0.98	0.85	0.56

A comparison of the fit of the polynomial equation curves to the HRU 1/72 curves for different durations which were used in this assessment is shown in Figure 4.8.

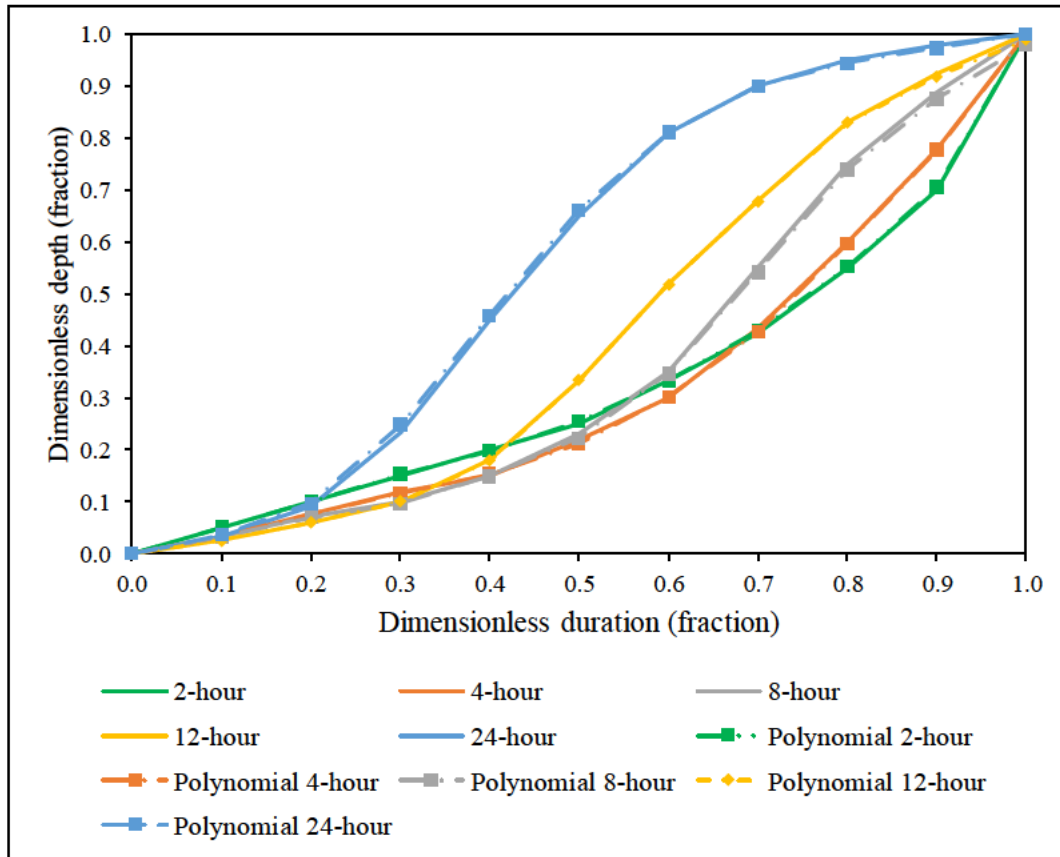


Figure 4.8 Fit of the polynomial equation curves for HRU 1/72 different duration curves

The HRU 1/72 24-hour distribution was selected and used to disaggregate the daily rainfall data. The disaggregated depths were then used to derive Huff curves. The HRU 1/72 24-hour is a fixed distribution. Hence, generation of Huff curves from the disaggregated daily rainfall using the 24-hour distribution results in a single distribution. This distribution was compared to the Huff curves derived from the observed daily rainfall data as shown in Figure 4.9 and Table 4.4.

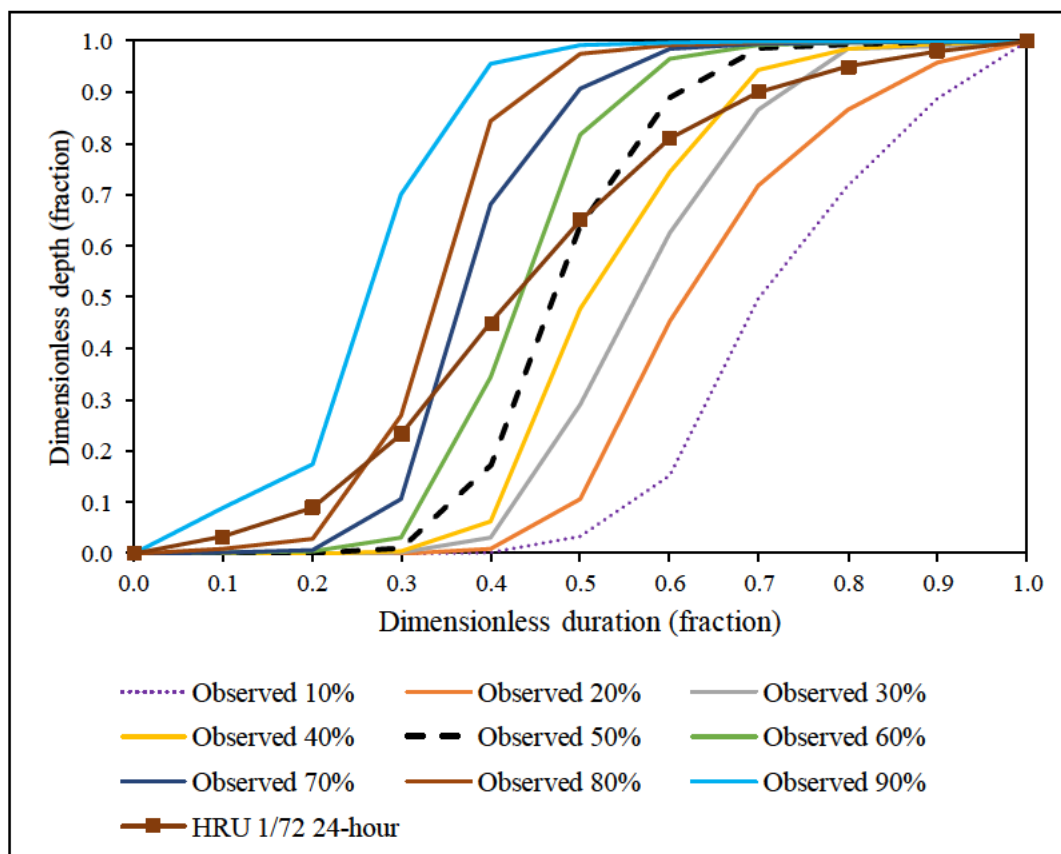


Figure 4.9 Comparison of observed daily rainfall Huff curves and HRU 1/72 24-hour distribution curve

Table 4.4 MARE values for the HRU 1/72 24-hour distribution applied to disaggregate daily rainfall

Variable	Percentile									Σ
	10 th	20 th	30 th	40 th	50 th	60 th	70 th	80 th	90 th	
HRU 1/72 24-hour MARE (%)	30.2	21.8	15.4	11.7	9.3	9.8	11.6	13.0	19.9	142.7

There is a degree of intersection with the 50th percentile observed curve in the middle of the duration. However, the curve appears most similar to the 30th percentile and 40th percentile observed Huff curves in the late sections of the duration. Overall, the HRU 1/72 24-hour distribution is characteristic of a more even distribution of rainfall over the duration than that which is displayed by the observed daily Huff curves (curves derived from the observed 15-minute depths for the 08:00 to 08:00 period).

4.5 Triangular Distribution

As detailed in Section 2.1.1.5, the methodology described in Lambourne and Stephenson (1987) and Chow *et al.* (1988) was adapted for application of the Triangular distribution. For the initial application on rainfall days, the peak intensity (h), peak location (timing of peak) and total duration (T_d) values obtained from each observed rainfall day were utilised. The peak intensity utilised was the highest 15-minute rainfall intensity for the given day.

4.5.1 Triangular ObsTP

The observed total depth P (mm) and observed daily duration T_d (hours) were used to calculate a suitable peak intensity h (mm.h⁻¹) according to Equation 4.2.

$$h \text{ (mm. h}^{-1}\text{)} = (2 * P)/T_d \quad (4.2)$$

Once the characteristics for each rainfall day were determined, it was necessary to derive a means for calculating the rainfall depth at each increment of time of the total duration. Straight line regressions were derived for sections of the Triangular distributions before the peak (t_a) and after the peak (t_b), as shown in Figure 4.10. The location of the peak was derived from the observed data. The equations allowed for the given rainfall intensity y (mm.h⁻¹) to be calculated for each corresponding increment in the daily duration x (hours).

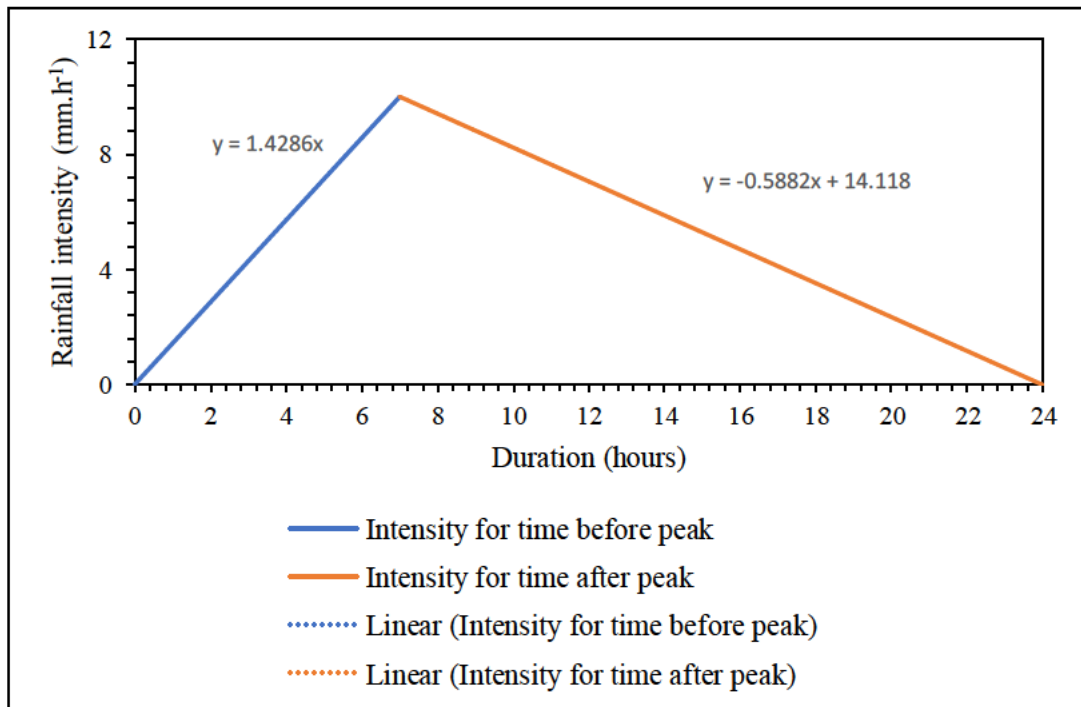


Figure 4.10 Derivation of straight line equations for rainfall intensity and depth values preceding and succeeding peak intensity

Once the rainfall intensity values at each point in the daily rainfall duration were determined, these were converted to rainfall depths for each 15-minute increment, thereby producing a distribution of 15-minute rainfall depths which could be summed to the daily total depth.

The rainfall days disaggregated using the Triangular distribution as derived using observed data parameters (Triangular ObsTP) were used to develop Huff curves. The comparison of these to the observed daily rainfall Huff curves can be seen in Figure 4.11. MARE values for this comparison are detailed in Table 4.5.

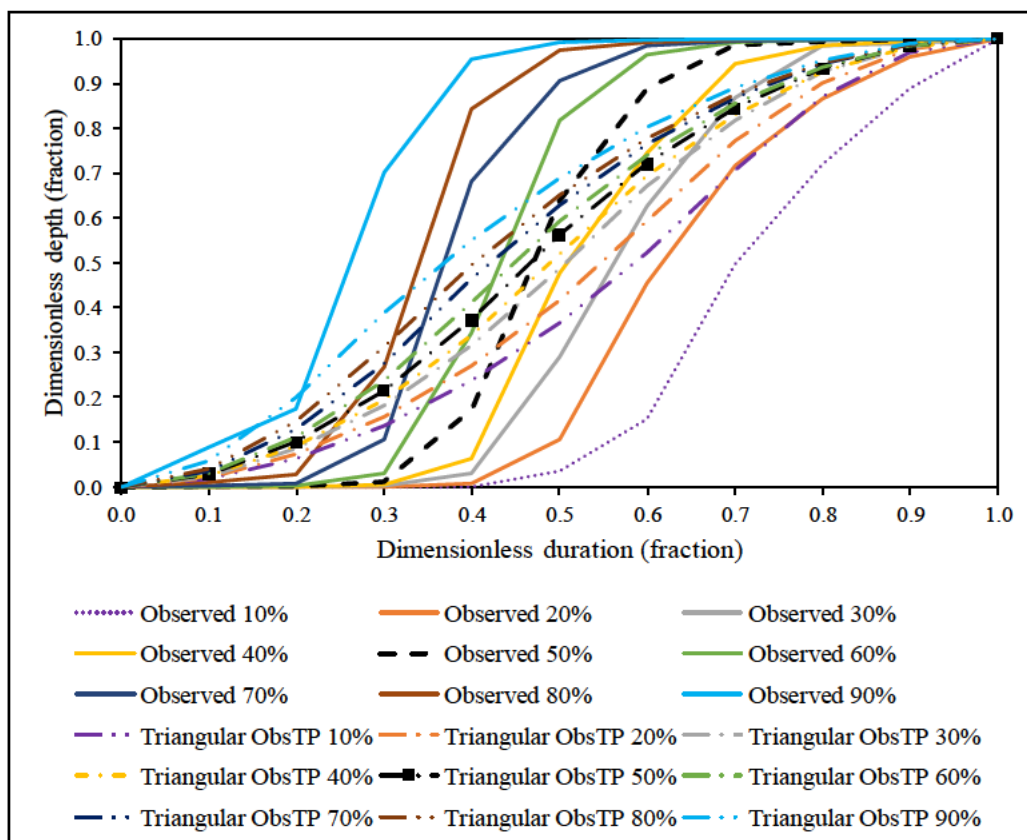


Figure 4.11 Comparison of observed daily rainfall Huff curves and Triangular distribution curves

Table 4.5 MARE values for Triangular ObsTP approach applied to daily rainfall

Variable	Percentile									Σ
	10 th	20 th	30 th	40 th	50 th	60 th	70 th	80 th	90 th	
Triangular ObsTP MARE (%)	16.9	11.7	10.3	9.4	10.9	11.7	13.6	13.9	15.9	114.2

The Huff curves produced from rainfall depths obtained through application of the Triangular ObsTP RTD approach are markedly different to the observed daily rainfall Huff curves. Each of the percentile Triangular ObsTP Huff curves displays a more gradual cumulative increase in dimensionless rainfall throughout the distribution as opposed to their counterparts in the set of observed Huff curves. This may be due to the calculated peak

intensities for the Triangular ObsTP being lower than the observed peak intensities, despite the locations of the peaks being the same.

4.5.2 Triangular Median TP

It is acknowledged that observed data will not always be available to derive parameters such as peak occurrence and peak intensity. However, if the total depth and the total duration are available, the Triangular distribution of rainfall may be determined using a generalized time of peak occurrence. The second approach for application of the Triangular distribution to daily rainfall involved using a generalised timing of the peak for development of the distribution. The median time to peak for the rainfall days was determined to be 10.5 hours. This value was utilised as well as a 24-hour fixed duration to calculate the peak 15-minute rainfall intensity for each rainfall day, according to Equation 3.2. The resulting distributions were then used to disaggregate the total daily rainfall depths in a similar manner as the methodology for the Triangular ObsTP.

Comparison of the observed daily Huff curves to the median time to peak Triangular distribution (Triangular Median TP) curve is shown in Figure 4.12 and by the MARE values in Table 4.6.

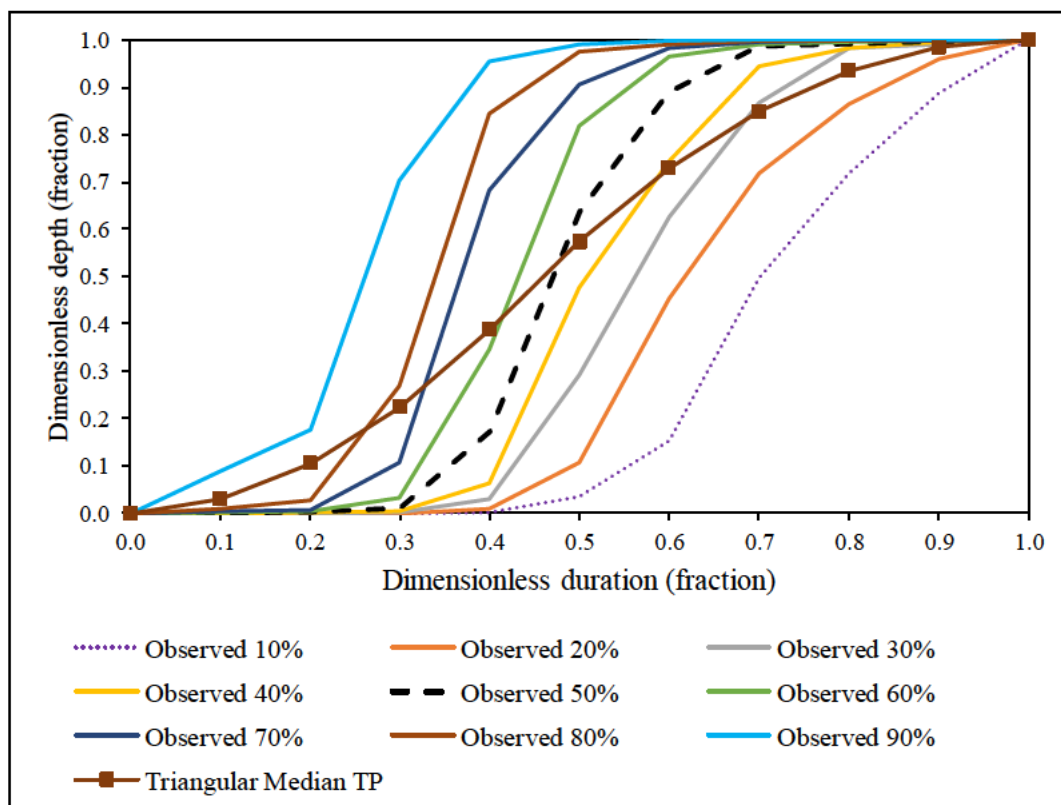


Figure 4.12 Comparison of observed daily Huff curves and Median time-to-peak Triangular distribution curve

Table 4.6 MARE values for Triangular Median TP approach applied to disaggregate daily rainfall

Variable	Percentile									Σ
	10 th	20 th	30 th	40 th	50 th	60 th	70 th	80 th	90 th	
Triangular Median TP MARE (%)	27.0	18.7	13.0	10.4	10.8	11.6	14.8	16.4	23.1	145.7

The Triangular Median TP does not perform better at approximating the observed Huff curves than the Triangular distributions derived using the observed peak locations for each rainfall day (Triangular ObsTP). When compared to the 50th percentile observed daily rainfall Huff curve, the Triangular Median TP curve displays a higher proportion of rainfall earlier for the earlier sections of the duration. However, the more gradual distribution of

rainfall, as shown by the less steep slope of the distribution curve, results in the cumulative total depth being lower in the later sections of the duration.

4.6 Average Variability Method (AVM)

A modified version of the AVM described in Chapter 2 was utilised in this assessment, which did not involve analysis of intense bursts of rainfall. Literature and case studies reviewed described the application of the approach for rainfall events. In this assessment, the approach was modified to be more suitable for application with the available daily rainfall data. The 24-hour rainfall days were divided into four sections of 6-hours in duration and the table for derivation of the AVM temporal pattern was followed. Rainfall data for Station C161 were ranked to identify the highest rainfall daily totals in each year on record, as shown in Table 4.7. The final pattern of rainfall was used to produce the AVM distribution shown in Figure 4.13. In order to apply to the approach to disaggregate daily rainfall total depths, the 6-hour sections of the distribution were fitted to straight line equations in a similar manner to the Triangular ObsTP approach. This allowed for the percentage of total rainfall to be calculated at each 15-minute increment of the 24-hour duration of each rainfall day. The percentages were then multiplied by the total depth to produce the distribution of rainfall depths over 24-hours.

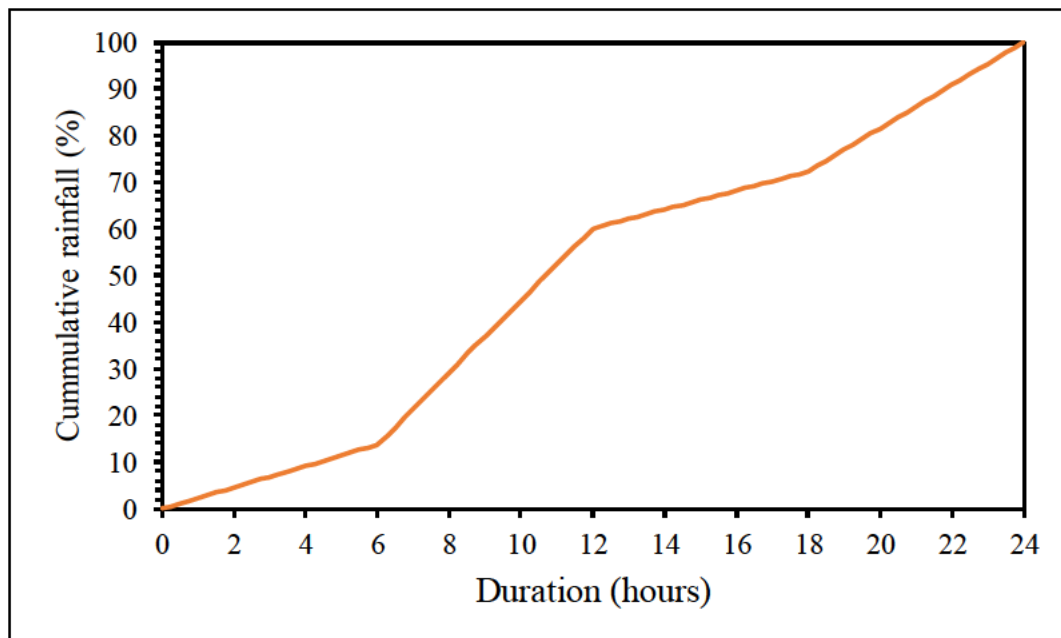


Figure 4.13 AVM 24-hourly distribution pattern at Station C161

Table 4.7 Derivation of 24-hourly AVM distribution

Date	Rain (mm)	Rank	Rain in each period (6 hours)				Rank of each period's rainfall period				Rain in period of each rank (%)			
			1	2	3	4	1	2	3	4	1	2	3	4
1982/02/16	57.605	1	0.00	23.39	33.26	0.95	4	2	1	3	57.74	0.00	1.65	40.61
1977/12/30	56.657	2	0.36	1.15	54.85	0.30	3	2	1	4	0.52	96.81	2.03	0.63
1978/09/08	51.402	3	0.00	11.50	12.50	27.40	4	3	2	1	22.38	24.31	0.00	53.31
1983/12/12	51.166	4	0.07	50.89	0.18	0.02	3	1	2	4	0.05	0.34	0.14	99.47
1984/04/09	48.308	5	18.77	12.07	10.56	6.91	1	2	3	4	21.86	24.99	14.30	38.85
1979/01/27	47.388	6	0.00	19.55	27.66	0.18	4	2	1	3	0.00	41.25	58.37	0.38
1989/01/06	46.797	7	0.07	4.00	20.74	21.99	4	3	2	1	8.55	44.31	46.99	0.15
1985/02/07	37.402	8	5.03	16.45	3.19	12.74	3	1	4	2	8.53	34.06	13.44	43.98
1981/02/16	36.772	9	0.00	36.24	0.41	0.12	4	1	2	3	1.12	98.55	0.33	0.00
1980/11/23	35.291	10	0.14	0.14	35.01	0.00	3	2	1	4	0.41	99.21	0.00	0.39
			Average				3.3	1.9	1.9	2.9	12.12	46.38	13.72	27.78
			Standard Deviation				0.95	0.74	0.99	1.20	18.24	38.66	21.41	33.52
			Assigned Rank				3	2	1	4				
			Period				1	2	3	4				
			Final Pattern (% of total rainfall)				13.72	46.38	12.12	27.78				

The approach for application of the AVM to disaggregate rainfall days involved disaggregating the total depths using the percentages of rainfall at each 15-minute interval of the 24-hour duration, as given by Figure 4.13. This produced a 24-hour distribution of depths for each rainfall day.

The disaggregated daily rainfall depths obtained by application of the AVM distribution were used to generate Huff curves. The AVM is a fixed distribution and therefore a single curve was produced, which is representative of the different percentiles. This curve was compared to the Huff curves derived from the observed daily rainfall, as shown in Figure 4.14 and using MARE values in Table 4.8.

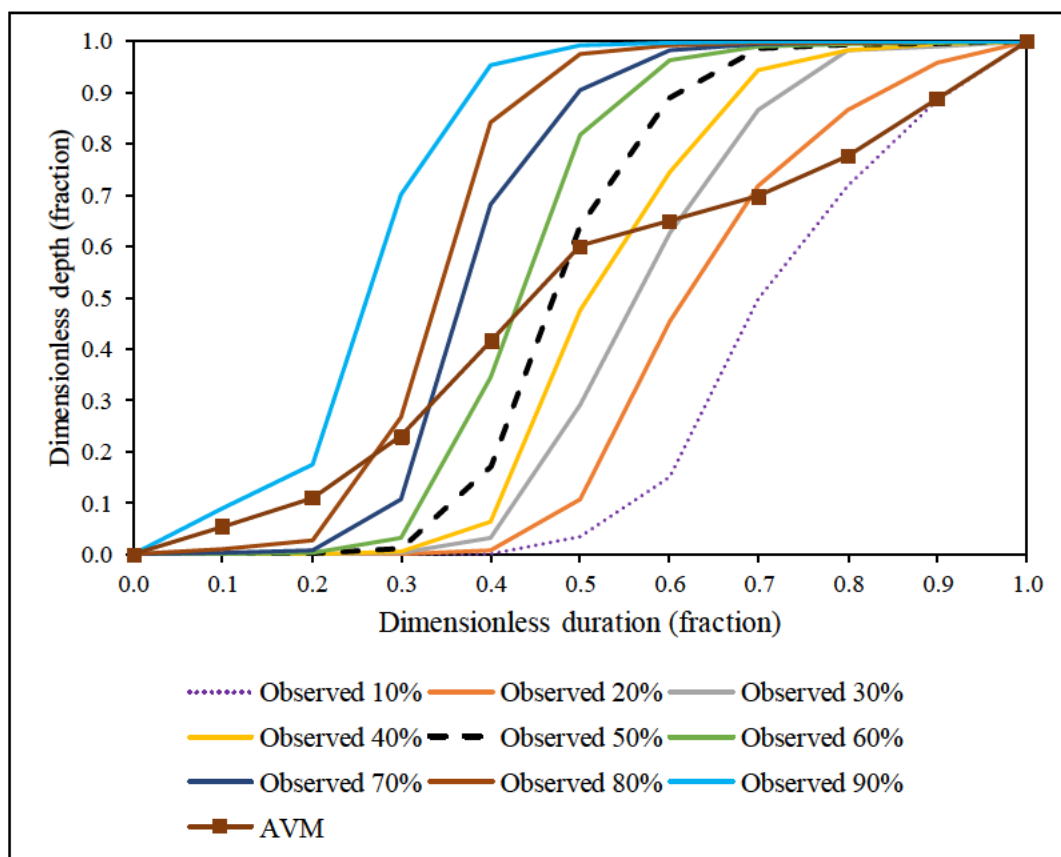


Figure 4.14 Comparison of observed daily rainfall Huff curves to AVM curve

Table 4.8 MARE values for AVM applied to disaggregate daily rainfall

Variable	Percentile									Σ
	10 th	20 th	30 th	40 th	50 th	60 th	70 th	80 th	90 th	
AVM MARE (%)	23.7	17.8	16.5	15.7	15.6	16.4	18.9	20.3	26.4	171.2

The dimensionless distribution generated for the AVM distribution does not appear to be similar to any of the observed daily rainfall Huff curves. The distribution displays a peak between 20 % and 50 % of the total duration. Therefore, such a distribution would be characteristic of rainfall days with peak intensities in the second quartile.

4.7 AVM-B

The methodology used for initial derivation of the AVM distribution used in this assessment displays a limitation relating to the 6-hour sections of daily rainfall depths utilised. The use of four 6-hour sections of rainfall results may not result in disaggregated daily depths with similar peak values to the observed rainfall. Therefore, the second approached the modified AVM distribution used in this study was developed using 96 sections of 15-minutes in duration, which is the same resolution as the observed daily rainfall (AVM-B). In the same manner as for the AVM, the Huff curves developed using the rainfall depths disaggregated with the AVM-B were compared to the observed Huff curves, as shown in Figure 4.15. The MARE values for this comparison are shown in Table 4.9.

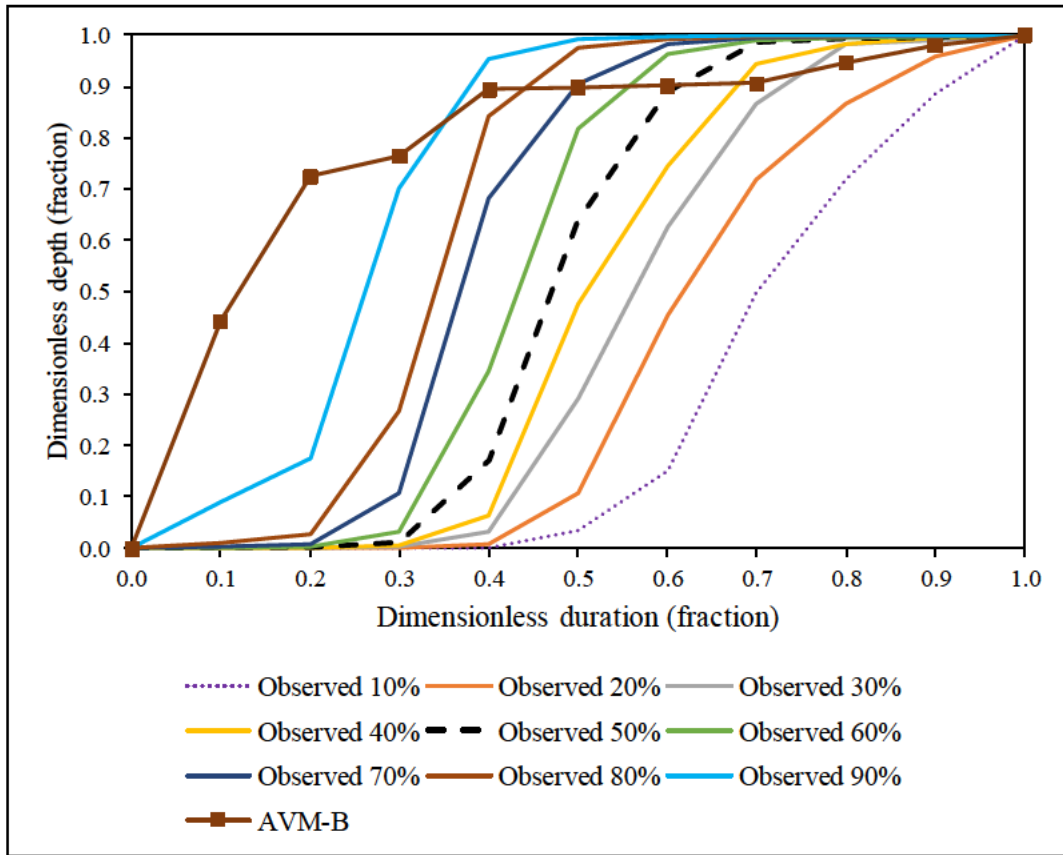


Figure 4.15 Comparison of observed daily rainfall Huff curves to AVM-B curve

Table 4.9 MARE values for AVM-B applied to disaggregate daily rainfall

Variable	Percentile									Σ
	10th	20th	30th	40th	50th	60th	70th	80th	90th	
AVM-B MARE (%)	42.8	36.5	34.7	32.0	31.2	29.8	26.4	26.0	21.9	281.7

It can be seen that the AVM-B Huff curve does not appear similar to any of the observed Huff curves. Furthermore, the MARE values show that it performs worse than the AVM, despite being developed with more sections of shorter periods of temporal resolution.

4.8 Knoesen Semi-stochastic Disaggregation Model

The Knoesen model as detailed in Chapter 2 was applied to stochastically generate rainfall depths over 24-hours for given daily rainfall total depths.

The Knoesen model was developed for application on 24-hourly data (00:00 to 00:00). The model programme developed by Knoesen (2005) was utilised to generate 24-hour distributions of daily rainfall total depths. It was determined that Station C161 falls within Range III of the regionalized distribution map of R values associated with the model (Knoesen, 2005). The Range type (Range III) and daily total depths were used as input to the programme to generate 15-minute rainfall depths distributed over 24 hours.

The stochastic nature of the model results in a different distribution with each successive run, as shown in Figure 4.16. For purposes of this assessment, a single distribution was generated for each respective rainfall day.

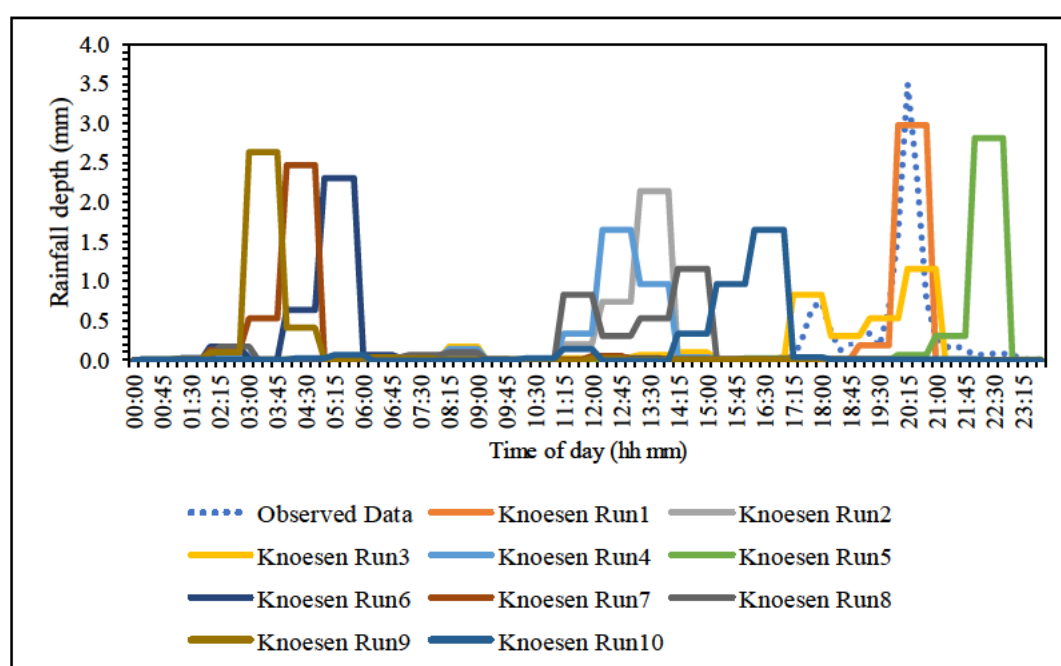


Figure 4.16 Stochastic generation of distribution of rainfall depths over 24-hours

Daily rainfall total depths were disaggregated using the Knoesen model program. For purposes of this assessment a single disaggregated distribution of 15-minute rainfall depths was derived for each rainfall day, i.e. 110 stochastic sequences were generated for total depths from the 110 rain days. The disaggregated depths were used to develop Huff curves, which were then compared to the Huff curves derived from the observed rainfall 15-minute depths, as can be seen in Figure 4.17 and Table 4.10.

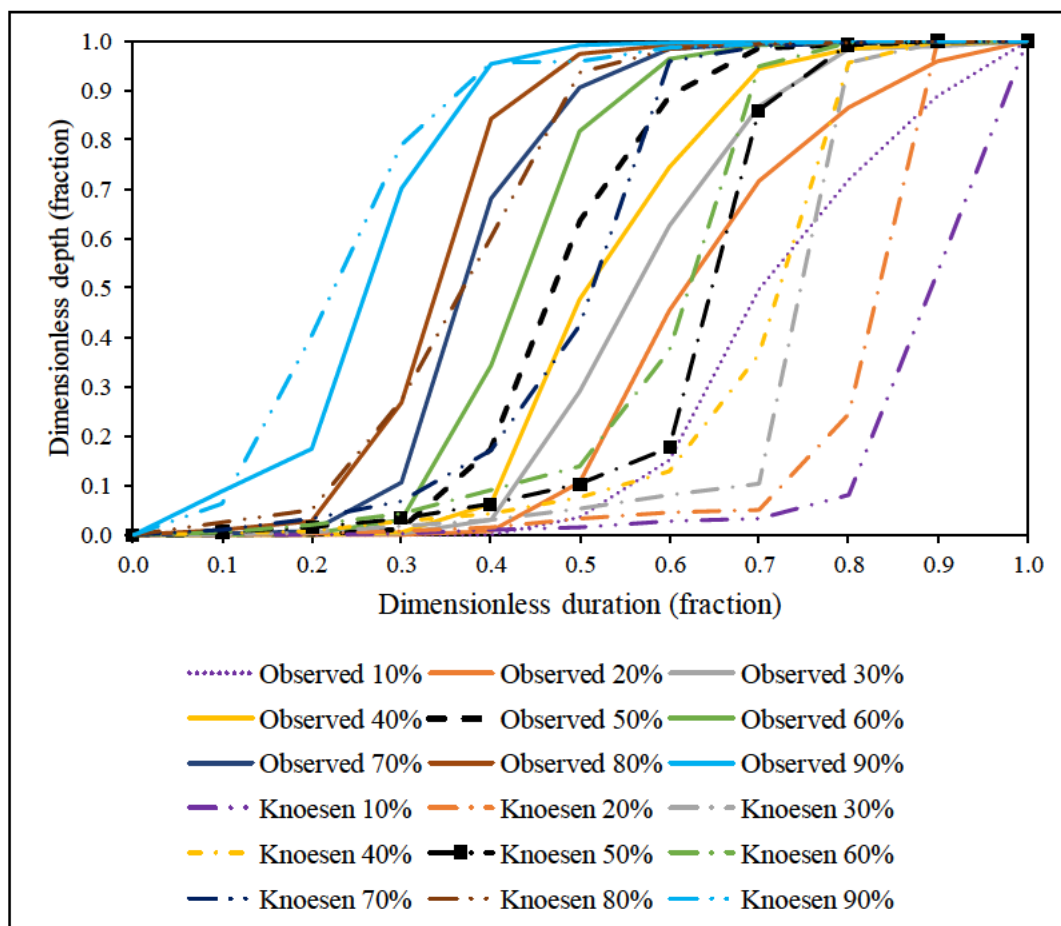


Figure 4.17 Comparison of observed daily Huff curves to Knoesen model daily Huff curves

Table 4.10 MARE values for Knoesen model applied to disaggregate daily rainfall

Variable	Percentile									Σ
	10 th	20 th	30 th	40 th	50 th	60 th	70 th	80 th	90 th	
Knoesen MARE (%)	14.0	19.9	17.7	18.6	16.9	17.8	12.2	3.7	4.4	125.2

It can be seen that there is a considerable difference between the Huff curves produced using the Knoesen model disaggregated rainfall depths and the observed data Huff curves. This is especially apparent for the lower to middle percentiles, which display the highest percentage of rainfall much later in the duration than the observed Huff curves. However, the 90th percentile and 80th percentile Knoesen model curves display a closer approximation to the

respective observed curves in each percentile, than is displayed by the other disaggregated rainfall Huff curves.

4.9 Comparison of The Performance of RTD Approaches

The RTD approaches which were applied to disaggregate daily rainfall total depths were assessed for their performance in approximating the observed temporal distribution of rainfall, as represented by the Huff curves developed. In addition, the disaggregated rainfall days were assessed on the basis of preservation of the peak rainfall intensities displayed by the observed data rainfall days. The results of the assessments are presented in this section.

4.9.1 Comparison of observed and disaggregated peak intensities

Comparison of the peak rainfall intensities of the observed rainfall days was compared to those of the disaggregated rainfall days obtained through application of each approach. An example of the comparison of the observed and disaggregated rainfall day peak intensities is shown in Figure 4.18 for the results of the application of the Triangular ObsTP distribution. The correlation coefficient values for the regression analysis and the PBIAS values for each approach can be seen in Table 4.11.

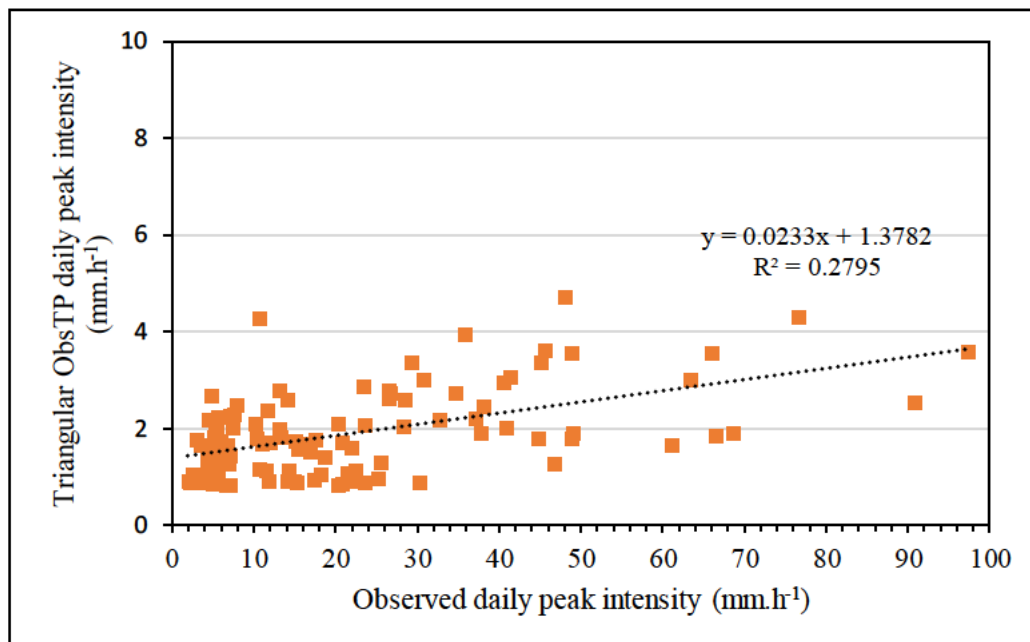


Figure 4.18 Regression analysis between peak intensities of rainfall days disaggregated using the Triangular ObsTP approach and observed rainfall day peak intensities for Station C161

Table 4.11 Comparison between observed and disaggregated peak intensities for each approach applied to daily rainfall for Station C161

RTD Approach	R ² Correlation	Pearson correlation	PBIAS (%)
Knoesen	0.15	0.39	-40.80
AVM	0.28	0.53	-91.90
AVM-B	0.16	0.40	-24.70
HRU 1/72	0.24	0.49	-91.00
Triangular ObsTP	0.28	0.53	-91.30
Triangular Median TP	0.28	0.53	-91.30
SCS1	0.28	0.53	-55.20
SCS2	0.28	0.53	-30.70
SCS3	0.28	0.53	1.60
SCS4	0.28	0.53	28.90

Disaggregation of daily rainfall totals at Station C161 results in distributions with peak intensity values that are markedly different to those of the observed data. This is shown by poor correlation values for all approaches. Furthermore, overestimation bias was displayed for each approach, with the exceptions of SCS3 and SCS4, which showed a relatively low degree of underestimation bias. In addition, it can be seen that the tendency for overestimation of the peak intensities is lower for the AVM-B and Knoesen model than for the other approaches which show overestimation bias. Overall, application of the disaggregation approaches using daily rainfall data does not result peak intensities similar to the observed data.

4.9.2 Comparison of temporal distribution accuracy

The MARE values calculated for the comparison between the observed daily rainfall Huff curves and those derived from the disaggregated daily rainfall depths obtained through application of the RTD approaches were determined. The MARE values for the 50th percentile curves comparison can be seen in Figure 4.19.

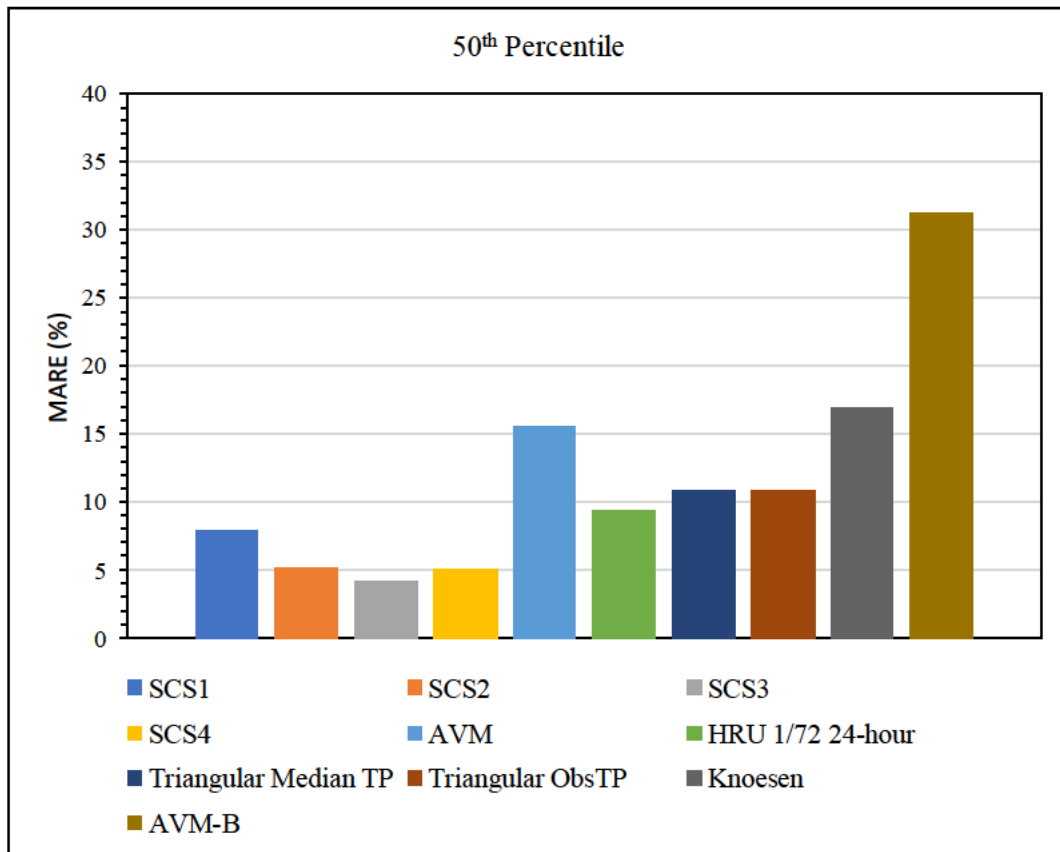


Figure 4.19 MARE between observed and disaggregated 50th percentile Huff curves

The 50th percentile observed daily Huff curve appears to be best approximated by the SCS3 distribution, followed by the SCS4 distribution. The Triangular ObsTP and Triangular Median TP distribution display similar values, and hence perform similarly. The AVM-B displays the worst performance, with the Knoesen model as second worst performance, followed by the AVM as the third worst.

4.9.2.1 Total MARE

\sum MARE values were determined for the application of RTD approaches on daily rainfall. The \sum MARE for each RTD approach is shown in Figure 4.20.

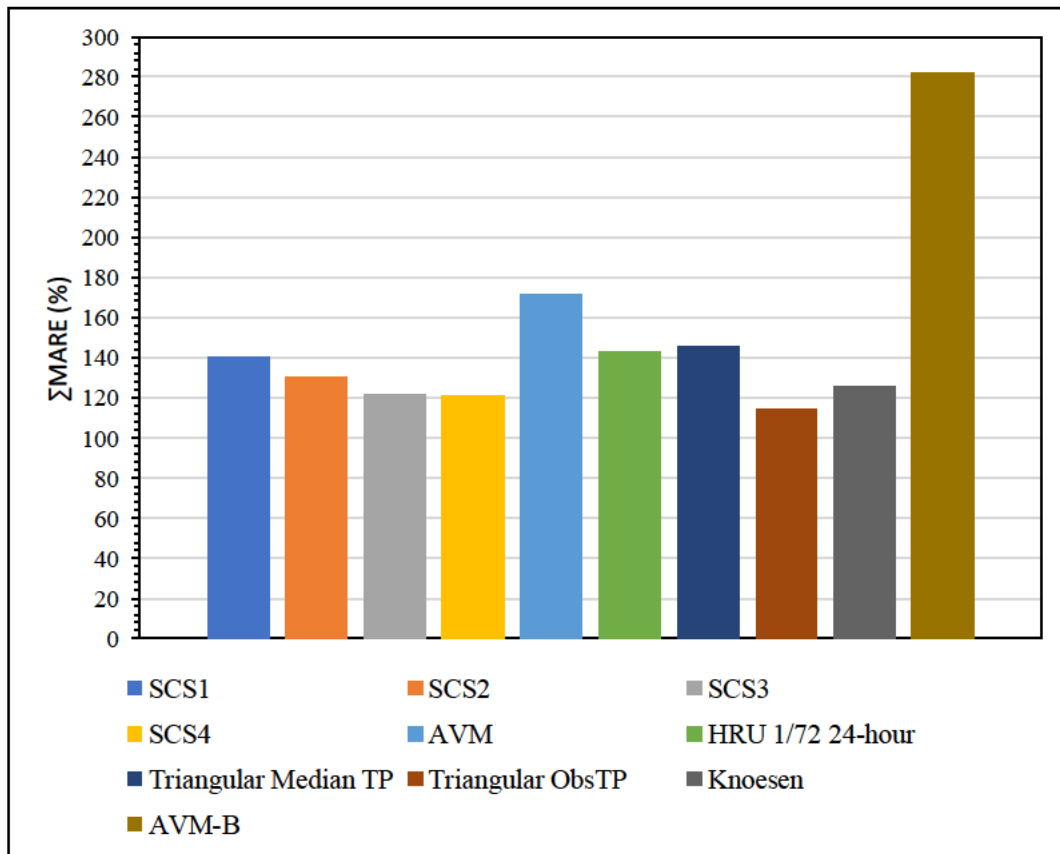


Figure 4.20 Total MARE across percentiles for each RTD approach

The Triangular ObsTP appears to perform the best out of the RTD approaches. However, it should be noted, that the approach was developed using observed rainfall total depths and the observed time to peak, which likely accounts for the good performance. The Triangular Median TP distribution, which was developed using the median time to peak value for all rainfall days and the daily total depth does not perform as well. Considering these factors, the Knoesen model performs the best out of the approaches which are not fixed distributions or do use observed parameters. The SCS3 and SCS4 distributions are quite similar in performance. However, the SCS4 distribution performs the best, despite the rainfall station from which the observed data was obtained falling within a SCS3 region.

4.9.2.2 NSE for observed and disaggregated Huff curves

The NSE values between the observed and disaggregated Huff curves were determined, and can be seen in Table 4.12. This serves as an additional assessment of how similar the distributions displayed by the disaggregated rainfall curves are to those of the observed rainfall curves.

Table 4.12 NSE values for comparison of observed and disaggregated Huff curves

RTD approach	NSE for each Percentile									Mean
	10 th	20 th	30 th	40 th	50 th	60 th	70 th	80 th	90 th	
SCS1	0.36	0.73	0.89	0.95	0.97	0.94	0.84	0.73	0.42	0.76
SCS2	0.26	0.69	0.88	0.96	0.99	0.96	0.85	0.73	0.38	0.74
SCS3	0.10	0.60	0.84	0.94	0.99	0.97	0.83	0.69	0.29	0.70
SCS4	-0.05	0.51	0.79	0.91	0.97	0.96	0.80	0.65	0.20	0.64
AVM	0.46	0.72	0.81	0.85	0.86	0.84	0.79	0.72	0.45	0.72
AVM-B	-1.29	-0.59	-0.20	-0.02	0.16	0.30	0.45	0.55	0.73	0.01
HRU 1/72 24-hour	0.18	0.61	0.81	0.89	0.93	0.95	0.92	0.85	0.63	0.75
Triangular ObsTP	0.75	0.88	0.92	0.93	0.93	0.92	0.89	0.86	0.77	0.87
Triangular Median TP	0.36	0.72	0.87	0.91	0.93	0.92	0.86	0.78	0.52	0.76
Knoesen	0.52	0.46	0.55	0.60	0.63	0.61	0.77	0.97	0.96	0.68

It can be seen that relatively high NSE values are displayed for each approach, particularly for the higher percentiles. An exception to this is the AVM-B which displays values indicative of overall poor performance. The results characterised by the NSE values are slightly different to those of the MARE and Σ MARE values previously shown, especially by the mean NSE values. The Knoesen model is shown to be the second least accurate RTD approach, based on approximation of the Huff curve temporal distributions, according to the NSE values. This is despite the result shown by the MARE values, which indicated that the Knoesen model was the best performing. However, the NSE values do provide a fair indication that there is a discernible difference between the observed Huff curves and the Huff curves derived from the disaggregated rainfall produced by each approach.

4.10 Chapter Discussion and Conclusions

The pilot study involved the analysis of daily rainfall data from Station C161 in Cedara, KwaZulu-Natal. Relationships for the distribution of rainfall over and daily rainfall durations were determined. Following analysis of the observed rainfall data, selected RTD approaches, identified from literature for their suitability to the scope of this study, were applied to disaggregate the daily rainfall total depths.

Key trends in the analysis of daily rainfall showed a low correlation between peak intensity and total depth. It should be noted that the highest rainfall intensity in a 15-minute duration for the 24-hour daily rainfall period was used as the peak intensity for the day. This peak is not the same as the peak generally utilised in studies relating to rainfall events. Rainfall events may occur across multiple rainfall days or occur multiple times within a 24-hour daily period. Rainfall days were found to display the highest proportion of peaks intensities in the second and third quartiles. Hence, they are more likely to peak towards midday or in the afternoon. Furthermore, the majority of rainfall days displayed totals between 10 mm to 20 mm.

In general, the RTD approaches did not perform well at maintaining the peak intensity values, as indicated by poor correlation values, underestimation and overestimation bias (PBIAS). However, some of the approaches performed relatively well in approximating the general temporal distribution of rainfall displayed by the observed Huff curves, in terms of the MARE values for each percentile and the \sum MARE value, which represented performance across all percentiles. This was slightly contrasted by the relatively fair performance indicated by the NSE values for higher percentiles, with some exceptions such as for the AVM-B. However, the NSE values did highlight that on average, across percentiles, there is a discrepancy between the observed rainfall Huff curves and disaggregated Huff curves. The MARE values are more suited to direct comparison between the Huff curves, as they do not relate to the 1:1 line, but rather the direct difference in fractions of rainfall displayed at each fraction of the duration, which is similar to the PBIAS values used for peak intensity comparisons. Therefore, the MARE values and \sum MARE values across percentiles, are utilised as the main means of assessment of performance, in addition to graphical analysis of the Huff curves.

The Triangular ObsTP distribution performed relatively well. However, the Triangular ObsTP distribution was developed using the location of peak intensities obtained from the observed data. This bias was removed through using a generalised timing of the peak for the Triangular Median TP distribution. This approach was also found to perform well with a relatively low \sum MARE, despite being higher than other approaches. The poor performance of the AVM and AVM-B may be attributed to the use of rainfall days with the highest total depths in their development. These are not representative of the temporal distributions displays by lower and medium total depth rainfall days, which make up the majority of the dataset.

The Knoesen model was found to perform the best out of the disaggregation model approaches when using disaggregating daily rainfall. The SCS4 distribution performed the best for the rainfall days out of all the approaches, followed second by the SCS3. The rainfall station is located in a region where the SCS3 is recommended, however, it is also close to a SCS4 region. The SCS4 region may need to be adjusted as other areas that are classified as being within an SCS3 region may be better characterised by the SCS4 distribution. Based on the results obtained, the Knoesen Model and Triangular ObsTP distribution performed well when disaggregating daily rainfall. However, the performance of the Knoesen model will be influenced by the stochastically distribution generated as it is a semi-stochastic approach. Generating multiple hyetograph variations for each rainfall day in future studies may result in different trends in performance.

The performance of these approaches will be further tested on data from additional rainfall stations, each from a different relatively Homogenous region. This will be performed to assess their potential for application in areas with different rainfall characteristics than the pilot site.

5. APPLICATION OF RTD APPROACHES: ALL SITES

The daily rainfall data for 14 additional rainfall stations, with one station selected from each of the 15 homogenous rainfall clusters as described in Chapter 3, were used for the application of RTD approaches using the same methodologies outlined in Chapter 4. This was undertaken to further assess the performance of the selected approaches for the disaggregation of rainfall data in different climatic locations in South Africa. This chapter contains the results of the application of the RTD approaches on the data from the 14 additional rainfall stations, analysis and discussion of the trends between results for each station. Selected sites from the additional 14 will be shown individually as examples and the overall results and trends will then be shown for all of the stations.

5.1 Performance of Disaggregation Approaches

The characteristics of the rainfall days from each station, which influence some of the relationships displayed in the results, were shown in Section 3.3.1. Huff curves were developed for the observed and disaggregated rainfall depths. The 50th percentile observed rainfall Huff curves derived using the observed 15-minute rainfall depths for each rainfall day from each station are shown in Figure 5.1.

The performance of the RTD approaches were assessed using MARE and \sum MARE values, as detailed in Equation 3.1 and Equation 3.2. \sum MARE values, which reflect the cumulative difference between observed and disaggregated Huff curves, serve as the overall standard for selection of the most suitable and least suitable RTD approaches for each rainfall station. In addition, NSE values were computed to indicate the level of approximation of the generalised temporal distribution (Huff curves) derived from disaggregated rainfall to those of the observed rainfall. NSE values were derived according to Equation 3.3. A comparison of the peak intensities between the observed and disaggregated rainfall days was also performed, utilising PBIAS values according to Equation 3.4, as well as Pearson and R^2 correlation coefficients.

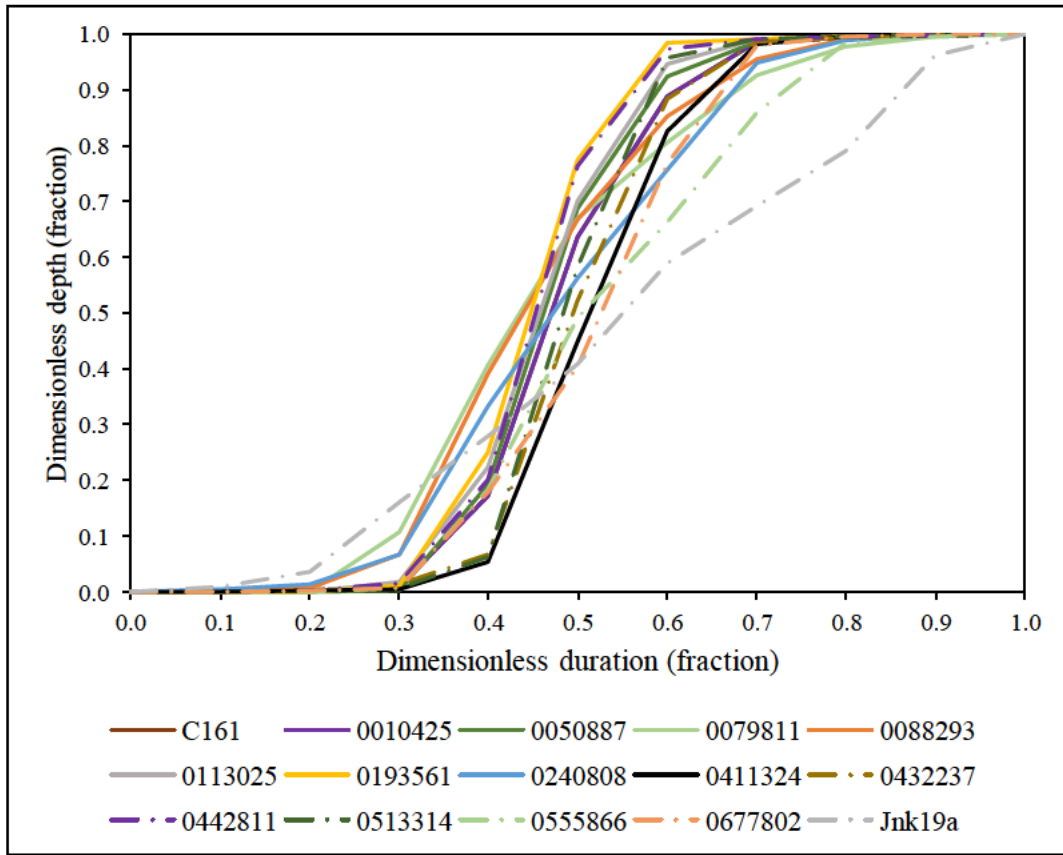


Figure 5.1 50th percentile Huff curves derived from observed daily rainfall at each station

It can be seen that the 50th percentile Huff curves for all the rainfall stations used in this assessment are similar in shape and distribution of rainfall. Some clear differences are seen for Station Jnk19a and Station 0555866 in the later sections of the duration, which display a greater proportion of rainfall later in the rainfall day. However, generally, the distribution displays a peak between the second and third quartiles of the daily rainfall 24-hour duration. Due to the similarities between the curves, the approach which displays the overall best performance in terms of the lowest $\sum \text{MARE}$ values and best NSE values across the different rainfall stations may be considered as suitable for representing rainfall distributions characteristic of those displayed by the Huff curves.

5.1.1 Station 0555866

The selected RTD approaches were applied to disaggregate rainfall days from Station 0555866. This was performed according to the same methodology utilised in Chapter 4. Daily rainfall peak intensity values were compared between observed and disaggregated data, as shown in Table 5.1. The direct comparison between Huff curves is given by the Σ MARE values in Figure 5.2 and the NSE values in Table 5.2.

Table 5.1 Comparison between observed and disaggregated peak intensities for Station 0555866 rainfall days

RTD Approach	R ² Correlation	Pearson correlation	PBIAS (%)
SCS1	0.25	0.50	-59.90
SCS2	0.25	0.50	-37.90
SCS3	0.25	0.50	-9.00
SCS4	0.25	0.50	15.40
AVM	0.25	0.50	-90.00
AVM-B	0.25	0.50	-31.20
HRU 1/72	0.25	0.50	-91.40
Triangular ObsTP	0.25	0.50	-92.20
Triangular Median TP	0.25	0.50	-92.20
Knoesen	0.12	0.34	-51.20

As shown by the correlation coefficients and PBIAS, the daily peak intensity values of the disaggregated rainfall days are not similar to those of the observed rainfall days. Overestimation bias is seen for each approach, with the exception of SCS4. Hence, for this station, as was seen for the pilot study, RTD approaches do not produce disaggregated rainfall with accurate peak intensity values.

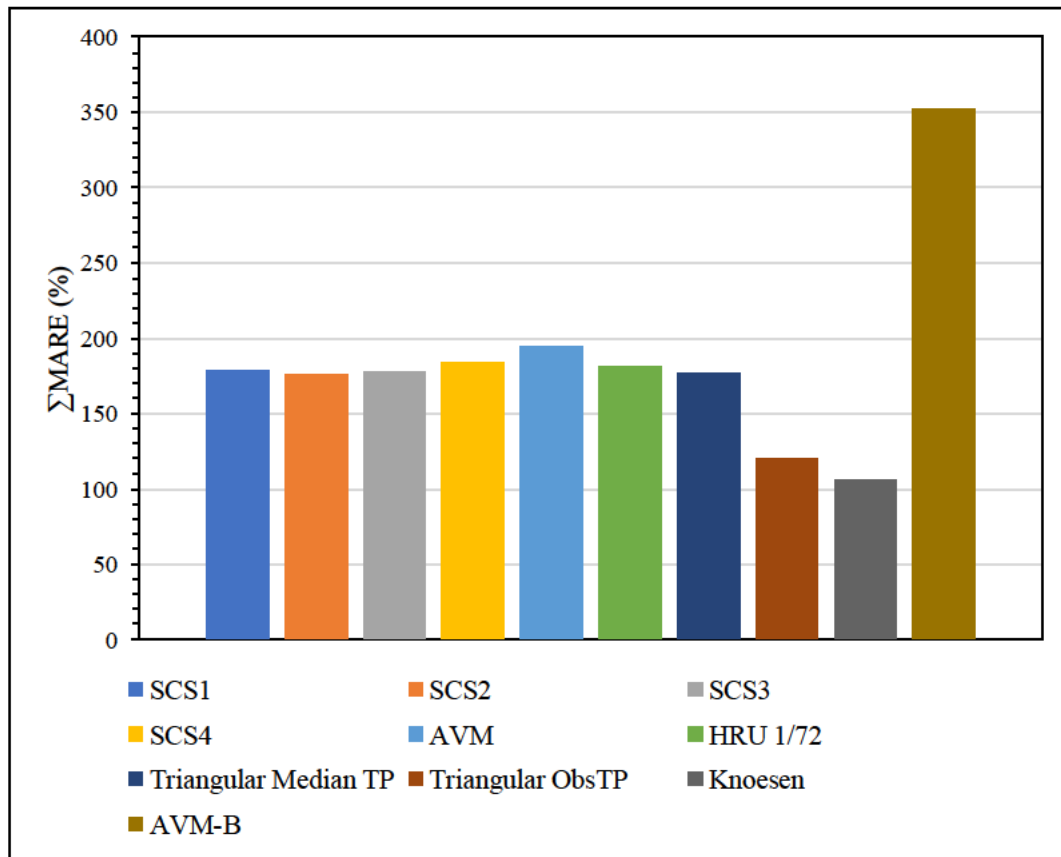


Figure 5.2 Σ MARE values for Station 0555866

Rainfall Station 0555866 is located in a summer rainfall region and SCS-SA rainfall region 2. It can be seen that the method with the lowest Σ MARE value, and hence the best performing approach for the station, is the Knoesen model. This is followed by the Triangular ObsTP approach, which displays the second lowest Σ MARE. However, as detailed in Chapter 3, this approach utilises the observed timing of the peak, which results in greater accuracy over the other RTD approaches. The Triangular Median TP which has less bias compared to the Triangular ObsTP, does not perform as well. However, it displays a similar Σ MARE to the SCS2, which is the best performing out of the SCS-SA distributions for this station. The performance of the SCS2 compared to the other SCS-SA distributions may be attributed to the station being located in SCS-SA Region 2.

Table 5.2 NSE values for comparison of observed and disaggregated Huff curves for 0555866 rainfall days

RTD approach	NSE for each Percentile									Mean
	10 th	20 th	30 th	40 th	50 th	60 th	70 th	80 th	90 th	
SCS1	-0.36	0.23	0.68	0.84	0.96	0.96	0.89	0.57	-0.13	0.51
SCS2	-0.52	0.12	0.63	0.81	0.95	0.95	0.87	0.53	-0.22	0.46
SCS3	-0.78	-0.05	0.53	0.75	0.92	0.92	0.83	0.45	-0.38	0.35
SCS4	-1.02	-0.22	0.43	0.68	0.87	0.87	0.77	0.36	-0.53	0.25
AVM	0.00	0.50	0.80	0.87	0.89	0.84	0.73	0.39	-0.21	0.53
AVM-B	-2.41	-1.43	-0.69	-0.44	-0.12	0.11	0.37	0.63	0.81	-0.35
HRU 1/72 24-hour	-0.62	0.05	0.56	0.74	0.91	0.97	0.96	0.74	0.15	0.50
Triangular ObsTP	0.49	0.67	0.87	0.92	0.95	0.96	0.96	0.84	0.55	0.80
Triangular Median TP	-0.30	0.28	0.70	0.84	0.95	0.96	0.90	0.62	-0.03	0.55
Knoesen	0.82	0.73	0.83	0.75	0.78	0.68	0.58	0.74	0.97	0.76

The mean NSE values for the station 0555866 rainfall stations appear more supportive of the results shown by the \sum MARE values than was seen for the results of the pilot study station data. The NSE values show that overall, the Knoesen model performs the best, with fair approximation of the observed temporal distributions throughout each percentile. Another noteworthy result is that the Triangular Median TP appears to perform the best out of the fixed distribution approaches, excluding the Triangular ObsTP. Therefore, the potential for use of a Triangular distribution which utilises a generalised timing of the peak is highlighted.

5.1.2 Station Jnk19a

The results for the application of the RTD approaches to disaggregate daily rainfall data from Station Jnk19a are detailed in this section. Peak intensity comparisons are given in Table 5.3, while \sum MARE values are can be seen in Figure 5.3. The NSE values for the comparison of the observed and disaggregated data Huff curves are shown in Table 5.4.

Table 5.3 Comparison between observed and disaggregated peak intensities for Jnk19a rainfall days

RTD Approach	R ² Correlation	Pearson correlation	PBIAS
SCS1	0.29	0.54	-10.40
SCS2	0.29	0.54	38.70
SCS3	0.29	0.54	103.30
SCS4	0.29	0.54	157.80
AVM	0.29	0.54	-82.70
AVM-B	0.29	0.54	-48.20
HRU 1/72	0.29	0.54	-80.80
Triangular ObsTP	0.00	0.02	-86.00
Triangular Median TP	0.00	0.02	-86.00
Knoesen	0.22	0.46	-8.50

It can be seen that for poor representation of daily peak intensity values in the disaggregated rainfall is displayed for Station Jnk19a as well. Considerable overestimation bias is seen for most approaches. However, the SCS3 and SCS4 display underestimation bias. The Knoesen model and SCS1 appear to perform fairly well, relative to the other RTD approaches.

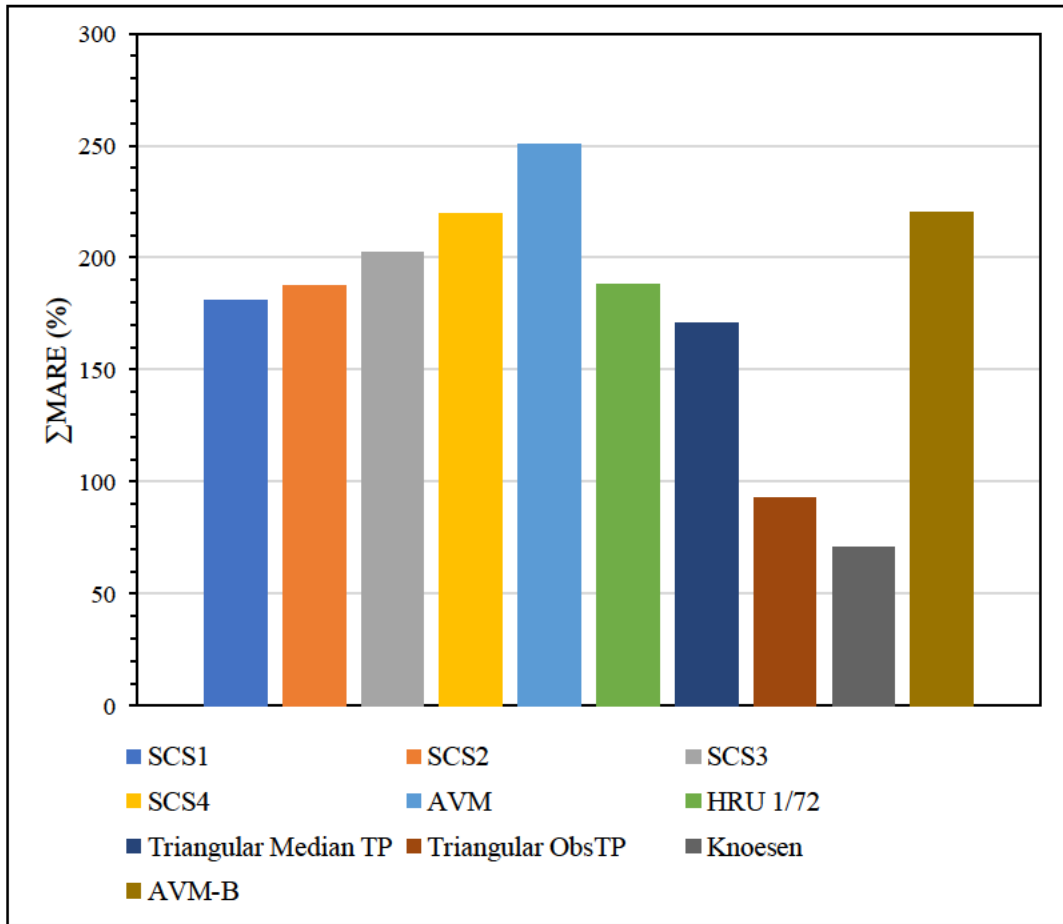


Figure 5.3 Σ MARE values for Station Jnk19a

The rainfall Station Jnk19a is located in a winter rainfall region, also in SCS-SA region 2 and displays considerably different trends in Σ MARE values for RTD approaches compared to Station 0555866. The best performing approaches are the Knoesen model, Triangular ObsTP and Triangular Median TP, respectively. The Σ MARE values for the Knoesen model and Triangular ObsTP are lower than those for Station 0555866. Furthermore, the values for the AVM and SCS4 approaches are relatively higher. However, the AVM-B presents a lower Σ MARE for this station. An additional difference in the trends in Σ MARE values is that the SCS-SA approaches, HRU 1/72 24-hour and Triangular Median TP do not perform similarly, which they did for Station 0555866. Furthermore, despite the station being located in a SCS2 region, SCS1 displays the lowest Σ MARE value out of the SCS-SA distributions.

Table 5.4 NSE values for comparison of observed and disaggregated Huff curves for Jnk19a rainfall days

RTD approach	NSE for each Percentile									Mean
	10 th	20 th	30 th	40 th	50 th	60 th	70 th	80 th	90 th	
SCS1	-0.89	-0.31	0.40	0.72	0.91	0.97	0.86	0.64	0.21	0.39
SCS2	-1.10	-0.47	0.30	0.64	0.85	0.93	0.81	0.59	0.12	0.30
SCS3	-1.41	-0.73	0.14	0.51	0.73	0.84	0.71	0.48	-0.03	0.14
SCS4	-1.69	-0.96	-0.02	0.38	0.61	0.74	0.61	0.36	-0.18	-0.02
AVM	-2.18	-1.42	-0.49	0.00	0.44	0.75	0.93	0.99	0.93	-0.01
AVM-B	0.82	0.91	0.90	0.80	0.60	0.28	-0.16	-0.71	-1.48	0.22
HRU 1/72 24-hour	-1.21	-0.57	0.21	0.59	0.85	0.98	0.95	0.79	0.43	0.34
Triangular ObsTP	0.38	0.60	0.85	0.94	0.98	1.00	0.98	0.91	0.83	0.83
Triangular Median TP	-0.42	0.08	0.65	0.87	0.98	0.96	0.78	0.49	-0.02	0.49
Knoesen	0.96	0.94	0.89	0.91	0.89	0.92	0.89	0.88	0.89	0.91

Similar results as were displayed by the \sum MARE values are shown by the NSE values in terms of the performance of the RTD approaches in providing accurate temporal distributions of rainfall. Overall, the Knoesen model provides the best performance, while the other approaches utilised provide relatively weak performances.

5.1.3 Results for all selected rainfall stations

Trends for all of the rainfall stations with regards to the performance of RTD approaches, as given by \sum MARE values, are shown in Table 5.5 and Figure 5.4. The overall performance across all sites was assessed by summing \sum MARE values for each RTD approach for all stations. The \sum MARE values for each approach, summed for all stations are shown in Figure 5.5. The computed mean NSE values for the results of each approach, for all stations can be seen in Table 5.6.

Table 5.5 Total MARE values for each RTD approach per station

Rainfall station	\sum MARE (%)									
	SCS1	SCS2	SCS3	SCS4	AVM	AVM-B	HRU 1/72 24-hour	Triangular ObsTP	Triangular Median TP	Knoesen
C161	140.6	130.2	121.5	120.9	171.2	281.8	142.7	114.2	145.7	125.2
0010425	174.0	173.1	178.9	190.4	187.8	249.2	171.8	107.8	172.3	25.1
0050887	150.4	139.8	131.9	130.6	188.4	380.7	151.0	120.0	154.8	103.1
0079811	141.7	138.0	139.6	148.5	218.7	262.8	136.3	40.5	139.6	40.5
0088293	170.6	164.7	164.0	170.6	181.4	333.6	166.5	40.5	170.6	40.5
0113025	169.2	159.7	152.1	151.0	162.3	225.8	168.8	131.7	173.1	84.3
0193561	159.5	149.0	137.9	134.7	195.4	334.5	157.3	127.7	164.4	135.1
0240808	168.2	167.3	169.3	177.7	174.0	323.7	166.7	112.8	166.6	112.1

Rainfall station	Σ MARE (%)									
	SCS1	SCS2	SCS3	SCS4	AVM	AVM-B	HRU 1/72 24-hour	Triangular ObsTP	Triangular Median TP	Knoesen
0411324	167.9	157.6	151.1	149.3	201.8	377.1	172.6	131.7	168.9	84.3
0432237	173.2	164.2	158.4	158.3	247.5	243.1	178.8	133.7	175.8	133.7
0442811	138.5	124.6	111.8	108.9	183.0	321.4	136.4	118.3	144.7	149.0
0513314	146.7	133.5	121.2	117.0	181.7	290.7	151.2	126.8	154.2	96.0
0555866	178.7	175.9	177.6	183.9	195.2	352.6	181.2	120.8	176.9	105.7
0677802	181.7	174.2	170.3	170.1	186.9	274.6	184.9	134.0	184.6	68.0
Jnk19a	181.3	187.8	202.4	219.6	250.8	220.0	188.3	93.0	171.1	70.9

It should be noted that for purposes of showing the overall performance of the SCS-SA approach, the SCS-SA distribution which was recommended for the region in which a particular station was located is utilised for the results shown in Figure 5.4. For example, SCS3 is recommended for Station C161, therefore, the Σ MARE shown for Station C161 is that of the SCS3 distribution, as indicated by the SCS label. The results are presented in a similar manner for Figure 5.5, where the SCS MARE values for each station (as given by the recommended SCS-SA distribution) are summed across all 15 stations to present the overall performance of the SCS-SA method in this assessment.

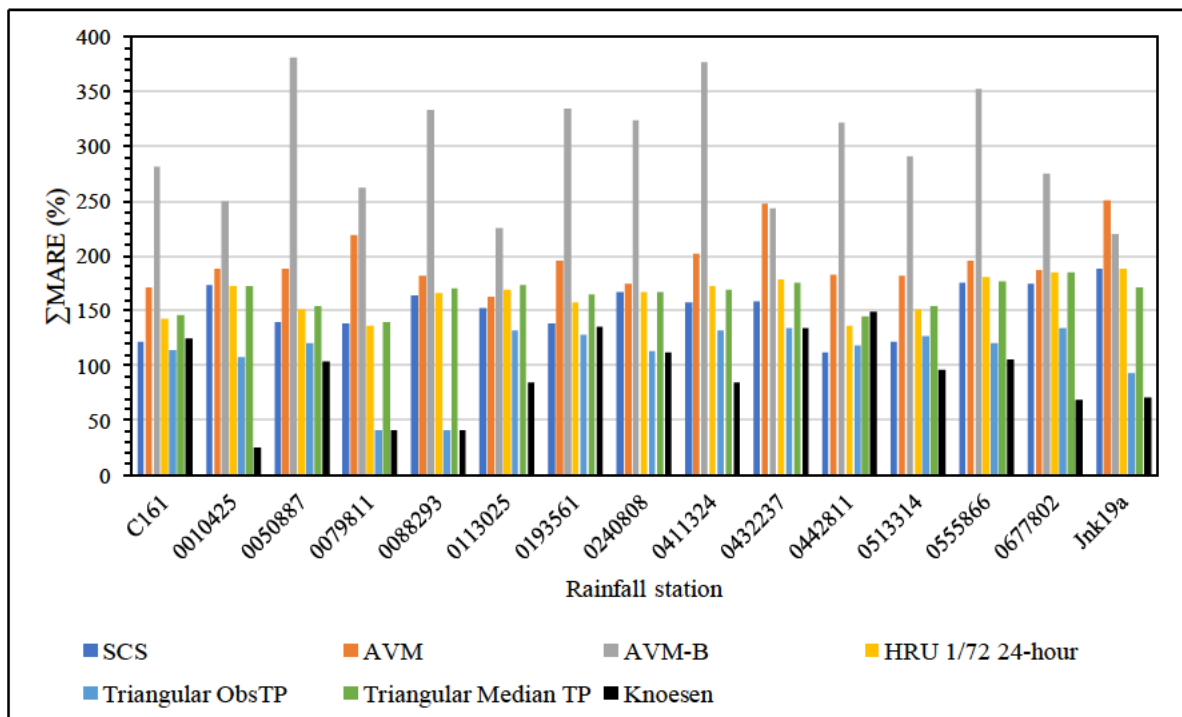


Figure 5.4 Σ MARE values per RTD approach for each rainfall station

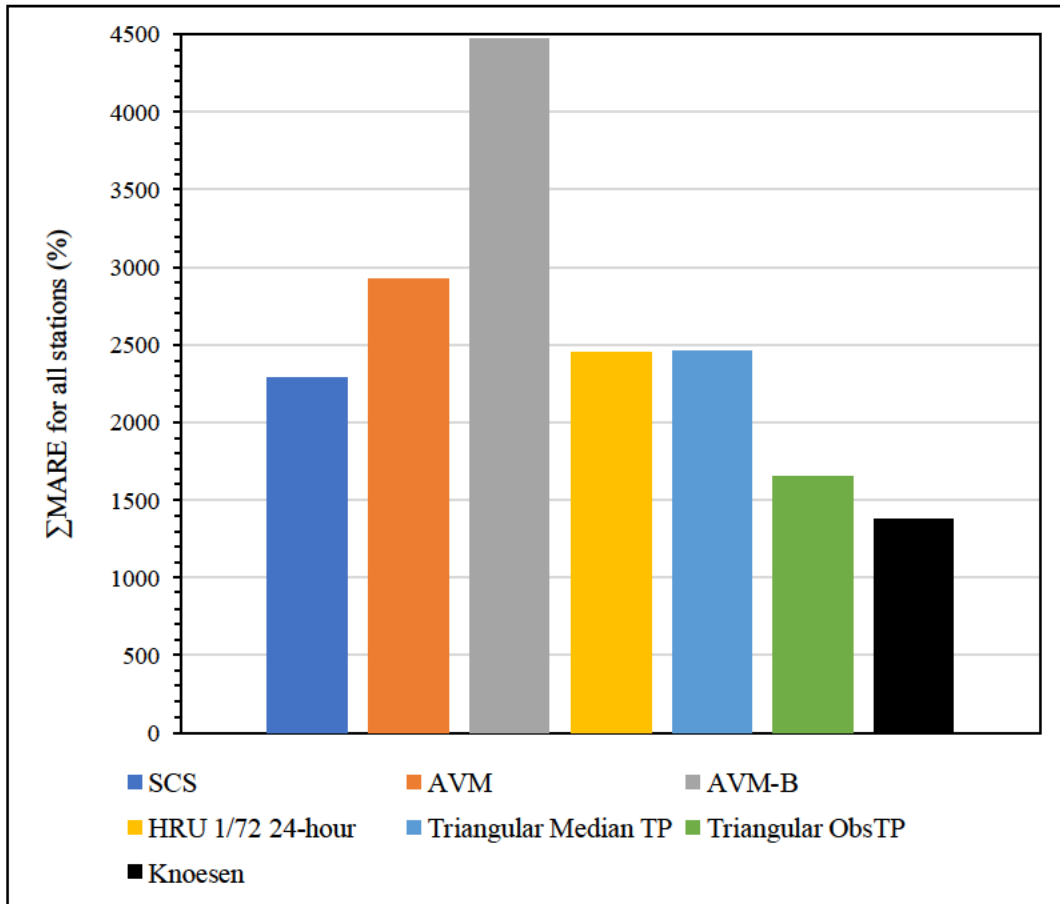


Figure 5.5 Σ MARE values for RTD approaches summed across all stations

The approach which provides the least realistic rainfall temporal distribution in terms of the Huff curves appears to be the AVM-B, followed by the AVM distribution. It can be seen that for all of the rainfall stations, the approaches which generally display the lowest Σ MARE values are the Knoesen, Triangular ObsTP and SCS. It is acknowledged that the good performance of the Triangular ObsTP can be attributed to the methodology used in its application. The approach was applied using available timing peak intensity for each application, which improves the performance in approximating the observed daily rainfall temporal distribution. The version of the approach which utilises a generalised timing of the peak intensity value and hence removes this bias, the Triangular Median TP distribution, does not perform as well and often displays relatively high Σ MARE values. Given the abovementioned factors, it can be said that the RTD approach which results in the best overall performance for the disaggregation daily rainfall totals into realistic temporal distributions is the Knoesen semi-stochastic disaggregation model, followed by the SCS-SA.

Table 5.6 Mean NSE values for each approach for each rainfall station

Rainfall station	Mean NSE for each method									
	SCS1	SCS2	SCS3	SCS4	AVM	AVM-B	HRU 1/72 24-hour	Triangular ObsTP	Triangular Median TP	Knoesen
C161	0.76	0.74	0.70	0.64	0.72	0.01	0.75	0.87	0.76	0.68
0010425	0.52	0.46	0.35	0.24	0.52	0.35	0.53	0.46	0.56	0.96
0050887	0.70	0.68	0.62	0.55	0.62	-0.54	0.68	0.84	0.70	0.77
0079811	0.72	0.69	0.61	0.53	0.53	0.31	0.73	0.97	0.74	0.97
0088293	0.54	0.50	0.41	0.31	0.48	-0.18	0.55	0.96	0.57	0.96
0113025	0.58	0.54	0.47	0.39	0.54	0.38	0.58	0.79	0.59	0.83
0193561	0.66	0.64	0.58	0.52	0.48	-0.05	0.67	0.83	0.67	0.64
0240808	0.53	0.47	0.37	0.26	0.49	-0.61	0.53	0.81	0.55	0.77
0411324	0.64	0.61	0.54	0.46	0.42	-0.43	0.61	0.81	0.66	0.85
0432237	0.54	0.50	0.42	0.34	0.20	0.32	0.51	0.78	0.56	0.78
0442811	0.78	0.77	0.74	0.69	0.61	-0.06	0.78	0.87	0.78	0.61
0513314	0.74	0.73	0.69	0.63	0.66	0.26	0.72	0.85	0.74	0.77

Rainfall station	Mean NSE for each method									
	SCS1	SCS2	SCS3	SCS4	AVM	AVM-B	HRU 1/72 24-hour	Triangular ObsTP	Triangular Median TP	Knoesen
0555866	0.51	0.46	0.35	0.25	0.53	-0.35	0.50	0.80	0.55	0.76
0677802	0.51	0.46	0.37	0.28	0.46	-0.05	0.48	0.79	0.53	0.86
Jnk19a	0.39	0.30	0.14	-0.02	-0.01	0.22	0.34	0.83	0.49	0.91

The mean NSE values shown in Table 5.6 are reflective of the results which have been previously shown by the Σ MARE values. Overall, the Knoesen model is RTD approach which provides the temporal distributions of that are most similar to those of the observed daily rainfall data. SCS-SA distributions also perform relatively well for stations in their respective recommended regions. However, some exceptions noted previously are seen, in cases where an SCS-SA distribution not recommended for the region may outperform the recommended distribution. It should also be noted, that relatively fair performance is shown by the Triangular Median TP approach is displayed as well, which outperforms other approaches in some instances and for certain percentiles.

5.2 Chapter Discussion and Conclusions

The analysis of the trends in the timing of the peak intensity of the rainfall days from each station revealed that the majority of rainfall days display peaks in the second and third quartiles. Hence approaches which time the peak intensity in similar sections of the duration are likely to perform better at disaggregating rainfall. Furthermore, as with the data used in the pilot study, rainfall days mainly fall within the 10-20 mm and 20-40 mm ranges of total depth.

The RTD approaches were applied to disaggregate daily rainfall data from 14 additional rainfall stations. It was generally found that the fixed distribution approaches were the least successful at characterising the general temporal distribution of rainfall as presented by the Huff curves developed using the daily rainfall observed 15-minute depths. Considering this, the overall best performing RTD approach for disaggregating daily rainfall into sub-daily rainfall which displays realistic temporal distributions is the Knoesen semi-stochastic disaggregation model. This was indicated by both the Σ MARE values and the NSE values utilised for comparison of the approaches. This was a different trend to that which was seen for the results of the pilot study, in which the Knoesen model was outperformed by the SCS-SA distributions. The performance of the Triangular Median TP was found to be similar to that which was displayed by the SCS-SA approaches and HRU 1/72 24-hour distribution. Further adjustment of the Triangular Median TP approach through development of ranges of values for use in the timing of the peak and regionalisation may yield an improvement in results.

It should be noted that no particular approach performed well at providing disaggregated data with accurate daily rainfall peak intensities. This is a limitation, despite the selected approaches providing relatively good temporal distributions of rainfall. Further assessments into what factors may influence accurate estimation of peak intensity values in disaggregated data may need to be performed in future studies. Adjustments may need to be made to the structure of RTD approaches in order to improve peak intensity estimation in disaggregated data. Furthermore, there is a need to investigate the impact which the peak rainfall intensity estimates resulting from each disaggregation approach may have of Design Flood Estimates.

6. DISCUSSION, CONCLUSIONS AND RECOMMENDATIONS

6.1 Overview

Design Flood Estimation (DFE) and other forms of hydrological modelling is required for the design of hydraulic structures and water resources management. Numerous rainfall-runoff models which are used in DFE require the generation of a hyetograph from rainfall data. DFE generally utilises daily rainfall data which is abundantly available in South Africa. Rainfall is highly variable both temporally and spatially. The temporal distribution of rainfall influences the magnitude and timing of peak charges and is of substantial importance to improvement of modelling, such as through the use of CSM approaches which need to be representative of processes at finer temporal scales. Improving the accuracy of modelling and simulation approaches requires data to be available in finer resolutions. However, sub-daily and sub-hourly rainfall data are not as readily available as daily rainfall. Sub-daily rainfall stations are relatively sparse and have shorter record lengths compared to daily rainfall stations, both in South Africa and internationally. Therefore, a means of disaggregating daily rainfall data into sub-daily rainfall hyetographs is required. RTD approaches may be utilised to disaggregate daily rainfall data into shorter temporal resolutions (time steps) from higher temporal resolution data, thereby extending record lengths and improving data availability.

The number of RTD approaches applied in South Africa is relatively limited compared to those which have been developed and applied international. The overall aim of this study was to assess the performance of various RTD methods and to recommend the adoption or adaptation of one or more of these approaches for application under South African conditions. The following objectives needed to be met for this aim to be achieved:

- Reviewing literature on disaggregation approaches.
- Acquiring an understanding of previously used methods as well as recently developed approaches.
- Assessing the performance of selected methods using South African daily rainfall data, either in their original form or as adapted methods.
- Recommendation of suitable options for adoption, adaptation or development of a regionalised rainfall disaggregation method(s) for design flood estimation in South African.

6.2 RTD Approaches Applied in South Africa

An extensive literature review was conducted to identify RTD approaches applied in South Africa and internationally, which is detailed in Chapter 2. The literature review revealed that RTD approaches can be classified into two broad categories, which encompass rainfall distribution curves or disaggregation models. Rainfall distribution curves are generally fixed distributions which provide a generalised temporal resolution for different durations of rainfall events, including 24-hourly periods. Disaggregation models can either be stochastic or deterministic in nature. An element of randomness may be introduced into the temporal distributions derived, as a result of the stochastic design of some approaches. Several RTD approaches have been applied in South Africa, including the SCS-SA distributions, Huff curves, Knoesen semi-stochastic disaggregation model and Triangular distribution. However, application of RTD approaches locally is relatively limited, both in terms of diversity of approaches and number of application, compared to those developed and applied internationally. Therefore, a need exists to further assess the performance of locally applied approaches as well update the list of available approaches through inclusion of internationally developed and applied RTD techniques. This forms the focus of this study in which selected locally applied and internationally applied approaches were applied to disaggregated daily rainfall data into depths which provide realistic temporal distributions.

6.3 Application and Performance of Selected Approaches

A pilot study was used to develop procedures to apply the methods and to develop performance indices to assess and compare the performance of the methods. Prior to application of the RTD approaches, 24-hour rainfall totals were computed from the available 15-minute digitised rainfall data for 08:00 to 08:00 periods for 15 rainfall stations, with one for each of the homogenous rainfall clusters, as outlined in Chapter 3. The rainfall daily totals were generally found to be between 10-20 mm and 30-40 mm in total depth and displayed the highest 15-minute rainfall intensity in either the second or third quartiles of the 24-hour duration. Station C161 data was used for the pilot study. Rainfall days were analysed for relationships in peak intensity, total depths and time-to-peak as a fraction of the total duration as detailed in Chapter 4. It was generally found that a low correlation existed between the timing of the peak and total depth. However, peak intensities generally occurred towards in the second and third quartiles, which was also seen for the other rainfall stations.

The approaches which were applied to disaggregate daily rainfall depths were the SCS-SA, HRU 1/72 24-hour, Triangular ObsTP, Triangular Median TP, AVM, AVM-B and Knoesen model, as detailed in Chapter 4. The results of the application of the RTD approaches revealed that generally, the approaches did not perform well in preserving the peak intensity values, with underestimation and overestimation bias shown in by the PBIAS values, seen for different approaches, and poor correlation coefficients. However, this did not translate into poor performance at producing temporal distributions which were similar to those of the observed data. Huff curves which provide generalised temporal distributions of rainfall depths were utilised for comparison of the observed and disaggregated rainfall depths. Furthermore, MARE, \sum MARE and NSE values served as indices for the quantifying the difference between Huff curves developed using observed depths and those developed from the disaggregated depths, as detailed in Chapter 3 and Chapter 4.

The Huff curves developed from daily rainfall disaggregated using the Knoesen model, SCS3, SCS4 and Triangular distribution performed well in approximating the observed Huff curves for the pilot study. Good performance of the Triangular ObsTP distribution was attributed to the inclusion of observed parameters in its application. However, the Triangular Median TP did not perform as well. The Triangular Median TP was developed using a generalised timing of the peak and the observed e durations in order to remove part of the performance bias of the Triangular ObsTP. Overall, the best performing approach for the disaggregating daily rainfall was the SCS4, despite the station falling within a SCS3 region. The approaches which performed well displayed peak intensities in the same quartiles of the duration as the observed rainfall days, hence, the timing of the peak intensity has a considerable influence on the accuracy of the distribution. The stochastic nature of the Knoesen model may be a disadvantage in this case, as the peak location varies for each stochastically generated distribution. Furthermore, as the methods do not preserve peak values well, the peak intensity value itself does not appear to greatly influence the accuracy of the resulting dimensionless distributions produced from disaggregated data.

The RTD approaches were further assessed using data from the remaining 14 rainfall stations for their performance in producing realistic daily rainfall temporal distributions. The approaches were applied using the same methodology as per the pilot study detailed in Chapter 4. It was found that the 50th percentile Huff curves derived from the observed 15-minute data for each station were similar in terms of the temporal distributions which they

presented. This can be attributed to the similarities in the timing of the peak intensities of rainfall days for all stations, which were determined to generally be between the second and third quartiles of the duration. Due to the similarities in temporal distribution displayed by the Huff curves, it was discerned that the approaches which were found to perform well at characterising the distributions would be similar for each station. Furthermore, the approaches would also perform well in future applications for stations which display similar generalised temporal distributions.

The results of the assessment of the RTD approaches according to \sum MARE and NSE values, as given in Chapter 5, were different to those seen for the pilot study. The best performing RTD approaches were found to be the SCS-SA and Knoesen model, when the Triangular ObsTP is appropriately excluded. However, the Triangular Median TP displayed fair performance and shows potential for further investigation into general use. Overall, the Knoesen model provided the lowest \sum MARE values and most appropriate NSE values across all stations and can therefore be considered the most suitable approach for disaggregating daily rainfall into realistic temporal distributions. In the case of the \sum MARE values of the recommended distribution were utilised for the final comparison, as detailed in Chapter 5. However, a finding was that in certain cases the recommended SCS-SA distribution for a station was outperformed by one which was recommended for a different region. This may be explained by some of the stations being located at the edge of one region, in close proximity to another region. The AVM and AVM-B approaches, which were adapted from the original application of the AVM in literature, performed exceptionally poorly and are therefore not recommended for use in disaggregation in the forms utilised in this assessment. However, it is noted that the AVM is no longer recommended as a temporal distribution in Australia due to limitations relating to the averaging of the distribution and use of high rainfall periods for its construction.

The objectives of this study were met through conduction of the literature review, selection and application of RTD approaches and analysis of the trends and results from both the pilot study and the application on data from additional rainfall stations. Furthermore, approaches have been recommended for usage in future studies and applications, as discussed above. In meeting the objective of this study, the overall aim has been achieved. Limitations of the study are acknowledged, which may be addressed in recommended future research.

6.4 Recommendations

The limitations of this research study can be attributed to the assumptions made, the methodology used for identifying rainfall days and the modifications made to the RTD approaches for application. The Triangular distribution approaches, including the Triangular ObsTP and Triangular Median TP, have shown considerable potential for providing a similar temporal distribution to observed daily rainfall in terms of the shape of the distribution when the observed value for the timing of the peak is utilised. Therefore, it is recommended that the approach be further developed using generalised values for the timing of the peak. This will require relationships between depths and this parameter to be derived at regional levels.

It was found that each of the four SCS-SA distributions for daily rainfall generally performed similarly, despite being applied in regions for which they were not recommended. Furthermore, in some cases the appropriate distribution for a station within region was outperformed by a distribution for a different region. Hence, the SCS-SA distributions could potentially be adjusted on the edges of regions. This could involve a zone between regions where an intermediate distribution that characterises the daily distribution such that it is representative of a mix of both regions is available for use.

The influence of spatial distributions of rainfall on the results and the relationship with rainfall temporal disaggregation has not been explored in this study. It may be necessary to derive such relationships in future research, as it may influence the development of regionalised RTD approaches. Regionalisation of RTD approaches may require analysis of trends in storm patterns, the types of rainfall which different storm types are likely to produce, and additional climatic factors which may influence temporal distributions at regional scales. Incorporations of such factors may result in improvements to the estimation of peak intensity values when RTD approaches are applied. Furthermore, such regionalisation will allow for production of sub-daily rainfall for ungauged sites, where modelling is necessary.

7. REFERENCES

- Adamson, PT. 1981. *Southern African storm rainfall* Department of Environment Affairs: Directorate of Water Affairs Pretoria, South Africa.
- Arnaud, P, Fine, JA and Lavabre, J. 2007. An hourly rainfall generation model applicable to all types of climate. *Atmospheric Research* 85 (2): 230–242.
- ARR. 2015. *Project 3: Temporal Patterns of Rainfall* Australian Rainfall and Runoff (ARR), Engineers Australia Barton, Australia
- ARR. 2019. *A Guide To Flood Estimation*. Australian Rainfall and Runoff, Engineers Australia Commonwealth of Australia.
- Ball, JE. 1994. The influence of temporal patterns on catchment response. *Journal of Hydrology* 158 (3/4): 285–303
- Bhuiyan, T, Rahman, A and Abbey, S. 2010. Derivation of Design Rainfall Temporal Patterns in Australia's Gold Coast Region. *IKE*: 113-119.
- Bonta, JV. 2004. Development and utility of Huff curves for disaggregating precipitation amounts. *Applied Engineering in Agriculture* 20 (5): 641-653.
- Boughton, WC. 2000. *A Model for Disaggregating Daily to Hourly Rainfall for Design Flood Estimation*. Cooperative Research Centre for Catchment Hydrology, Monash University, Australia.
- Brunner, MI and Sikorska-Senoner, AE. 2019. Dependence of flood peaks and volumes in modeled discharge time series: Effect of different uncertainty sources. *Journal of Hydrology* 572 620-629.
- Burn, DH and Hag Elnur, MA. 2002. Detection of hydrologic trends and variability. *Journal of Hydrology* 255 (1-4): 107-122.
- Calver, A, Crooks, S, Jones, D, Kay, A, Kjeldsen, T and Reynard, N. 2004. *Flood Frequency Quantification for Ungauged Sites using Continuous Simulation: a UK approach*. Centre for Ecology & Hydrology, Wallingford, United Kingdom.
- Calver, A, Crooks, S, Jones, D, Kay, A, Kjeldsen, T and Reynard, N. 2005. *National river catchment flood frequency method using continuous simulation. R&D Technical Report FD2106/TR*. Centre for Ecology & Hydrology, Wallingford, United Kingdom.
- Carreau, J, Mhenni, NB, Huard, F and Neppel, L. 2019. Exploiting the spatial pattern of daily precipitation in the analog method for regional temporal disaggregation. *Journal of Hydrology* 568: 780-791.

- Chow, VT, Maidment, DR and Larry, W. 1988. *Applied Hydrology International Edition*. MacGraw-Hill, Inc, New York, NY, United States of America.
- Cowpertwait, PSP. 1991. Further Developments of the Neyman-Scott Clustered Point Process for Modeling Rainfall. *Water Resources Research* 27 (7): 1431-1438.
- Engida, AN and Esteves, M. 2011. Characterization and disaggregation of daily rainfall in the Upper Blue Nile Basin in Ethiopia. *Journal of Hydrology* 399 226-234.
- Entekhabi, D, Rodriguez-Iturbe, I and Eagleson, PS. 1989. Probabilistic Representation of the Temporal Rainfall Process by a Modified Neyman-Scott Rectangular Pulses Model: Parameter Estimation and Validation *Water Resources Research* 25 (2): 295-302.
- Frezghi, MS and Smithers, JC. 2008. Merged rainfall fields for continuous simulation modelling (CSM). *Water SA* 34 (5): 523-528.
- Frost, AJ, Srikanthan, R and Cowpertwait, PSP. 2004. *Stochastic generation of point rainfall data at subdaily timescales: a comparison of DRIP and NSRP*. Cooperative Research Centre for Catchment Hydrology, Monash University Australia.
- Glasbey, CA, Cooper, G and McGechan, MB. 1995. Disaggregation of daily rainfall by conditional simulation from a point-process model. *Journal of Hydrology* 165 (1-4): 1-9.
- Green, J, Walland, D, Nandakumar, N and Nathan, R. 2005. Temporal patterns for the derivation of PMPDF and PMF estimates in the GTSM region of Australia. *Australian Journal of Water Resources* 8 (2): 111-121.
- Güntner, A, Olsson, J, Calver, A and Gannon, B. 2001. Cascade-based disaggregation of continuous rainfall time series: the influence of climate. *Hydrology and Earth System Sciences* 5 (2): 145-164.
- Hassini, S and Guo, Y. 2017. Derived flood frequency distributions considering individual event hydrograph shapes. *Journal of Hydrology* 547: 296-308.
- Hingray, B and Ben Haha, M. 2005. Statistical performances of various deterministic and stochastic models for rainfall series disaggregation. *Atmospheric Research* 77 (1-4): 152-175.
- Hingray, B, Monbaron, E, Jarrar, I, Favre, AC, Consuegra, D and Musy, A. 2002. Stochastic generation and disaggregation of hourly rainfall series for continuous hydrological modelling and flood control reservoir design. *Water Science and Technology* 45 (2): 113-119.

- HRU. 1972. *Design Flood Determination in South Africa Report No. 1/72*. Hydrological Research Unit, University of the Witwatersrand Department of Civil Engineering South Africa
- Hu, P, Zhang, Q, Shi, P, Chen, B and Fang, J. 2018. Flood-induced mortality across the globe: Spatiotemporal pattern and influencing factors. *Science of the Total Environment* 643: 171-182.
- Huff, FA. 1967. Time Distribution of Rainfall in Heavy Storms. *Water Resources Research* 3 (4): 1007-1019.
- Huff, FA. 1990. *Time Distributions of Heavy Rain storms in Illinois*. Illinois State Water Survey, Champaign.
- Huff, FA and Angel, JR. 1992. *Rainfall frequency atlas of the Midwest*. Illinois State Water Survey, Champaign, Illinois.
- Knoesen, DM. 2005. The Development and Assessment of Techniques for Daily Rainfall Disaggregation in South Africa. . Unpublished thesis, School of Bioresources Engineering and Environmental Hydrology, University of KwaZulu-Natal Pietermaritzburg, South Africa
- Knoesen, DM and Smithers, JC. 2008. The development and assessment of a regionalised daily rainfall disaggregation model for South Africa. *Water SA* 34 (3): 323-330.
- Kossieris, P, Makropoulos, C, Onof, C and Koutsoyiannis, D. 2018. A rainfall disaggregation scheme for sub-hourly time scales: Coupling a Bartlett-Lewis based model with adjusting procedures. *Journal of Hydrology* 556: 980-992.
- Koutsoyiannis, D.2003. Rainfall disaggregation methods: Theory and applications. *Workshop on Statistical and Mathematical Methods for Hydrological Analysis*, Rome.
- Koutsoyiannis, D and Onof, C. 2001. Rainfall disaggregation using adjusting procedures on a Poisson cluster model. *Journal of Hydrology* 246 (1-4): 109-122.
- Koutsoyiannis, D, Onof, C and Howard, SW. 2003. Multivariate rainfall disaggregation at a fine timescale. *Water Resources Research* 39 (7):
- Lambourne, J and Stephenson, D. 1987. Model study of the effect of temporal storm distributions on peak discharges and volumes. *Hydrological Sciences* 32 (2): 215-226.
- Li, X, Meshgi, A, Wang, X, Zhang, J, Tay, SHX, Pijcke, G, Manocha, N, Ong, M, Nguyen, MT and Babovic, V. 2018. Three resampling approaches based on method of

- fragments for daily-to-subdaily precipitation disaggregation. *International Journal of Climatology* 38: e1119–e1138.
- Lisniak, D, Franke, J and Bernhofer, C. 2013. Circulation pattern based parameterization of a multiplicative random cascade for disaggregation of observed and projected daily rainfall time series. *Hydrology and Earth System Sciences* 17 (7): 2487-2500.
- Marsalek, J and Watt, WE. 1984. Design storms for urban drainage design. *Canadian Journal of Civil Engineering* 11 (3): 574-584.
- Moriassi, DN, Arnold, JG, Van Liew, MW, Bingner, RL, Harmel, RD and Veith, TL. 2007. Model Evaluation Guidelines for Systematic Quantification of Accuracy in Watershed Simulations *Transactions of the American Society of Agricultural and Biological Engineers* 50 (3): 885–900
- Müller, H and Haberlandt, U. 2018. Temporal rainfall disaggregation using a multiplicative cascade model for spatial application in urban hydrology. *Journal of Hydrology* 556: 847-864
- Na, W and Yoo, C. 2018. Evaluation of Rainfall Temporal Distribution Models with Annual Maximum Rainfall Events in Seoul, Korea. *Water* 10 (10): 1468.
- Nguyen, CC, Gaume, E and Payrastre, O. 2014. Regional flood frequency analyses involving extraordinary flood events at ungauged sites: further developments and validations. *Journal of Hydrology* 508: 385-396.
- Nguyen, TA, Grossi, G and Ranzi, R. 2008. Design storm selection for mixed urban and agricultural drainage systems: A case study in the Northern delta-Vietnam. *Proceedings of 11th International Conference on Urban Drainage, Edinburgh, UK* 31
- Olsson, J and Burlando, P. 2002. Reproduction of temporal scaling by a rectangular pulses rainfall model. *Hydrological Processes* 16 (3): 611-630.
- Ormsbee, LE. 1989. Rainfall Disaggregation Model for Continuous Hydrological Modelling *Journal of Hydraulic Engineering* 115 (4): 507-525.
- Parkes, B and Demeritt, D. 2016. Defining the hundred year flood: A Bayesian approach for using historic data to reduce uncertainty in flood frequency estimates. *Journal of Hydrology* 540: 1189-1208.
- Pilgrim, DH, Cordery, I and French, R. 1969. Temporal patterns of design rainfall for Sydney. *Civil Engineering Transactions* : 9-14.
- Prodanovic, P and Simonovic, SP. 2004. *Generation of Synthetic Design Storms for the Upper Thames River Basin CFCAS Project: Assessment of Water Resources Risk*

- and Vulnerability to Changing Climatic Condition* University of Western Ontario: Department of Civil and Environmental Engineering Canada
- Pui, A, Sharma, A, Mehrotra, R, Sivakumar, B and Jeremiah, E. 2012. A comparison of alternatives for daily to sub-daily rainfall disaggregation. *Journal of Hydrology* 470: 138-157
- Rodriguez-Iturbe, I, Cox, DR and Isham, V. 1987. Some models for rainfall based on stochastic point processes. *Proceedings of the Royal Society of London A* 410 (1839): 269-288.
- Rowe, TJ. 2019. Development and Assessment of an Improved Continuous Simulation Modelling System for Design Flood Estimation in South Africa using the ACRU Model. Unpublished thesis, Centre for Water Resources Research, School of Agricultural, Earth and Environmental Sciences, University of KwaZulu-Natal, Pietermaritzburg, South Africa.
- Rowe, TJ and Smithers, JC. 2018. Continuous simulation modelling for design flood estimation – a South African perspective and recommendations. *Water SA* 44 (4): 691-705.
- Schulze, RE. 1984. *Hydrological models for application to small rural catchments in Southern Africa: Refinements and developments*. University of Natal Pietermaritzburg, South Africa.
- Segond, M-L, Onof, C and Wheeler, HS. 2006. Spatial–temporal disaggregation of daily rainfall from a generalized linear model. *Journal of Hydrology* 331 (3-4): 674-689.
- Serinaldi, F. 2010. Multifractality, imperfect scaling and hydrological properties of rainfall time series simulated by continuous universal multifractal and discrete random cascade models. *Nonlinear Processes in Geophysics* 17 (6): 697-714.
- Sivakumar, B, Sorooshian, S, Gupta, HV and Gao, X. 2001. A chaotic approach to rainfall disaggregation. *Water Resources Research* 37 (1): 61-72.
- Smithers, JC. 1998. Development and Evaluation of Techniques for Estimating Short Duration Design Rainfall in South Africa. Unpublished thesis, Department of Agricultural Engineering, University of Natal, Pietermaritzburg, South Africa.
- Smithers, JC, Gergens, A, Gericke, OJ, Jonker, V and Roberts, C. 2016. *The Initiation of a National Flood Studies Programme for South Africa*. South African National Committee on Large Dams (SANCOLD), Pretoria, South Africa.

- Smithers, JC, Pegram, GGS and Schulze, RE. 2002. Design rainfall estimation in South Africa using Bartlett–Lewis rectangular pulse rainfall models. *Journal of Hydrology* 258 (1-4): 83-99.
- Smithers, JC and Schulze, RE. 2000. *Development and Evaluation of Techniques for Estimating Short Duration Design Rainfall in South Africa*. WRC Report No. 681/1/00. Water Research Commission, Pretoria, South Africa.
- Smithers, JC and Schulze, RE. 2001. A methodology for the estimation of short duration design storms in South Africa using a regional approach based on L-moments. *Journal of Hydrology* 241 (1-2): 42-52.
- Smithers, JC and Schulze, RE. 2002. *Design Rainfall and Flood Estimation in South Africa*. School of Bioresources Engineering and Environmental Hydrology, University of Natal, Pietermaritzburg, South Africa.
- Socolofsky, S, Adams, EE and Entekhabi, D. 2001. Disaggregation of daily rainfall for continuous watershed modeling. *Journal of Hydrologic Engineering* 6 (4): 300-309.
- Walker, S and Tsubo, M. 2003. *Estimation of rainfall intensity for potential crop production on clay soil with in-field water harvesting practices in a semi-arid area*. WRC Report No 1049/1/02 Water Research Commission Pretoria, South Africa.
- Ward, PJ, Kumm, M and Lall, U. 2016. Flood frequencies and durations and their response to El Niño Southern Oscillation: Global analysis. *Journal of Hydrology* 539: 355-378.
- Weddepohl, JP. 1988. Design Rainfall Distributions for Southern Africa. Unpublished thesis, Department of Agricultural Engineering, University of Natal Pietermaritzburg, South Africa.
- Westra, S, Evans, JP, Mehrotra, R and Sharma, A. 2013. A conditional disaggregation algorithm for generating fine time-scale rainfall data in a warmer climate. *Journal of Hydrology* 479 86-99.
- Westra, S, Fowler, HJ, Evans, JP, Alexander, LV, Berg, P, Johnson, F, Kendon, EJ, Lenderink, G and Roberts, NM. 2014. Future changes to the intensity and frequency of shortduration extreme rainfall. *Reviews of Geophysics* 52: 522–555.